

ROLE OF COARSE SOIL FRACTION ON  
RESILIENT MODULI PROPERTIES  
OF CLAYEY SOIL

by

CHATUPHAT SAVIGAMIN

Presented to the Faculty of the Graduate School of  
The University of Texas at Arlington in Partial Fulfillment  
of the Requirements  
for the Degree of

MASTER OF SCIENCE IN CIVIL ENGINEERING

THE UNIVERSITY OF TEXAS AT ARLINGTON

May 2014

Copyright © by Chatuphat Savigamin 2014

All Rights Reserved

*To my religion and family*

## Acknowledgements

First of all, I would like to deferentially thank the University of Texas at Arlington as my second home where I always feel peaceful and comfortable whenever I stay or walk around. Being a graduate student here is a great honor for me.

Simultaneously, I must respectfully thank my advisor, Dr. Anand J. Puppala. Without his help, I would never have a chance of being a graduate student who experienced and worked in many valuable projects, dealt with many well-known people in the geotechnical engineering field, and formed many eternal friendships. I also would like to respectfully thank my committee, Dr. Shih-Ho Chao and Dr. Xinbao Yu for their time and kind consideration given to help my thesis. I sincerely appreciate their assistance.

Since a tree cannot stand without its roots, my geotechnical engineering path could not begin without the guidelines from my primary advisors as well. I hereby would like to respectfully thank Dr. Suched Likitlersuang and Dr. Tanate Srisirojanakorn for their inspiration and encouragement given to me since I was an undergraduate student at Chulalongkorn University, Thailand.

Including my dear friends, I have to thank them all. Let me start with my postdoctoral associate, Dr. Aravind Pedarla, who always protected me from suspicion, and Tom (Pinit Ruttanaporamakul), my senior Thai friend who helps me even in the smallest to the largest things. In addition, I sincerely thank Raju Acharya, Tejo V. Bheemasetti, Durga Praveen Reddy Vanga, Nan (Victor) Zhang, Ujwal K.



Patil, Asheesh Pradhan, Justin D. Thomey, Nagasreenivasu Talluri, Spoorthi Reballi, Rathna P. Mothkuri, Jorge I. Almendares, and Humberto Johnson for giving me true friendship that will last forever.

As to my beloved parents, I gratefully thank my father, Mr. Chatuporn Savigamin, and my mother, Mrs. Orapin Savigamin, for their hearty kindness and love that never end. As for my brothers, I want to thank Chatupark and Chatuthanai Savigamin who always have been my support of everything. I will not miss thanking my girlfriend, Chollada Soonyakanit, for creating my beautiful world that cannot be better. Lastly, I reverently thank my precious religion, Buddhism. Without this leading light, my soul will never walk properly.

April 16, 2014

Abstract

ROLE OF COARSE SOIL FRACTION ON  
RESILIENT MODULI PROPERTIES  
OF CLAYEY SOIL

Chatuphat Savigamin, M.S.

The University of Texas at Arlington, 2014

Supervising Professor: Anand J. Puppala

As one of the major methods of soil stabilization used in the present, mechanical stabilization improves a native soil by admixing a coarse and/or fine material. This method of soil stabilization aims to reach a composition in which coarser particles form the skeleton and the surrounding space is filled with fine grains. As a result, higher soil strength can be achieved.

To study the soil strength improvement behavior, resilient modulus and unconfined compressive strength are used as evaluation parameters in this research. Since the present research focuses on subgrade soils, Dallas clay was selected as a reference clayey soil representing a native subgrade. Industrial silica sand was an admixing material. Six types of clay-sand mixtures were prepared from Dallas clay with 0%, 5%, 10%, 20%, 30%, and 50% sand admixture, respectively.

Unconfined compression tests and resilient modulus tests were performed on six types of the clay-sand mixtures. The preparation of the test samples was adhered

to their maximum dry density and optimum moisture content obtained from Proctor tests. The unconfined compression test results showed that unconfined compressive strength linearly increased with an increase in the sand admixture. For the resilient modulus ( $M_R$ ) tests, the measured  $M_R$  results were analyzed with the universal model in order to determine the predicted  $M_R$  results, which were found to be well matched with the measured results. Based on both measured and predicted  $M_R$  results, the turning point of the clay-sand mixture from a stress-softening to stress hardening material was exhibited when the percentage of the sand admixture was increased to 10%. Both deviatoric stress and confining pressure are also found to have a significant effect on the resilient modulus. In addition, the resilient modulus ( $M_R$ ) improvement analysis showed that the  $M_R$  significantly increased when the amount of the sand admixture was increased. The threshold of the effective resilient modulus improvement was also found at Dallas clay with 10% sand admixture.

## Table of Contents

Acknowledgements .....	iv
Abstract.....	vi
List of Illustrations .....	xii
List of Tables .....	xvi
Chapter 1 Introduction.....	1
1.1 General.....	1
1.2 Research Objectives and Tasks .....	3
1.3 Thesis Organization .....	6
Chapter 2 Literature Review .....	7
2.1 Pavement Failure Caused by Poor Soils .....	7
2.1.1 Compressible Soils.....	7
2.1.2 Collapsible Soils .....	8
2.1.3 Expansive Soils.....	8
2.2 Soil Stabilization for Pavements .....	9
2.2.1 Mechanical Stabilization .....	10
2.2.1.1 Application of mechanical stabilization .....	12
2.2.2 Chemical Stabilization .....	13
2.3 Resilient Modulus.....	14
2.3.1 Parameters Influencing Resilient Modulus .....	16
2.3.1.1 Types of soil.....	16
2.3.1.2 Loading condition .....	16

2.3.1.3 Compaction method .....	19
2.3.1.4 Moisture content .....	20
2.3.1.5 Density.....	21
2.3.1.6 Soil index properties.....	22
2.3.1.7 Thixotropy .....	22
2.3.1.8 Freeze-thaw.....	23
2.3.2 Methods for Resilient Modulus Measurement .....	23
2.3.2.1 Laboratory methods.....	23
2.3.2.2 Field methods.....	28
2.3.2.3 Direct correlation methods .....	36
2.3.3 Resilient Modulus Prediction Models.....	47
2.3.3.1 Bulk stress model.....	47
2.3.3.2 Uzan model.....	47
2.3.3.3 Octahedral shear stress model.....	48
2.3.3.4 Universal model.....	48
2.4 Summary .....	49
Chapter 3 Experimental Program.....	50
3.1 Introduction.....	50
3.2 Laboratory Testing Program .....	50
3.2.1 Physical Soil Properties.....	50
3.2.1.1 Particle size analysis.....	50
3.2.1.2 Atterberg limits .....	52

3.2.1.3 Specific gravity .....	52
3.2.2 Clay-Sand Mixtures .....	53
3.2.3 Standard Proctor Compaction Test .....	53
3.2.4 Unconfined Compressive Strength Test.....	58
3.2.5 Repeated Load Triaxial Test.....	60
3.2.5.1 Resilient modulus sample preparation .....	60
3.2.5.2 Cyclic triaxial system components.....	63
3.2.5.3 Resilient modulus test procedures.....	68
3.3 Summary .....	71
Chapter 4 Test Results and Analysis .....	72
4.1 Introduction .....	72
4.2 Unconfined Compression Test .....	72
4.3 Resilient Modulus Test .....	74
4.3.1 Example of Complete Resilient Modulus Test Results.....	75
4.3.2 Measured Resilient Modulus Results.....	80
4.3.3 Analysis of Resilient Modulus Test Results.....	88
4.3.4 Analysis of Resilient Modulus Improvement by Sand Admixture.....	93
4.4 Summary .....	97
Chapter 5 Conclusions and Recommendations.....	98
5.1 Conclusions .....	98
5.2 Recommendations .....	100
References.....	102

Biographical Information..... 121

## List of Illustrations

Figure 1.1 Flowchart representing the research tasks .....	5
Figure 2.1 Pavement failure due to the swelling of subgrade ( <a href="http://www.pavemanpro.com/index.php?/article/identifying_asphalt_pavement_defects">http://www.pavemanpro.com/index.php?/article/ identifying_asphalt_pavement_defects</a> ) .....	9
Figure 2.2 Relationship between CBR value and the percentage of clay-size particles (Hopkins et al., 1995) .....	12
Figure 2.3 Gradation of soils – Batticaloa airport runway (modified from Saparamado, 1962) .....	13
Figure 2.4 Definition of the resilient modulus (Selig and Waters, 1994) .....	15
Figure 2.5 Effect of the deviatoric stress on the resilient modulus of cohesive soils (Wilson et al., 1990) .....	17
Figure 2.6 Effect of the deviatoric stress on the resilient modulus of cohesionless soils (Wilson et al., 1990) .....	18
Figure 2.7 Effect of moisture content on the resilient modulus of cohesive soils (Lee et al., 1997) .....	20
Figure 2.8 Effect of density on the resilient modulus (Hicks and Monismith, 1971) .....	22
Figure 2.9 Repeated load triaxial testing system (Titi et al., 2006) .....	24
Figure 2.10 Operation of the resonant column test (Barksdale et al., 1997) .....	26
Figure 2.11 Hollow cylinder schematic layout (Thom and Dawson, 1989) .....	27
Figure 2.12 Operation of the Simple Shear test (Barksdale et al., 1997) .....	28
Figure 2.13 GeoGauge schematic layout (Lenke et al., 2001) .....	30



Figure 2.14 Seismic pavement analyzer schematic layout (Nazarian et al., 1995).....	31
Figure 2.15 Dynamic cone penetrometer schematic layout (ASTM D6951-03 Standard) .....	32
Figure 2.16 Resilient modulus measurements of PMT (Cosentino and Chen, 1991).	35
Figure 2.17 Stabilometer test schematic layout (Yoder and Witczak, 1975) .....	40
Figure 3.1 Pictures of soils using in this research.....	51
Figure 3.2 Particle size distribution of Dallas clay .....	51
Figure 3.3 Flowchart of the clay-sand mixtures .....	53
Figure 3.4 Standard Proctor compaction procedure.....	54
Figure 3.5 Compaction curve of Dallas clay with no sand admixture .....	55
Figure 3.6 Compaction curve of Dallas clay with 5% sand admixture .....	55
Figure 3.7 Compaction curve of Dallas clay with 10% sand admixture .....	56
Figure 3.8 Compaction curve of Dallas clay with 20% sand admixture .....	56
Figure 3.9 Compaction curve of Dallas clay with 30% sand admixture .....	57
Figure 3.10 Compaction curve of Dallas clay with 50% sand admixture .....	57
Figure 3.11 Total compaction curves of the clay-sand mixtures .....	58
Figure 3.12 Unconfined compressive strength equipment .....	59
Figure 3.13 Soil specimen compaction steps from Lift 1 to Lift 5 .....	61
Figure 3.14 Soil specimen preparation for the repeated load triaxial test .....	62
Figure 3.15 Cyclic triaxial system components.....	63
Figure 3.16 Triaxial load frame with pneumatic actuator .....	64
Figure 3.17 Integrated Multi-Axis Control System (IMACS).....	65

Figure 3.18 Auxiliary air reservoir.....	66
Figure 3.19 Water distribution panel.....	66
Figure 3.20 Triaxial cell .....	67
Figure 3.21 Linear Variable Displacement Transducers (LVDTs).....	68
Figure 3.22 Load cycle duration of each deviatoric stress (Titi et al., 2006) .....	70
Figure 4.1 Average of the UCS results with various percentages of the sand admixture .....	73
Figure 4.2 Example of the complete $M_R$ test results, Sequence No. 0 and 1 .....	75
Figure 4.3 Example of the complete $M_R$ test results, Sequence No. 2, 3, and 4.....	76
Figure 4.4 Example of the complete $M_R$ test results, Sequence No. 5, 6, and 7.....	77
Figure 4.5 Example of the complete $M_R$ test results, Sequence No. 8, 9, and 10.....	78
Figure 4.6 Example of the complete $M_R$ test results, Sequence No. 11, 12, and 13...	79
Figure 4.7 Example of the complete $M_R$ test results, Sequence No. 14 and 15.....	80
Figure 4.8 $M_R$ results of Dallas clay with no sand admixture, Sample A .....	81
Figure 4.9 $M_R$ results of Dallas clay with no sand admixture, Sample B .....	81
Figure 4.10 $M_R$ results of Dallas clay with 5% sand admixture, Sample A.....	82
Figure 4.11 $M_R$ results of Dallas clay with 5% sand admixture, Sample B .....	82
Figure 4.12 $M_R$ results of Dallas clay with 10% sand admixture, Sample A.....	83
Figure 4.13 $M_R$ results of Dallas clay with 10% sand admixture, Sample B .....	83
Figure 4.14 $M_R$ results of Dallas clay with 20% sand admixture, Sample A.....	84
Figure 4.15 $M_R$ results of Dallas clay with 20% sand admixture, Sample B .....	84
Figure 4.16 $M_R$ results of Dallas clay with 30% sand admixture, Sample A.....	85

Figure 4.17 $M_R$ results of Dallas clay with 30% sand admixture, Sample B .....	85
Figure 4.18 $M_R$ results of Dallas clay with 50% sand admixture, Sample A .....	86
Figure 4.19 $M_R$ results of Dallas clay with 50% sand admixture, Sample B .....	86
Figure 4.20 Predicted $M_R$ results of Dallas clay with no sand admixture .....	89
Figure 4.21 Predicted $M_R$ results of Dallas clay with 5% sand admixture .....	89
Figure 4.22 Predicted $M_R$ results of Dallas clay with 10% sand admixture.....	90
Figure 4.23 Predicted $M_R$ results of Dallas clay with 20% sand admixture.....	90
Figure 4.24 Predicted $M_R$ results of Dallas clay with 30% sand admixture.....	91
Figure 4.25 Predicted $M_R$ results of Dallas clay with 50% sand admixture.....	91
Figure 4.26 Comparison between the predicted and measured $M_R$ results of the clay- sand mixtures .....	92
Figure 4.27 Relationship between an increase in the measured resilient modulus and percentage of the sand admixture (at deviatoric stress of 13.8 kPa).....	94
Figure 4.28 Relationship between an increase in the measured resilient modulus and percentage of the sand admixture (at deviatoric stress of 27.6 kPa).....	94
Figure 4.29 Relationship between an increase in the measured resilient modulus and percentage of the sand admixture (at deviatoric stress of 41.4 kPa).....	95
Figure 4.30 Relationship between an increase in the measured resilient modulus and percentage of the sand admixture (at deviatoric stress of 55.2 kPa).....	95
Figure 4.31 Relationship between an increase in the measured resilient modulus and percentage of the sand admixture (at deviatoric stress of 68.9 kPa).....	96

## List of Tables

Table 3.1 Physical properties of Dallas clay.....	52
Table 3.2 Standard Proctor compaction specifications (ASTM D 698 Standard).....	54
Table 3.3 Summary of standard Proctor compaction results.....	58
Table 3.4 Testing sequence for subgrade soil (AASHTO T 307-99 Standard).....	69
Table 4.1 Summary of unconfined compression test results .....	73
Table 4.2 Material specific regression coefficients of the clay-sand mixtures.....	88

## Chapter 1

### Introduction

#### 1.1 General

Transportation plays as an important role in the development of any nation while creating opportunities for people through better accessibility. Form of transportation includes roads, railways, water, and air. In this research, the main concerned form is roads or pavements.

Pavements have long been developed from the past starting from purely empirical methods to scientific methods. Many theories were developed and improved. Although pavement construction methods and materials have significantly progressed over the past century, several theories behind them are still principally empirical. Nowadays, pavements can be roughly categorized into three types, flexible pavements, rigid pavements, and composite pavements (Huang, 2003). Flexible pavements are constructed using bituminous and granular materials, rigid pavements are constructed using Portland cement concrete, and composite pavements are constructed using both bituminous and Portland cement. Regardless of types, pavements need to be supported on a strong native material which is called subgrade or subgrade layer.

In general, the performance of subgrade is governed by two characteristics, strength and deformation (Selig and Lutenegeger, 1991). To characterize subgrade materials; three basic strength/stiffness characterizations are typically used; which are

Resilient Modulus ( $M_R$ ), California Bearing Ratio (CBR), and Modulus of Subgrade Reaction (k-value).

For several times, native subgrade soil can cause various road failure problems since it cannot stand a large amount of transferred load resulting in loss of excessive money or sometime life. A number of ground improvement techniques were developed to improve these soil characteristics in order to match the designed purpose and prevent roads from failure. Among these methods of soil stabilization, mechanical stabilization is one of the appropriate methods for improving subgrade layer since it can provide a higher strength to the native soil immediately after the mixing process, and also does not create any environmental problem (O'Flaherty, 2002). This method performs by adding soil materials into the native soil. After the soil mixing process is completed, the soil mixture is then compacted (O'Flaherty, 2002; Liu and Evett, 2008). Mechanical stabilization is an ideal method of improvement especially when suitable materials are available near the construction area (Jones et al., 2010).

To determine the improvement of subgrade after being stabilized, the most referred parameter for pavement design is the resilient modulus. According to the AASHTO Guide for Design of Pavement Structures 1993 (AASHTO, 1993), Resilient Modulus has been used as the only definitive material property of roadbed soil (subgrade). The resilient modulus is a measure of soil elastic property recognizing certain nonlinear characteristics. Additionally, the resilient modulus can be used directly for the flexible pavement design, but must be converted to a modulus

of subgrade reaction (k-value) in order to use for the rigid or composite pavement design (AASHTO, 1993). However, a lack of equipment still forces many agencies to use some parameters such as standard CBR or k-value to determine the resilient modulus.

### 1.2 Research Objectives and Tasks

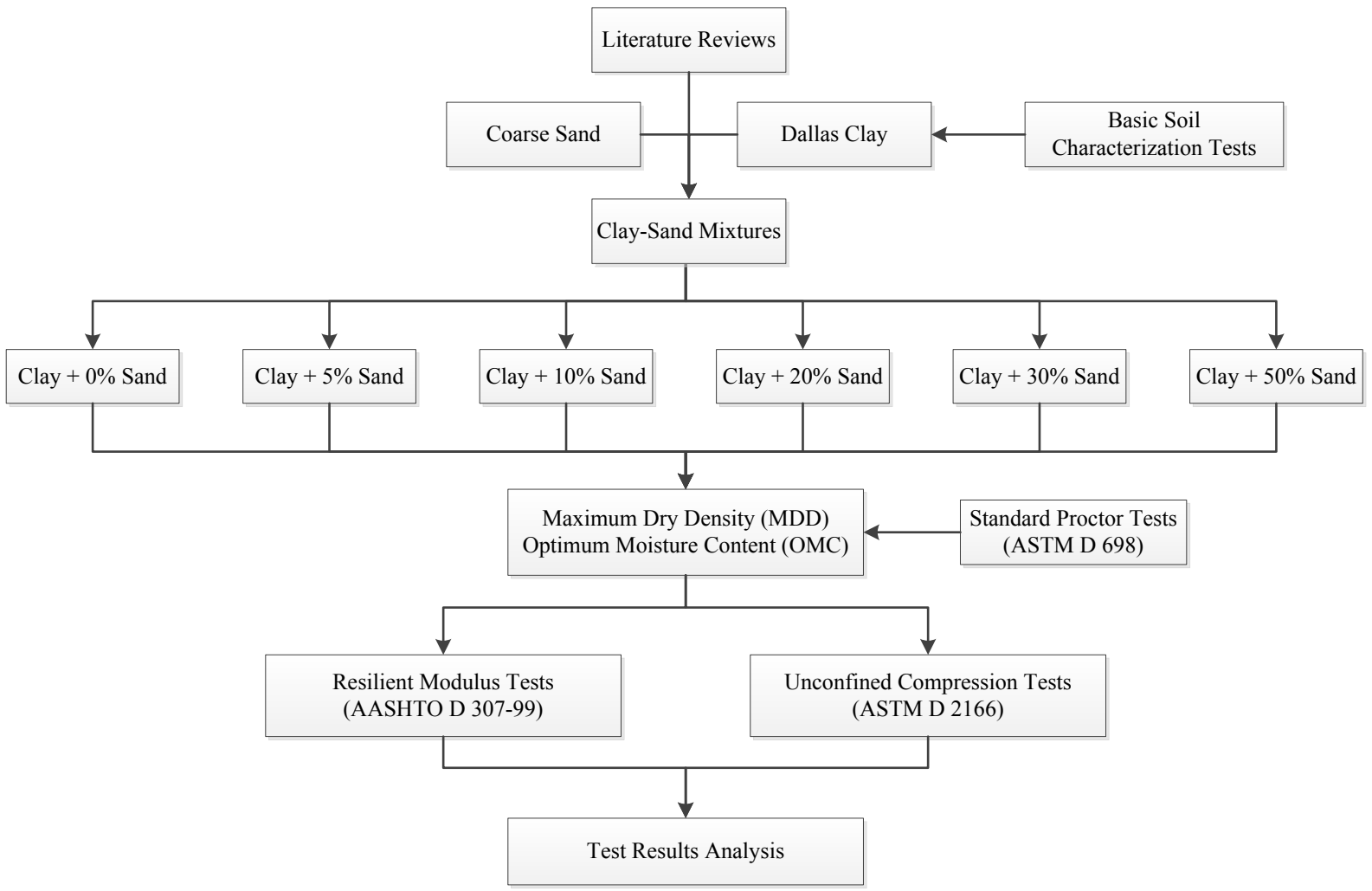
The primary objective of this research is to study the behavior of resilient moduli properties due to the respective increase of coarse sand particles in the clayey soil which referred as the mechanical stabilization method. The secondary objective is to analyze the soil strength improvement by the mechanical stabilization method. To achieve these objectives, the following tasks are created and listed as follows.

1. Study all the available literature on soil stabilization methods, resilient modulus properties, and related theories of soil mechanics.
2. Conduct basic soil characterization tests on Dallas clay, which include specific gravity tests, hydrometer tests, sieve analysis, plastic limit tests, and liquid limit tests with respect to the appropriate ASTM standards.
3. Prepare six types of clay-sand mixtures by inclusion of Dallas clay and coarse sand of 0, 5, 10, 20, 30, and 50 percent by weight of the total mixture.
4. Determine the maximum dry density (MDD) and optimum moisture content (OMC) for six types of the clay-sand mixtures by conducting standard Proctor compaction tests with respect to the ASTM D 698 standard.

5. Prepare two statically compacted specimens for one type of the clay-sand mixtures in compliance with their optimum moisture content and maximum dry density.
6. Conduct unconfined compression tests on the statically compacted specimens with respect to the ASTM D 2166 standard.
7. Prepare two resilient modulus specimens for one type of the clay-sand mixtures in compliance with their optimum moisture content and maximum dry density.
8. Conduct resilient modulus tests by using the repeated load triaxial (RLT) test equipment with respect to the AASHTO T 307-99 standard.
9. Analyze the resilient modulus test results as well as the unconfined compression test results corresponding to various percentages of the sand admixture.

Figure 1.1 presents a flow chart representing the research tasks.





5

Figure 1.1 Flowchart representing the research tasks

### 1.3 Thesis Organization

This thesis consists of five chapters: Chapter 1: Introduction, Chapter 2: Literature Review, Chapter 3: Experimental Program, Chapter 4: Test Results and Analysis, and Chapter 5: Conclusions and Recommendations.

Chapter 1 provides an introduction to the mechanical stabilization method using the resilient modulus as a main evaluation parameter of soil improvement. Research tasks and thesis organization are also included in this chapter.

Chapter 2 presents literature reviews on soil stabilization methods with a focus on mechanical stabilization. Concept of the resilient modulus; parameters influencing the resilient modulus; several methods of resilient modulus measurement; and resilient modulus models are addressed therein.

Chapter 3 offers the experimental programs conducted in this research. Basic soil properties of Dallas clay and coarse sand; standard Proctor compaction test and results; unconfined compression test; resilient modulus sample preparation; and methodology of the repeated load triaxial (RLT) test are presented.

Chapter 4 contains the unconfined compression test results obtained from six types of the clay-sand mixtures. The measured and predicted resilient modulus results from each clay-sand mixture are then presented. Graphical analyses of the resilient modulus improvement are also performed by comparing an increase in the resilient modulus results with various percentages of the sand admixture.

Chapter 5 summarizes the results and addresses some recommendations for future research.

## Chapter 2

### Literature Review

#### 2.1 Pavement Failure Caused by Poor Soils

Pavement failure can be categorized into two types, structural failure and functional failure (Yoder and Witczak, 1975). Structural failure is a breakdown of one or more pavement layers causing the pavement to inefficiently sustain the loads imposed on its surface. Functional failure takes place when the pavement is unable to carry on its intended function without causing any discomfort to drivers or creating imposing stresses on vehicles. Pavement failures may occur due to various reasons, such as poor soils, poor moisture control, transition between cuts and fill, non-uniformity of foundation, and utility cuts (Schaefer et al., 2008).

Poor soils can severely damage construction as well as affecting a long-term performance of the pavement during its service life. Using as a subgrade layer, poor soils often lack strength and stability to provide enough support for trucks hauling construction materials causing project delays and wasting of excessive money. Poor soils that related to pavement design generally have three types, compressible soils, collapsible soils, and expansive soils. Figure 2.1 shows a pavement failure by a localized upward movement due to the swelling of subgrade.

##### *2.1.1 Compressible Soils*

Compressible soils are susceptible to large deformations or settlements. These soils generally are clays, silts, peat, and organic alluvium which are low in density. When they are not treated properly, large surface depressions can be developed. Then

the surface depressions can allow water to pond on the pavement surface and infiltrate into the pavement structure causing severe damage to pavement. Additionally, the ponding water can create a safety hazard to the driver who passes during wet weather (Schaefer et al., 2008).

### *2.1.2 Collapsible Soils*

Collapsible soils can also cause significant settlements to the pavement. Collapsible soils are very low density silt soils which are generally a combination of alluvium or wind-blown deposits. These soils are susceptible to decreases in volume when wetted. Many times, collapsible soils are cemented by clay binders or other deposits which easily dissolve upon saturation, allowing a large decrease in volume. Residual soils can often become collapsible due to leaching of colloidal or soluble materials. If pavement systems have to be constructed over collapsible soils, special investigations may be required in order to prevent large-scale cracking or differential settlements (Lawton et al., 1992; Coduto, D. P., 2000; Schaefer et al., 2008).

### *2.1.3 Expansive Soils*

Expansive or swelling soils are susceptible to changes in volume with fluctuations in moisture content. The magnitude of volume changes depends on the type of soil and moisture content (Al-Rawas and Goosen, 2006). When moisture content decreases, these soils will shrink. On the other hand, if moisture content increases, these soils will expand. This volume changing behavior can cause longitudinal cracks near the edge of pavement and surface roughness along the length of pavement (Nelson and Miller, 1992).



Figure 2.1 Pavement failure due to the swelling of subgrade

([http://www.pavemanpro.com/index.php?/article/identifying\\_asphalt\\_pavement\\_defects](http://www.pavemanpro.com/index.php?/article/identifying_asphalt_pavement_defects))

## 2.2 Soil Stabilization for Pavements

Soil stabilization is any treatment applied to the soil in order to improve its strength and lower its susceptibility to water (O’Flaherty, 2002). To define as a stable soil, the treated soil is required to withstand the imposed stress by traffic loading under weather conditions without any significant deformation (O’Flaherty, 2002). Conventionally, pavement layers that have been constructed by using selected soils and aggregates are easy to estimate the load-bearing capacity of each layer. However, since a subgrade layer is a native soil, proper treatments are often necessary in order to prevent pavement failure and ensure a long-lasting pavement which does not

require excessive maintenance. In some cases of subgrade soils, which do not perform well; excavation may be preferred by the agencies. However, excavation generally is not the most economical or desirable method since it can cause a great disturbance and losing lots of excessive money. In practice, the main methods of soil stabilization for pavement are mechanical stabilization and chemical (or additive) stabilization (Joint Departments of the Army and Air Force, USA, 1994; Liu and Evett, 2008). This present research mainly focuses on the mechanical soil stabilization method.

### *2.2.1 Mechanical Stabilization*

Mechanical stabilization, also known as granular stabilization, is a method of improving a native soil by admixing a coarse and/or fine material (generally 10 to 50 percent), with the purpose of achieving a denser homogeneous mass when compacted. Soil particles of the additional non-fines materials contributed in this method have a diameter of more than 0.06 mm (O’Flaherty, 2002). According to Hick (2002), the suitable soils for mechanical stabilization method include silty sands, sandy clays, silty clays, poor-graded products, dune or deposited sands, crusher run products, waste quarry products, and high-plasticity pavement materials. For the improvement concept, after adding coarse grains to the existing fine-grained soil, the coarse grains form the skeleton and the pores that occurred around the skeleton are filled with fine grains. Therefore, the mutual contact between coarse and fine grains forms better soil conditions that possess more internal friction and cohesion. As a result, more workability and stability will be obtained after the

completion of mixing and compaction processes (Vanicek, 2008; Liu and Evett, 2008). The mechanical stabilization can be used in preparing soils to function as subgrades, bases, and surfaces (Department of the Army, 1992). In addition, one of the outstanding benefits of mechanical stabilization method is that it can be used for a situation where traffic must be routed onto the subgrade immediately after compaction. In this situation, chemical stabilization may not be appropriate since the time required for curing of the chemically-treated subgrade is not enough (Hopkins et al., 1995).

The main parameters which control the supporting performance of this method are degree of saturation and the percentage of clay-size particles (Hopkins et al., 1995). The degree of saturation significantly controls the short-term bearing capacity during the construction process. Often, a large decrease in bearing capacity will occur if the soil mixture is exposed to periods of rainfall or melting snow since the soil mixture may swell, increase in volume, and thus decrease in strength. For the percentage of clay-size particles, both total strength and loss strength during weather conditions depend on this parameter. Therefore, the percentage of aggregate to be mixed with the native soil must be determined during the design process in order to achieve an adequate bearing capacity to avoid deep ruts or tire sinkage (Hopkins et al., 1995).

According to Hopkins (1991), for an anticipated ground contact stress of 552 kPa (80 psi), the CBR value must be in a range between 8 and 10 to avoid rutting. Also, Hopkins et al. (1995) presented a relationship between Kentucky CBR value

and the percentage of clay-size particles using Kentucky subgrade soil data obtained from the Kentucky Geotechnical Data Bank (Pfalzer et al., 1995) in Figure 2.2. As observed from the figure, the greater of the percent finer resulted in the lower of the CBR value, which represented soil strength. In addition, this figure clearly illustrated that soaked soils had lower strength than unsoaked soils.

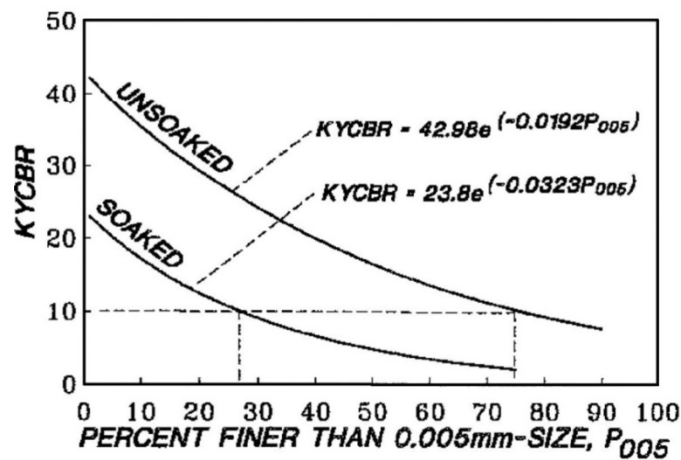


Figure 2.2 Relationship between CBR value and the percentage of clay-size particles  
(Hopkins et al., 1995)

#### 2.2.1.1 Application of mechanical stabilization

A construction project of Batticaloa airport runway was carried out by Public Works Department (PWD) in Sri Lanka. Mechanical stabilization method was selected to improve the base course of this airport (Saparamado, 1962).

Batticaloa airstrip soil is a deposit of beach sand about 4.5 feet thick over a formation of hard rock. The sand is poorly graded non-plastic with a gradation as shown in Figure 2.3. Since a source of gravel material was available at a distance of about 1.5 miles from the site, it had been selected as an admixture to improve the



quality of native soil by using the mechanical stabilization method. This gravel has a maximum diameter of 0.75 inch with 25% of fines particle passing No. 200 sieve. The fine part of this gravel has a liquid limit of 60 and a plastic index of 16. After mixing, the soil mixture was found to give a better well-gradation, which is preferred for a base course material, as shown in Figure 2.3.

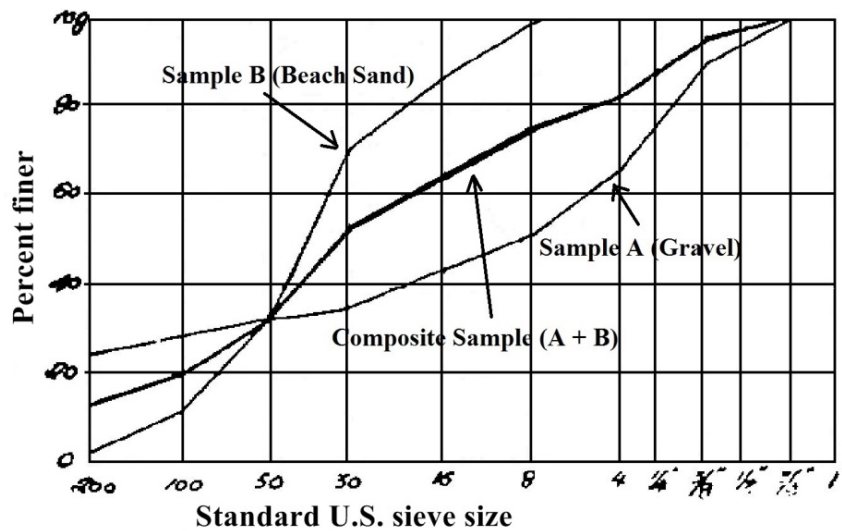


Figure 2.3 Gradation of soils – Batticaloa airport runway  
(modified from Saparamado, 1962)

### 2.2.2 Chemical Stabilization

Chemical (or additive) stabilization is a method of adding proper percentages of additives including lime, fly ash, portland cement, bitumen, calcium chloride, bioremediation, and combinations of these materials to the existing soil. This method is often used to stabilize soils when a mechanical stabilization is inadequate, and/or replacing an undesirable soil with desirable soil is not possible or too costly. In order to determine the appropriate type and percentage of the additive; the controlled

parameters are the type of soil to be stabilized, purpose for which the stabilized layer will be used, required strength and durability of the stabilized layer, type of soil quality improvement desired, and environmental conditions. (Department of the Army, 1992; Joint Departments of the Army and Air Force, USA, 1994; Hopkins et al., 1995; Hick, 2002).

### 2.3 Resilient Modulus

In the conventional elastic theories, elastic properties of any material are defined in terms of the elastic modulus ( $E$ ) and Poisson's ratio ( $\nu$ ). However, soils exhibit as nonlinear elasto-plastic materials which mean that they act partially elastic under an applied load but experience some permanent deformation. At the initial state after applying cyclic loads, soils perform like they are under a static load. Then after a number of certain loads, the permanent deformation under each load cycle is almost entirely recoverable. At this stage, if the applied loads are still small enough, soils can be considered as elastic materials. To find an appropriate approach, Resilient Modulus ( $M_R$ ) has been used in order to represent the nonlinear behavior with respect to the stress increasing (Lekarp et al., 2000). It was first introduced by H.C. Seed in the 1960s. From 1986, AASHTO started to require using of the resilient modulus for the flexible pavement design. Resilient Modulus ( $M_R$ ) is defined as a deviatoric stress ( $\sigma_d$ ), divided by the elastic strain ( $\epsilon_r$ ) experienced under number of repetitive loading conditions that simulate the real traffic (Puppala, 2008). This definition can be written as Equation 2.1 which is the slope of a relationship between the deviator stress and

resilient strain shown in Figure 2.4. The figure shows that each load cycle has two strain components which are plastic strain and elastic strain. The resilient strain or elastic strain ( $\epsilon_r$ ) is measured when plastic strain is approximately equal to zero.

$$M_R = \frac{\sigma_d}{\epsilon_r} \quad (2.1)$$

where the deviatoric stress ( $\sigma_d$ ) and elastic strain ( $\epsilon_r$ ) can be written as Equation 2.2 and 2.3 respectively.

$$\sigma_d = \frac{P}{A_i} \quad (2.2)$$

where P = applied load, and  $A_i$  = initial cross-sectional area of the soil specimen.

$$\epsilon_r = \frac{\Delta H}{H_i} \quad (2.3)$$

where  $\Delta H$  = change in soil specimen height due to the applied load, and  $H_i$  = initial height of soil specimen.

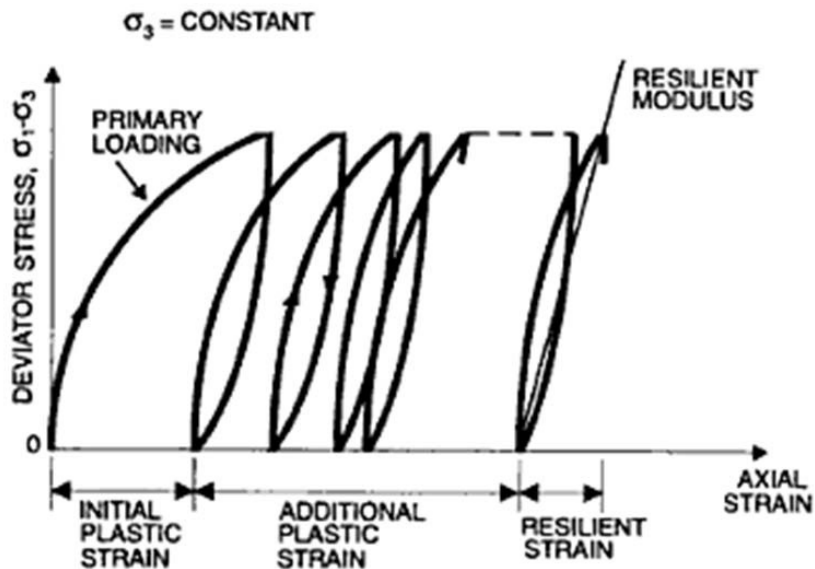


Figure 2.4 Definition of the resilient modulus (Selig and Waters, 1994)

### *2.3.1 Parameters Influencing Resilient Modulus*

Significant parameters that influence resilient modulus have been investigated by many researchers including types of soil, loading condition, compaction method, water content, dry density, and freeze-thaw cycles.

#### *2.3.1.1 Types of soil*

According to Thom and Brown (1987), an increase in fine content of the partially crushed aggregates results in decreasing of the resilient modulus. On the other hand, Hicks and Monismith (1971) investigated that an increase in fine content of the fully crushed aggregates results in increasing of the resilient modulus. Since the pore space between the soil particles is filled by the fine soil, the resilient modulus initially increases. However, after an increase in fine content reaches a certain point, the excess fine particles will change the soil behavior from coarse soil to fine soil causing a decrease in the resilient modulus (Jorenby and Hicks, 1986).

In general, an increase in the amount of fine content results in decreasing of the resilient modulus (Lekarp et al., 2000). Additionally, lower clay content and higher silt content result in the lower resilient modulus (Thompson and Robnett, 1979). According to Janoo and Bayer II (2001), an increase in maximum particle size results in increasing of the resilient modulus.

#### *2.3.1.2 Loading condition*

Since the resilient modulus is a function of stress and strain, the most significant loading condition factor that impacts on resilient properties is the stress level (Rada and Witczak, 1981).

According to Thompson and Robnett (1979), at low levels of the deviatoric stress, an increase in the deviatoric stress of cohesive soils results in decreasing of the resilient modulus. When the deviatoric stress is increased to a certain value, an increase in deviatoric stress results in a minor decrease or reaching a constant value of the resilient modulus as shown in Figure 2.5. Similarly, for cohesionless soils, an increase in the deviatoric stress results in decreasing of the resilient modulus as shown in Figure 2.6 (Wilson et al., 1990).

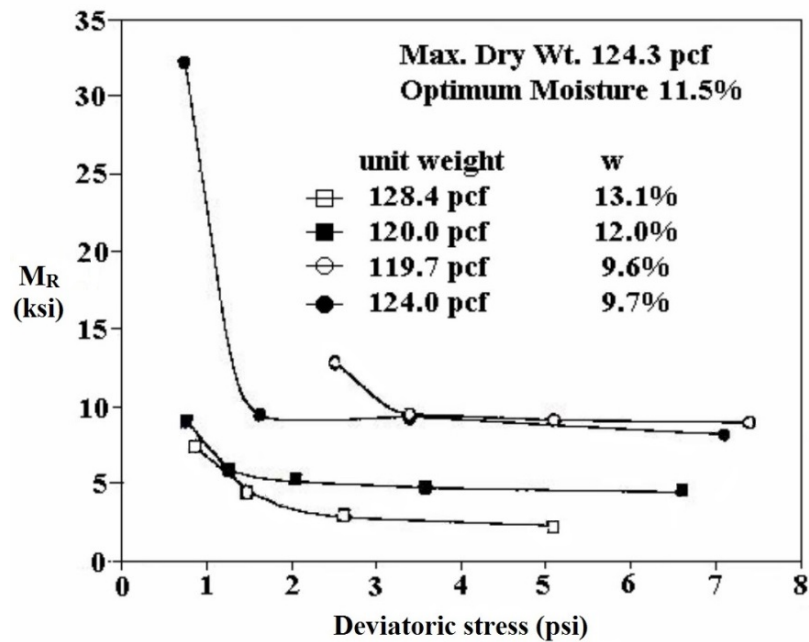


Figure 2.5 Effect of the deviatoric stress on the resilient modulus of cohesive soils

(Wilson et al., 1990)

As for the impact of confining stress, previous investigations show that an increase in the confining stress results in increasing of the resilient modulus (Seed et al., 1962; Thomson and Robnett, 1976; Rada and Witczak, 1981; and Pezo and

Hudson, 1994). However the changing in confining stress of cohesionless soils affects the resilient modulus more than cohesive soils (Thompson and Robnett, 1979; Rada and Witzak, 1981).

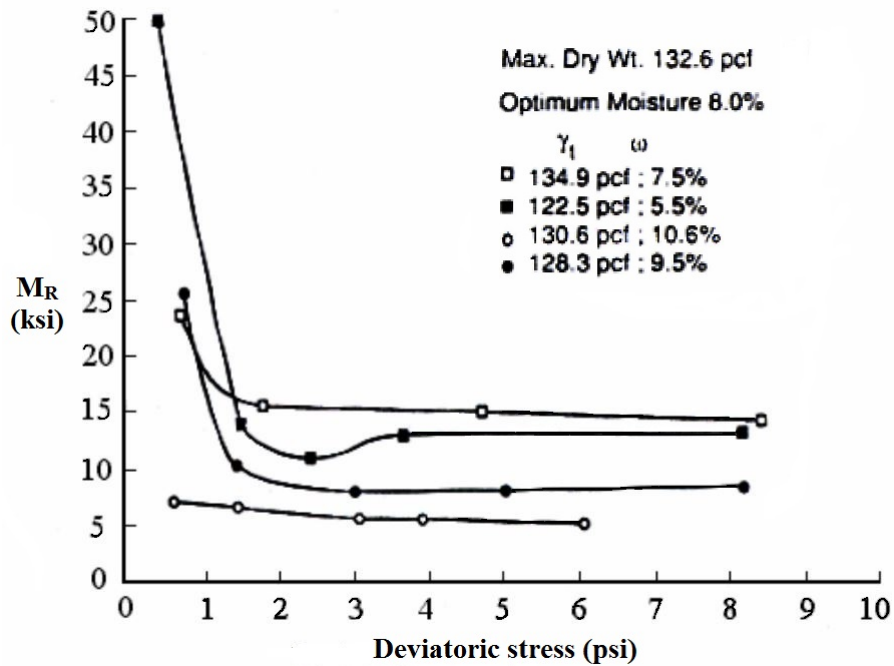


Figure 2.6 Effect of the deviatoric stress on the resilient modulus of cohesionless soils (Wilson et al., 1990)

According to Pezo et al. (1992) and Nazarian et al. (1993), stress history has a significant effect on the resilient modulus. Since an increase in the repeated loads reduces the moisture content of soils, the resilient modulus increases (Huang, 2001).

Other loading condition factors such as stress duration, sequence of load, and repetition of stress after getting into an equilibrium stage have only little effect on the resilient modulus (Rada and Witzak, 1981).

### 2.3.1.3 Compaction method

Normally when preparing a soil specimen for pavement design, the specimen should be prepared following its optimum density to achieve the required performance. Specimens that are compacted at higher density will result in higher resilient modulus. According to Lee (1993), the compaction method has a small effect on the resilient modulus when soil specimens are compacted at low degrees of saturation by reason of a flocculated arrangement of clay particles. On the other hand, the compaction method will have a large effect on the resilient modulus when soil specimens are compacted above their optimum moisture content due to a dispersed arrangement of clay particles.

In addition to the effect of compaction method on preparing soil specimens, Seed and Chan (1959) reported that when soil specimens are prepared by using the vibratory compaction method at the dry side of the compaction curve, a flocculated particle arrangement will be generated. In the same manner, when soil specimens are prepared at the wet side of the compaction curve, a dispersed arrangement will be generated. However, the static compaction method causes only a flocculated arrangement to soil particles both dry and wet sides. They also investigated that the recoverable strains for soil specimens prepared by vibratory and static compaction are similar. With these reasons, soil specimens prepared by a static compaction method give higher resilient modulus than a vibratory compaction method (Seed et al., 1962; Elliot and Thornton, 1988), and also soil specimens prepared by a static compaction method are less repeatable (Seim, 1989).

In addition, the resilient modulus obtained from the dry side is higher than the wet side of the compaction curve (Seed et al., 1962; Tanomota and Nishi, 1970; Thompson and Robnett, 1979).

#### 2.3.1.4 Moisture content

Many literatures in the past have found that moisture content has a significant effect on the resilient modulus. For cohesive soils, an increase in the moisture content results in decreasing of the resilient modulus as shown in Figure 2.7. Moreover, at the wet side of the compaction curve, it has been noticed that the resilient modulus value is lower than the dry side of the compaction curve (Lee et al., 1997).

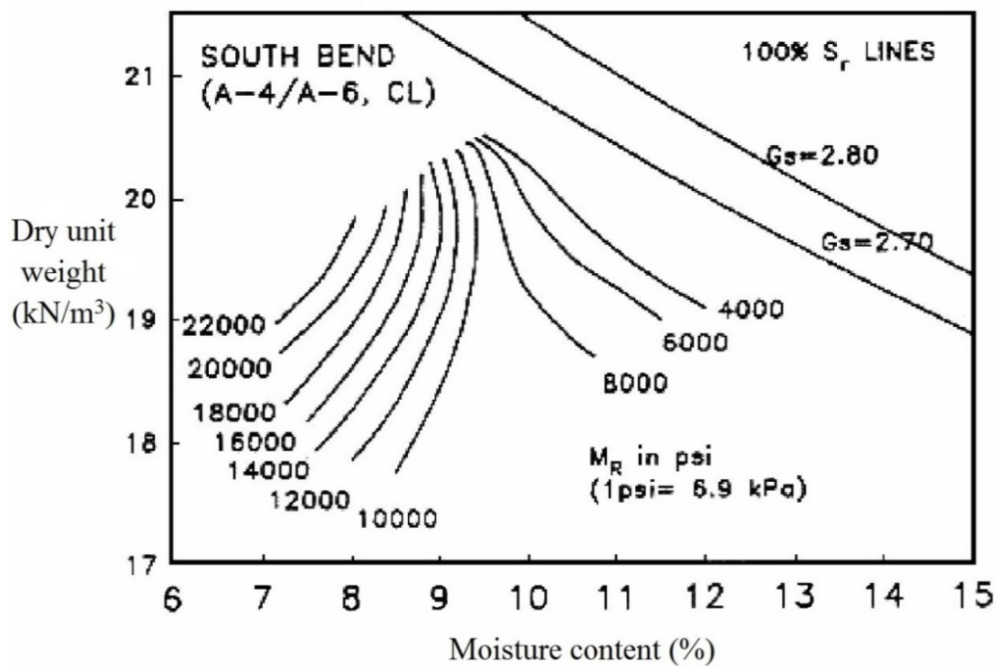


Figure 2.7 Effect of moisture content on the resilient modulus of cohesive soils  
(Lee et al., 1997)



As for granular materials, the resilient modulus of saturated soil specimen is significantly affected by the moisture content. However, when the soil specimen is dry or most partially saturated, the resilient modulus is constant with regard to the changing of moisture content. Since the saturated granular materials form excess pore-water pressure while accepting the cyclic load, the effective stress decreases and thus the resilient modulus also decreases (Smith and Nair, 1973; Vuong, 1992). According to Dawson et al. (1996), who studied the relationship of well-graded granular materials, at the dry side of the compaction curve, stiffness increases when the moisture content increases. On the other hand, at the wet side of the compaction curve, stiffness decreases rapidly when the moisture content increases.

#### 2.3.1.5 Density

In general, an increase in density of granular materials causes the materials to become stronger. Likewise, it happens to the resilient modulus. According to Hicks (1970), Robinson (1974), and Rada and Witczak (1981); the resilient modulus normally increases along with an increase of density. Kolisoja (1997) stated that when the density increases, the particle contact areas are increased which results in decreasing of the average contact stress receiving from the external load. Therefore, the resilient modulus increases because the deformation ( $\Delta H$ ) decreases. In addition, Hick and Monismith (1971) investigated that the effect of density on partially crushed granular materials is larger than fully crushed granular materials since the fine content of partially crushed granular materials is higher than fully crushed granular materials. They also reported that an increase in dry density results in increasing of

the resilient modulus for both coarse grading and fine grading materials as shown on Figure 2.8.

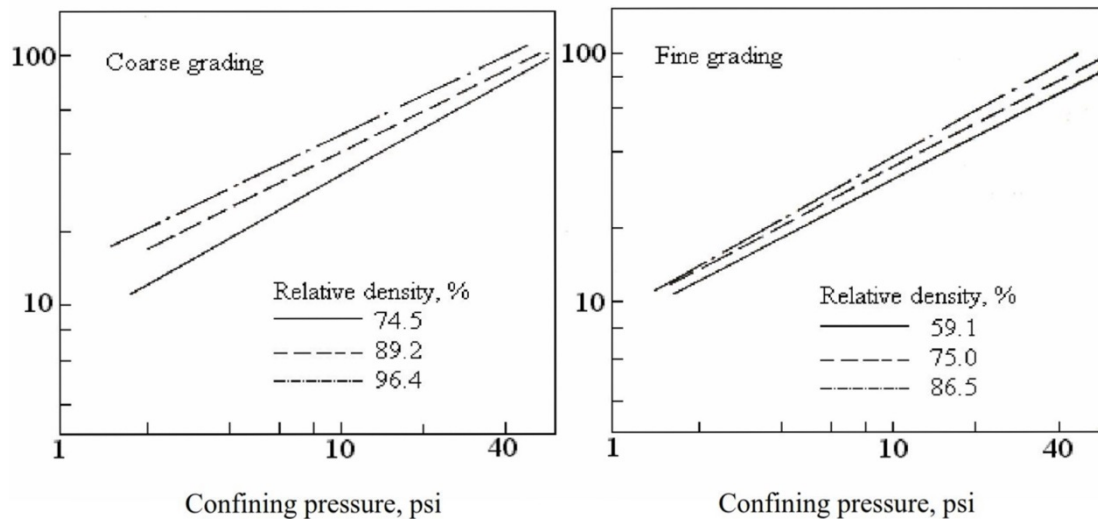


Figure 2.8 Effect of density on the resilient modulus (Hicks and Monismith, 1971)

#### 2.3.1.6 Soil index properties

According to Thompson and Robnett (1979), soil index properties which have an effect on the resilient modulus are plasticity index, liquid limit, specific gravity, and organic content. They also reported that low plasticity index, low liquid limit, low specific gravity, and high organic content lead to the lower resilient modulus.

#### 2.3.1.7 Thixotropy

The effect of thixotropy is particularly related to cohesive soil. Seed and Chan (1957) reported that soil specimens which are prepared at high degree of saturation and allowed to rest before testing show higher strength. They also investigated that if soil specimens are tested after certain number of cyclic loads, thixotropy will no longer affect the recoverable strain.

#### 2.3.1.8 Freeze-thaw

According to many researchers such as Bergan and Fredlund (1973), Chamberlain (1973), Elliott and Thornton (1988), and Lee (1993), freeze-thaw cycles have a significant effect on the resilient modulus. They all mentioned that a large reduction in the resilient modulus will occur only after the soil passes a small number of freeze-thaw cycles.

### 2.3.2 *Methods for Resilient Modulus Measurement*

#### 2.3.2.1 Laboratory methods

The resilient modulus can be determined by several laboratory tests using undisturbed or remolded soil specimens. Various laboratory methods can be used directly to determine the resilient modulus but in some laboratory methods need to use an empirical correlation to calculate for the resilient modulus. This section will provide a brief discussion of these laboratory methods including repeated load triaxial test, resonant column test, hollow cylinder test, and simple shear test.

##### 2.3.2.1.1 *Repeated load triaxial (RLT) test*

The repeated load triaxial test was designed to simulate real traffic loading using repeated cyclic loads to simulate a number of wheel passing loads. The test is performed by inserting a soil specimen, which can be both undisturbed and remolded, into the triaxial chamber that will be filled with water. Then a number of different confining pressures will be applied together with various levels of cyclic deviatoric stress following the AASHTO T 307-99 standard. At each cycle, which has a certain number of confining pressure and deviatoric stress, the resilient modulus is

determined by using the average of the last five resilient deformation values. Figure 2.9 shows an RLT testing system.

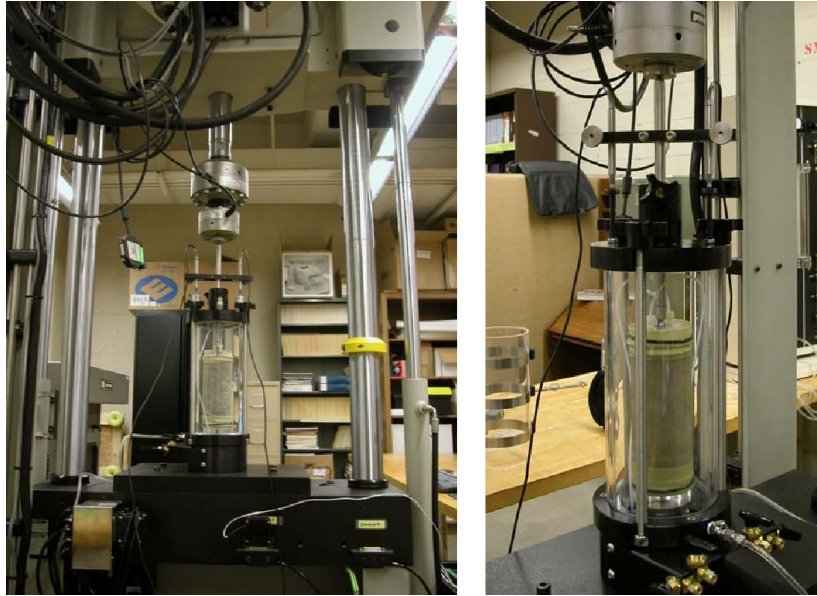


Figure 2.9 Repeated load triaxial testing system (Titi et al., 2006)

The full name of the AASHTO T 307-99 standard is “Standard Method of Test for Determining the Resilient Modulus of Soils and Aggregate Materials.” According to Puppala (2008), the development history of this standard tracks down to the Strategic Highway Research Programs (SHRP) protocol P 46-94 of which name is “Resilient Modulus of Unbound Base/Subbase Materials and Subgrade Soil.” After using this protocol for a few years, the protocol had been developed a few times by AASHTO who named the standard in chronological order as T-274, T-292, and T-294. In the current standard (AASHTO T 307-99 Standard), the test procedures are based on the Strategic Highway Research Program (SHRP) and Long Term Pavement Performance Program (LTPP). Maher et al (2000) noticed about some significant

changes from the previous AASHTO T274-82 and T294-92 procedures to the current AASHTO T307-99 procedures as follows:

- The range of maximum axial stress was changed from 1–20 psi to 3–40 psi for base and subbase materials and from 1–10 psi to 2–10 psi for roadbed materials.
- The number of loading sequences was changed from 27 to 15, and the number of loading cycles per a loading sequence was changed from 200 to 100 cycles.
- The confining pressure of subbase material testing was changed from 0 to 2 psi.
- The addition of a contact axial stress of 10% of the total deviatoric stress was to maintain full contact between the soil specimen and the loading piston.

#### *2.3.2.1.2 Resonant column test*

The resonant column test was designed to study dynamic characterization of materials since 1930s. The test is performed by inserting a soil specimen into a chamber on a pedestal. Then the top cap with torsional drive plate will be attached at the top of the soil specimen. Figure 2.10 shows the operation of the resonant column test. When the test begins, the torsional force is applied to the soil specimen at the top part with a constant amplitude and different frequency. The occurred displacement is recorded and shows in the frequency response curve. According to Richart (1975),

the frequency response curve can be used to define a small-strain shear modulus ( $G$ ) as follows:

$$G = \rho (2\pi L)^2 \left(\frac{f_r}{F_r}\right)^2 \quad (2.4)$$

$$F_r = \sqrt{\frac{I_R}{I_o}} \quad (2.5)$$

where  $\rho$  = soil density,  $L$  = sample length,  $f_r$  = resonant frequency,  $F_r$  = driver constant,  $I_R$  = polar moment of inertia (soil column), and  $I_o$  = polar moment of inertia (driver system).

After getting the small-strain shear modulus ( $G$ ), the resilient modulus can be determined by the provided equation below.

$$M_R = 2 G (1 + \mu) \quad (2.6)$$

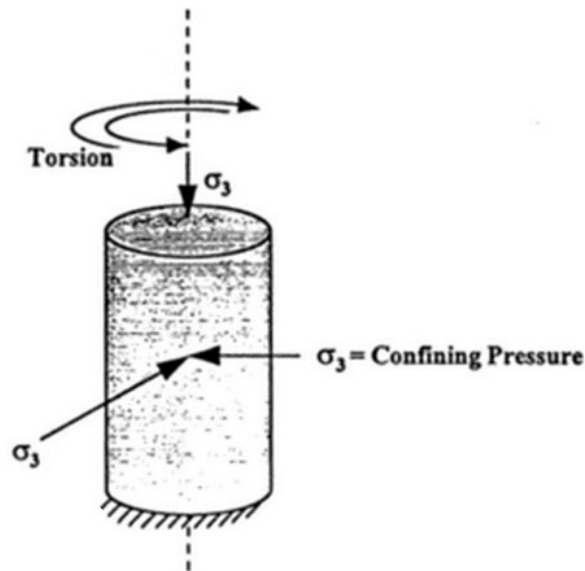


Figure 2.10 Operation of the resonant column test (Barksdale et al., 1997)

### 2.3.2.1.3 Hollow cylinder test

The hollow cylinder test can be used to simulate many different stress conditions which are vertical, radial, and torsional directions. From the benefit of multiple directions, this test generates a closer condition to the real traffic and represents an advanced tool for the advanced research. The soil specimen is prepared to be as a cylindrical shape enclosing a membrane both inside and outside. Since the test procedure and specimen preparation are complicated, the hollow cylinder test is not appropriate to the normal resilient modulus testing (Barksdale et al., 1997).

Figure 2.11 shows the Hollow Cylinder apparatus.

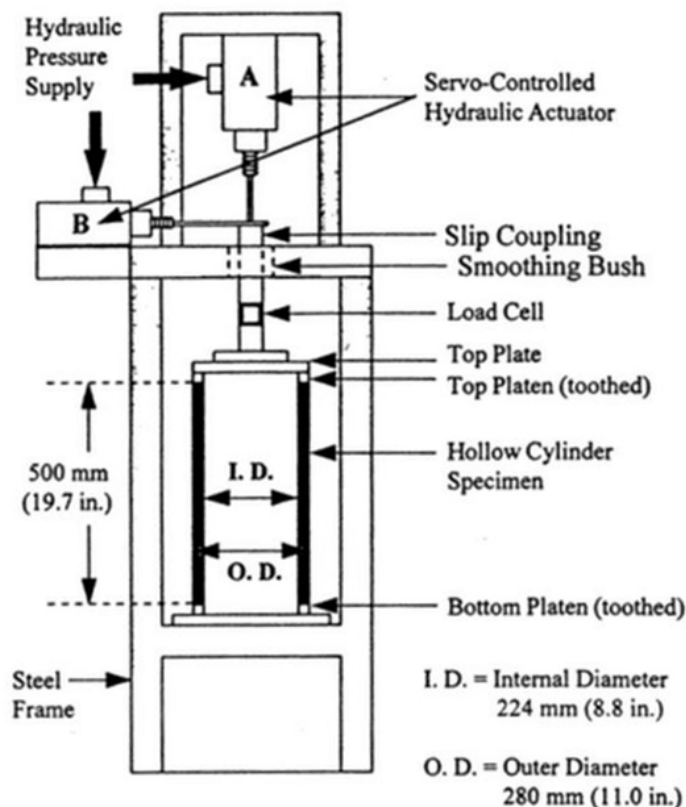


Figure 2.11 Hollow cylinder schematic layout (Thom and Dawson, 1989)

#### 2.3.2.1.4 Simple shear test

The simple shear test simulates the real condition that subsoil receives from the traffic wheel loading. After preparing a soil specimen into the mold, the shear stress will be applied alternatively in each direction both top part and bottom part of the specimen as shown in Figure 2.12.

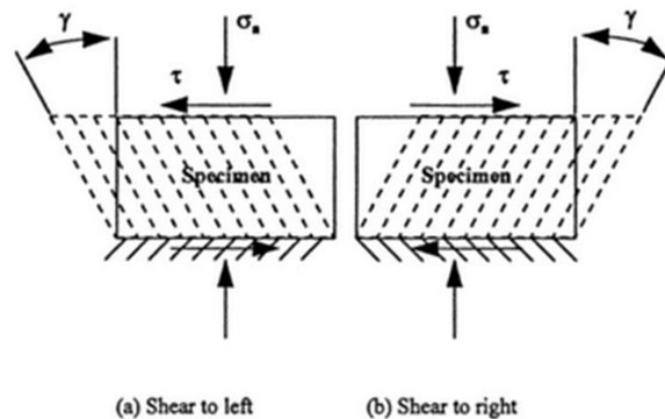


Figure 2.12 Operation of the Simple Shear test (Barksdale et al., 1997)

#### 2.3.2.2 Field methods

Various methods can be used to determine the resilient modulus value in the field. These methods are roughly separated into two types which are nondestructive and destructive methods. This section briefly presents both methods as follows:

##### 2.3.2.2.1 Dynaflect

The Dynaflect is a two-wheel towed trailer that applies load to the considered pavement by its two counter-rotating steel weights. The total applied load is a combination of the dynamic loads created by the two steel weights and the weight of the trailer itself. After the load is applied, a set of five geophones inside the Dynaflect



will detect the pavement deflection. This deflection data is used to determine the resilient modulus.

#### 2.3.2.2.2 Falling weight deflectometer

The falling weight deflectometer (FWD) is performed by applying an impulse load on the pavement surface, and simultaneously measures the pavement deflection at various longitudinal distances from the point of impulse load. This test has many benefits such as cost-effectiveness, nondestructive method, short duration, testing under in-situ condition, and can be designed to cover an interested area. The assumption behind this test is that the impulse load is considered as a static load applying to an elastic body (Kim et al., 2006). Equation 2.7 shows how to calculate the weight of the falling mass.

$$W_1(H + \delta_{max}) - 0.5 K \delta_{max}^2 = 0 \quad (2.7)$$

where  $W_1$  = weight corresponding to the mass M,  $H$  = height that mass M was dropped from,  $\delta_{max}$  = maximum pavement deflection, and  $K$  = spring constant. Also, the impulse load is calculated by using Equation 2.8.

$$P_{dyn} = W_1 \left\{ 1 + \left[ 1 + \left( \frac{2H}{\delta_{st}} \right) \right]^{0.5} \right\} \quad (2.8)$$

where  $P_{dyn}$  = impulse load, and  $\delta_{st}$  = static deflection. However, since the difficulty of determining an impulse load, force (F) is calculated by multiplying weight by height as shown in Equation 2.9.

$$F = WH \quad (2.9)$$

Thus, the uniformly distributed load (q) can be derived from Equation 2.10.

$$q = \frac{F}{A} \quad (2.10)$$

where  $A$  = loading plate area.

The deflection measured under different impulse loads will be used to analyze by various theoretical models in order to determine the resilient modulus.

### 2.3.2.2.3 GeoGauge

The GeoGauge is an instrument which applies loads to the soil by a harmonic oscillator with a frequency about 100–196 Hz. Soil stiffness properties can be obtained from the measurement of both displacement and applied forces. The final soil stiffness value is an average of the stiffness values obtained from 25 frequencies (Lenke et al., 2001). Figure 2.13 shows the GeoGauge schematic layout.

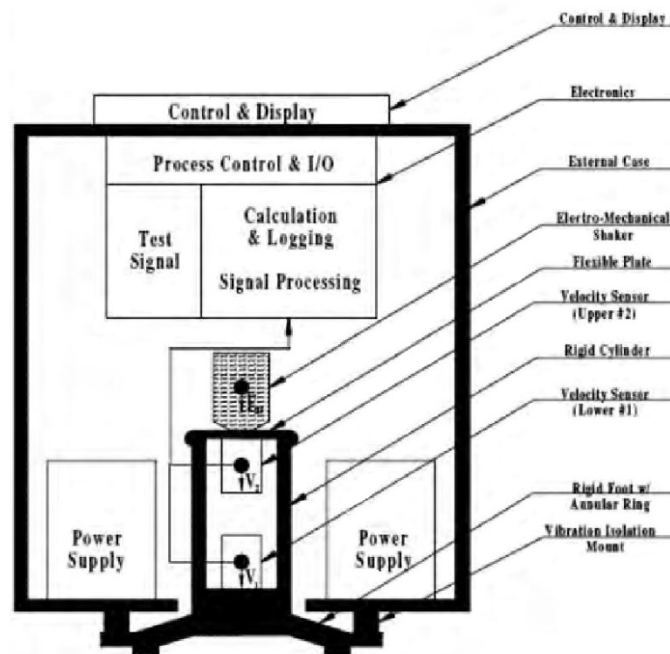


Figure 2.13 GeoGauge schematic layout (Lenke et al., 2001)

#### 2.3.2.2.4 Seismic pavement analyzer

According to Nazarian et al. (1995, 2003, 2005), the seismic pavement analyzer (SPA) has been designed to monitor both construction and deterioration of the pavement layers. Two hammers which are attached at the lower part of the SPA are used to induce surface deformations that will be recorded by the geophones and accelerometers as shown in Figure 2.14. Then the analyzer software that receives information from the geophones and accelerometers will determine the related soil moduli and shear wave velocities. Test procedure takes only about one minute which is relatively short duration.

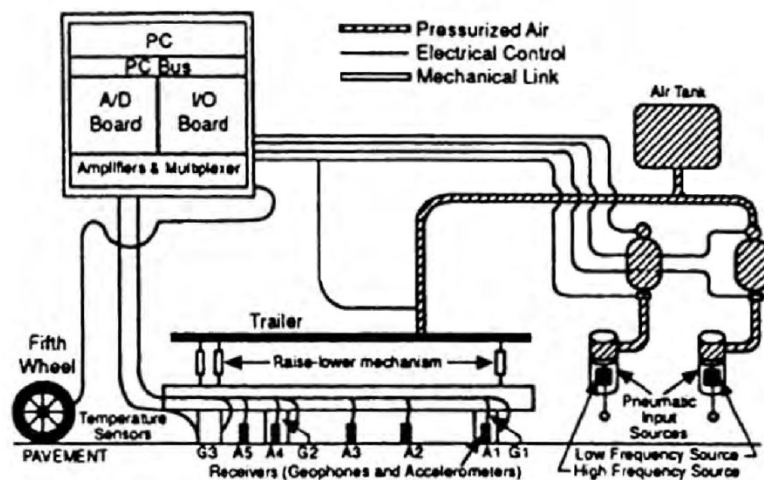


Figure 2.14 Seismic pavement analyzer schematic layout (Nazarian et al., 1995)

#### 2.3.2.2.5 Dynamic cone penetrometer

The dynamic cone penetrometer (DCP) consists of a hammer at the top half, and measurement scales at the bottom half as shown in Figure 2.15. The slender shaft is driven into the pavement layers by the weight of the falling hammer at the same

time the rate of penetration is measured until reaching the designed depth (ASTM D6951-03 Standard). The measured data will be converted to a penetration index which is referred to as a dynamic cone resistance ( $q_d$ ) or DCP index (DCPI).

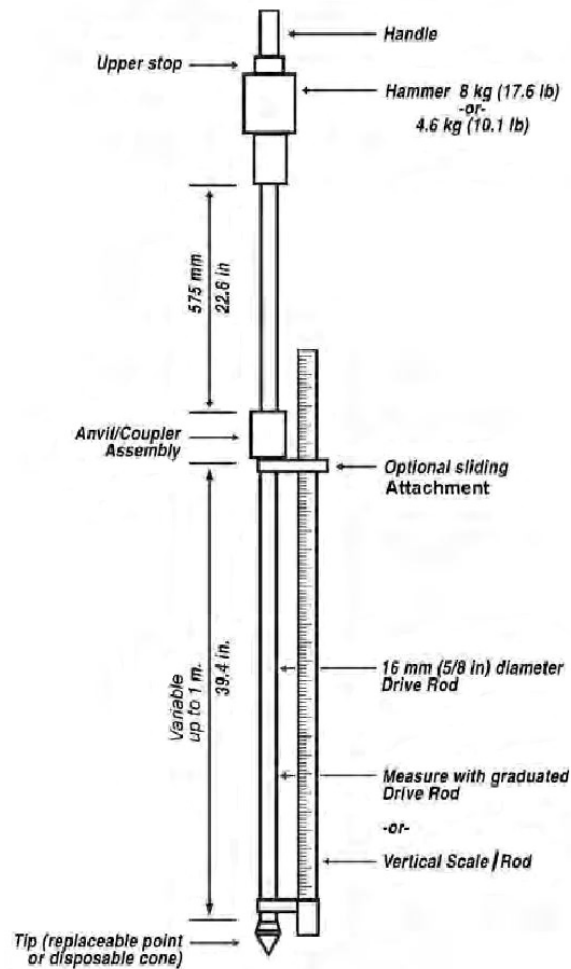


Figure 2.15 Dynamic cone penetrometer schematic layout

(ASTM D6951-03 Standard)

To obtain the resilient modulus value, Hassan (1996) proposed a correlation of the resilient modulus value with a DCPI parameter as shown in Equation 2.11.

$$M_R = 7013.0 - 2040.8 \ln(DCPI) \quad (2.11)$$

where  $M_R$  is in psi, and  $DCPI$  is in inches per blow. However, this correlation is only valid for testing at the original site with compaction moisture content on the wet side of optimum.

George and Uddin (2000) stated a correlation between a DCP index and the resilient modulus of fine-grained and coarse-grained subgrades in Equation 2.12 and 2.13 respectively.

$$M_R = 532.1 \times DCPI^{-0.49} \quad (2.12)$$

$$M_R = 235.3 \times DCPI^{-0.48} \quad (2.13)$$

where  $M_R$  is in MPa, and  $DCPI$  is in millimeters per blow.

Chen et al. (2007) also provided a resilient modulus correlation based on their studies since 2001 (Chen et al., 2001), which covers both base and subgrade soils, in Equation 2.14.

$$M_R = 78.05 \times DPI^{-0.67} \quad (2.14)$$

where  $M_R$  is in ksi, and  $DPI$  is in millimeters per blow.

#### 2.4.2.2.6 Cone penetration test

The cone penetration test (CPT) is a destructive method using an instrumented cone to penetrate through the soil layers. It was first developed by Dutch Laboratory for Soil Mechanics in 1950s. Because of this reason, the initial name of this test is given as “Dutch cone test.” The conventional test results give three main parameters which are cone tip resistance ( $q_c$ ), cone frictional resistance ( $f_s$ ), and total pore pressure ( $u_t$ ). Nowadays, various interpretation and correlation theories have been

produced. According to Mohammad et al. (2000, 2002, and 2007), the research that provided the correlation between CPT results and the resilient modulus was presented. CPTs were performed by using both miniature and large types of cones at the heavy clay material site. Resilient modulus tests were also performed in order to find a relationship with CPT results. Two correlation models were generated. The first model represented in-situ subgrade conditions as shown in Equation 2.15. The second model represented overburden and traffic conditions as shown in Equation 2.16.

$$\frac{M_R}{\sigma_c^{0.55}} = \frac{1}{\sigma_v} \left( 31.8 \times q_c + 74.8 \times \frac{f_s}{w} \right) + 4.08 \times \frac{\gamma_d}{\gamma_w} \quad (2.15)$$

$$\frac{M_R}{\sigma_c^{0.55}} = \frac{1}{\sigma_v} \left( 47.0 \times q_c + 170.4 \times \frac{f_s}{w} \right) + 1.70 \times \frac{\gamma_d}{\gamma_w} \quad (2.16)$$

where  $M_R$  is in MPa,  $q_c$  = cone resistance (MPa),  $f_s$  = cone frictional resistance (MPa),  $\sigma_c$  = vertical stress (kPa),  $w$  = water content (in decimal number format),  $\gamma_d$  = dry unit weight (kN/m<sup>3</sup>), and  $\gamma_w$  = unit weight of water (kN/m<sup>3</sup>).

#### 2.3.2.2.7 Pressuremeter

The pressuremeter (PMT) has two major components which are the probe and read-out unit. PMTs can be classified into prebored PMTs, push-in PMTs, and self-bored PMTs based on the method of installation. By inserting a pressuremeter probe into the borehole at the considered depth, the probe which is an inflatable membrane will expand corresponding to the applied pressure and generate displacements that will be recorded. The obtained pressure-strain profiles can be used to determine the in-situ strength and compressibility characteristics of soil.

To find the resilient modulus, Cosentino and Chen (1991) proposed the adapted PMT procedure and named as “Resilient Modulus PMT Test.” According to the procedure, six unload-reload cycles are performed in order to determine six resilient modulus values from several load durations along the in situ stress-strain response as shown in Figure 2.16. The total test duration is 17 minutes and the recorded cycles for obtaining the resilient modulus values are 10, 20, 30, 60, 120, and 240 seconds. Various cycle lengths were designed to appropriately simulate the real traffic conditions.

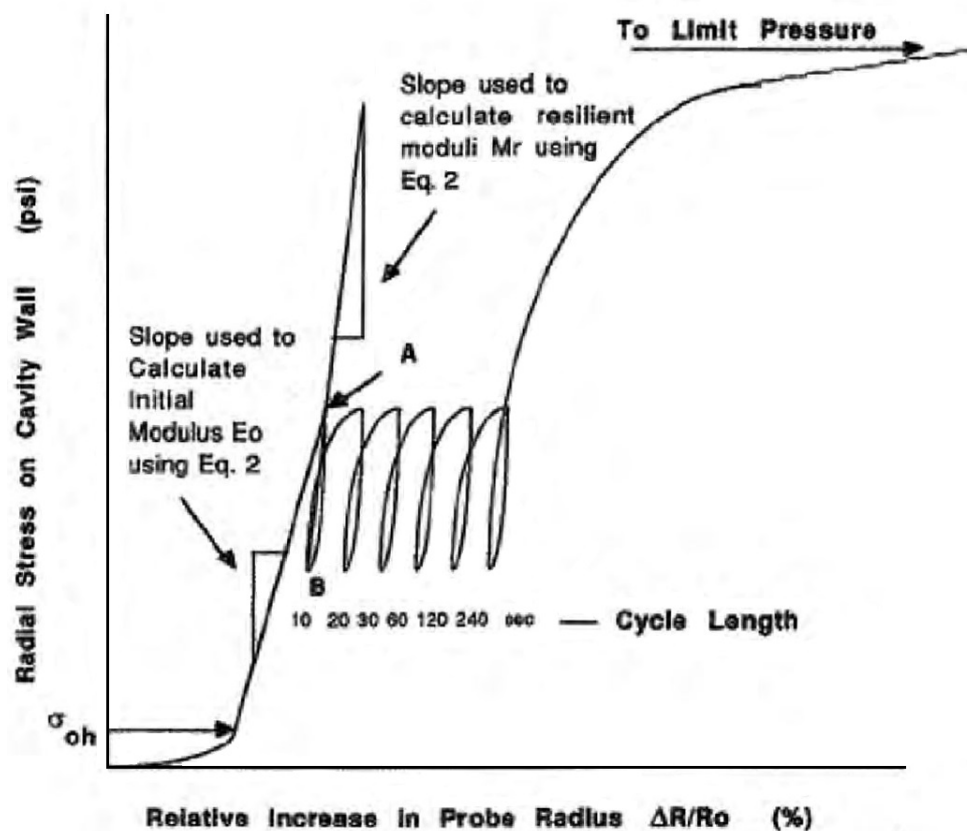


Figure 2.16 Resilient modulus measurements of PMT (Cosentino and Chen, 1991)

#### *2.3.2.2.8 Plate load test*

The plate load test (PLT) is operated by compressing a circular or equivalent rectangular plate to the attached soil layer by a hydraulic jack. The deflections from the applied load are measured and used to determine the soil modulus, which is  $E_{PLT}$ . When the test is performed cyclically, the stress-strain results can be used to specify the resilient modulus (Nelson et al., 2004).

#### *2.3.2.3 Direct correlation methods*

Since the first introduction of the resilient modulus in 1986 by H.C. Seed, several efforts have been made to create a relationship between the resilient modulus and basic soil parameters, which are easier to determine. This section will present various literatures based on the correlation between the resilient modulus and three main parameters; CBR, R-value, and basic soil properties.

##### *2.3.2.3.1 Correlation between CBR and $M_R$*

The California Bearing Ratio (CBR) test was developed in the 1930s before World War II by the California Department of Transportation and became a well-known method after the end of the war (Huang, 2004). The concept of the CBR test is to determine the penetration resistance of soils referred to the standard crushed rock. CBR tests can be categorized into two groups, laboratory and field tests with respect to the ASTM D 1883 and ASTM D 4429 standards, respectively. Although it has been categorized into two groups, the test procedure remains the same. The test is performed by penetrating a standardized piston into the soil. Then the pressure that the piston uses to penetrate until reaching the required depth is measured. To



determine the CBR, the measured pressure from the soil is divided by the measured pressure obtained from the standard crushed rock as shown in Equation 2.17.

$$CBR = \frac{p}{p_s} \times 100 \quad (2.17)$$

where CBR is in percentage,  $p$  is the measured pressure from the soil ( $\text{N}/\text{mm}^2$ ), and  $p_s$  is the measured pressure from the standard crushed rock ( $\text{N}/\text{mm}^2$ ).

As to the correlation between the CBR and resilient modulus, Heukelom and Klomp (1962) started developing the in-situ CBR results that correlated with dynamic modulus measurements. Although it was not determined directly from the repeated load triaxial test, the study has been referred by several literatures (Asphalt Institute, 1982; Drumm et al., 1990; Witczak et al., 1995; Sukumaran et al., 2002; Puppala, 2008) as shown in Equation 2.18.

$$M_R = 1.5 \times CBR \quad (2.18)$$

where  $M_R$  is in ksi, and CBR is determined from fine-grained soils with a CBR range from 10 or less.

Similar to the previous correlation, Green & Hall (1975) provided a correlation as shown in Equation 2.19 which is based on the in-situ CBR values and wave propagation measurements.

$$M_R = 5.409 \times CBR^{0.711} \quad (2.19)$$

where  $M_R$  is in ksi, and CBR is in a range between 2 and 200.

In the same way, Powell et al. (1984) developed a correlation based on in-situ CBR tests and wave propagation measurements as shown in Equation 2.20 for the

structural design method of asphalt roads in the United Kingdom. The authors also used data collected by Jones (1958) in this correlation.

$$M_R = 2.554 \times CBR^{0.64} \quad (2.20)$$

where  $M_R$  is in ksi, and  $CBR$  is in a range between 2 and 12.

According to Lofti (1984) and Lofti et al. (1988), a correlation between the resilient modulus and CBR was developed using repeated load triaxial (RLT) tests and laboratory CBR tests. The tests were performed on fabricated pulverized kaolinite clay at 13 different moisture-density types with a confining pressure ( $\sigma_3$ ) of 3 psi and different deviatoric stress ( $\sigma_d$ ) including 3, 5, 10, 15, 20, 40, and 80 psi. In addition, the measured data from Barker (1982) were included in determining of the correlation as shown in Equation 2.21.

$$\log M_R = 1.0016 + (0.043 \times CBR) - 1.9557 \left( \frac{\log \sigma_d}{CBR} \right) - 0.1705 \log \sigma_d \quad (2.21)$$

where  $M_R$  is in ksi,  $CBR$  is in a range between 2 and 21, and  $\sigma_d$  is in psi.

Several state departments of transportation generated their own correlations based on their literatures. For example, the Ohio Department of Transportation (ODOT) provided a correlation between the resilient modulus and CBR value, which was estimated from the group index (GI) of the soil. After determining the CBR value, the resilient modulus is estimated by the Equation 2.22 (ODOT, 2008).

$$M_R = 1.2 \times CBR \quad (2.22)$$

where  $M_R$  is in ksi, and  $CBR$  is in a range between 3 and 12.

In South Africa, the South African Council on Scientific and Industrial Research (CSIR) also developed a correlation from laboratory CBR tests to determine the resilient modulus as shown in Equation 2.23 (Witczak et al., 1995; Sukumaran et al., 2002).

$$M_R = 3.0 \times CBR^{0.65} \quad (2.23)$$

where  $M_R$  is in ksi, but there is no information about the CBR range.

#### 2.3.2.3.2 Correlation between R-Value and $M_R$

The R Value test or Stabilometer was first developed by the California Division of Highways in order to use with the pavement design method. According to the ASTM D 2844 standard, the test purpose is to determine the suitability of the material being use under paved roads. The cylindrical soil specimen is placed in a Hveem Stabilometer device and then compression will be applied. The annular space inside the Stabilometer is filled with oil in order to transfer lateral pressure to the soil specimen. Under the compression, the occurred horizontal pressure is measured by the Stabilometer. The R-value is a measured resistance to deformation as shown in Equation 2.24. Figure 2.17 also shows the Stabilometer test schematic layout.

$$R = 100 - \frac{100}{\left(\frac{2.5}{D_2}\right) \left[\left(\frac{P_v}{P_h}\right) - 1\right] + 1} \quad (2.24)$$

where  $R$  is the resistance value,  $P_v$  = applied vertical pressure (160 psi),  $P_h$  = transmitted horizontal pressure, and  $D_2$  = number of turns of the screw (to inject fluid oil into the specimen chamber).

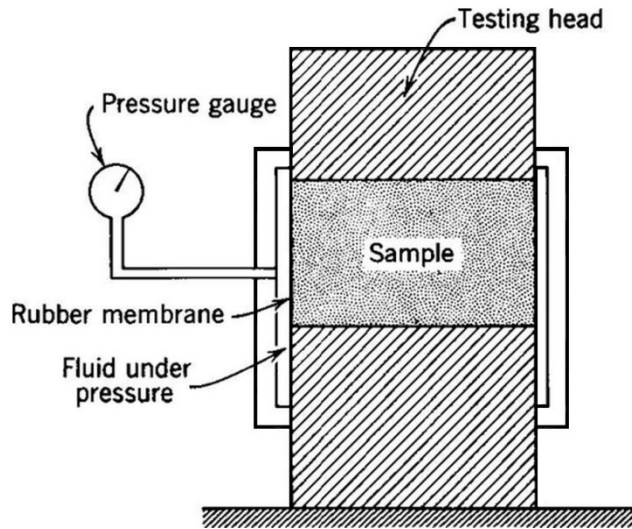


Figure 2.17 Stabilometer test schematic layout (Yoder and Witczak, 1975)

To correlate the R-value with the resilient modulus, several literatures have been generated. Starting from the Asphalt Institute (1981, 1982), since many state departments of transportation did not have an RLT test equipment which was recommended by the institute, hence the institute design method provided two correlations as shown in Equation 2.25 and 2.26.

$$M_R = 0.772 + 0.369 \times R \quad (2.25)$$

$$M_R = 1.155 + 0.555 \times R \quad (2.26)$$

where  $M_R$  is in ksi, and R-value in this correlation was developed from road tests in San Diego, California.

According to the information provided by the institute, Equation 2.26 is more appropriate when the R-value is lower than 21. However, for the R-value that is more than 60, the resilient modulus value obtained from both correlations tends to be overestimated.

As to the state departments of transportation, correlations between the R-value and resilient modulus have been found in many state pavement design manuals. Beginning with the Idaho Transportation Department (ITD), Buu (1980) reported that the RLT tests were performed at the University of Idaho and the R-value tests were performed at ITD headquarters in Boise, Idaho. Two correlations were generated as shown in Equation 2.27 and 2.28 (Yeh and Su, 1989). Equation 2.27 was developed for fine-grained soils with R-values between 46 and 68 and Equation 2.28 was developed for coarse-grained soils with R-values between 9 and 82.

$$M_R = 1.455 + 0.057 \times R \quad (2.27)$$

$$M_R = 1.600 + 0.038 \times R \quad (2.28)$$

where  $M_R$  is in ksi.

For the Colorado Department of Transportation (CDOT), Yeh and Su (1989) developed a correlation between R-value and the resilient modulus with soil ranges from cohesionless to cohesive soils. The RLT tests were conducted with respect to the AASHTO T 274 standard, and the R-value tests were conducted with respect to CDOT's method. Equation 2.29 shows the correlation that was tested at a deviatoric stress of 6 psi and a confining pressure of 3 psi.

$$M_R = 3.5 + 0.125 \times R \quad (2.29)$$

where  $M_R$  is in ksi.

For the Washington Department of Transportation (WSDOT), Muench et al. (2009) provided a correlation between R-value and the resilient modulus with soil

ranges from coarse to silty and clay materials. The R-value was tested at an exudation pressure of 400 psi with respect to WSDOT's method, and the RLT tests were performed with respect to the AASHTO T 274 standard. Equation 2.30 shows the referred correlation.

$$M_R = 0.72 \times (e^{0.0521 \times R} - 1.0) \quad (2.30)$$

where  $M_R$  is in ksi, and R-value used in this study range from 25 to 75.

#### 2.3.2.3.3 Correlation between soil properties and $M_R$

Many literatures present several correlations based on the resilient modulus and basic soil properties such as moisture content, dry unit weight, clay content, silt content, and plastic index. This section provides some of the correlations listed in chronological order as follows.

According to Jones and Witczak (1972), a correlation of the resilient modulus with the compaction moisture content and degree of saturation was developed by using California clayey soils. The resilient modulus values in this correlation were obtained from the RLT tests with a maximum deviatoric stress of 6 psi and a confining pressure of 2 psi. Equation 2.31 shows the referred correlation.

$$\log M_R = -0.111w + 0.0217S + 1.179 \quad (2.31)$$

where  $M_R$  is in ksi,  $w$  = compaction moisture content (percent), and  $S$  = degree of saturation (percent).

Thompson and Robnett (1979) proposed a correlation between the resilient modulus and basic soil properties of Illinois subgrade soils collected from 50

locations. The RLT tests in this correlation were conducted at a deviatoric stress of 6 psi and zero confining pressure. Equation 2.32 shows this correlation that is valid only for cohesive soils.

$$M_R = 6.37 + 0.034 \times \%C + 0.45 \times PI - 0.0038 \times \%M - 0.244 \times CLASS \quad (2.32)$$

where  $M_R$  is in ksi,  $\%C$  = clay content (percent),  $PI$  = plasticity index,  $\%M$  = silt content (percent), and  $CLASS$  is the AASHTO classification (for clay, use 7.6 in the equation).

Thompson and Robnett (1979) also provided two correlations between the resilient modulus and degree of saturation for soils that were compacted to 95% standard Proctor dry density and 100% standard Proctor dry density as shown in Equation 2.33 and 2.34 respectively.

$$M_R = 32.9 - 0.334 \times S \quad (2.33)$$

$$M_R = 45.2 - 0.428 \times S \quad (2.34)$$

where  $M_R$  is in ksi, and  $S$  = degree of saturation (percent).

Carmichael and Stuart (1985) analyzed a number of the resilient modulus data over the U.S. and developed two correlations between the resilient modulus and basic soil properties for fine-grained soils and coarse-grained soils as shown in Equation 2.35 and 2.36 respectively.

$$M_R = 37.43 - 0.457(PI) - 0.618w - 0.142(p\#200) \\ + 0.179\sigma_3 - 0.325\sigma_d + 36.42(CH) + 17.10(MH) \quad (2.35)$$

$$M_R = 0.523 - 0.0225w + 0.544 \log \sigma_T + 0.173(SM) + 0.197(GR) \quad (2.36)$$

where  $M_R$  is in ksi,  $PI$  = plasticity index,  $w$  = water content (percent),  $p_{\#200}$  = percent passing the #200 sieve,  $\sigma_3$  = confining pressure (ksi),  $\sigma_d$  = deviatoric stress (ksi),  $CH$  = 1 (for CH soil, 0 otherwise),  $MH$  = 1 (for MH soil, 0 otherwise),  $\sigma_T$  = total stress (ksi),  $SM$  = 1 (for SM soil, 0 otherwise), and  $GR$  = 1 (for GM, GW, GC, and GP soils, 0 otherwise).

Thompson and LaGrow (1988) reported a correlation of the resilient modulus with the clay content and plastic index for the Illinois compacted subgrades as shown in Equation 2.35.

$$M_R = 4.46 + 0.098 \times \%C + 0.119 \times PI \quad (2.35)$$

where  $M_R$  is in ksi,  $\%C$  = clay content (percent), and  $PI$  = plasticity index.

Elliott et al. (1988) generated two correlations between the resilient modulus and basic soil properties using Arkansas subgrade soils. Equation 2.36 was developed for  $\sigma_d = 4$  psi, and Equation 2.37 was developed for  $\sigma_d = 8$  psi. Both equations are valid only for cohesive soils.

$$M_R = 11.21 + 0.17\%C + 0.20PI - 0.73w_{opt} \quad (2.36)$$

$$M_R = 9.81 + 0.13\%C + 0.16PI - 0.60w_{opt} \quad (2.37)$$

where  $M_R$  is in ksi,  $\%C$  = clay content (percent),  $PI$  = plasticity index, and  $w_{opt}$  = optimum water content (percent).

Drumm et al. (1990) developed two correlations between the resilient modulus and basic soil properties using Tennessee subgrade soils. The first correlation, Equation 2.38, presents the breakpoint resilient modulus which is the



intersection of the resilient modulus and deviatoric stress by assuming both to be a bilinear relationship. Equation 2.39 presents the breakpoint resilient modulus by assuming both the resilient modulus and deviatoric stress to be a hyperbolic relationship. Both correlations are valid only for a zero confining pressure.

$$M_R = 45.8 + \frac{0.00052}{a} + 0.19 \times q_u + 0.45 \times PI - 0.22 \times \gamma_d - 0.25 \times S - 0.15 \times p\#200 \quad (2.38)$$

$$M_R = \frac{a' + b' \sigma_d}{\sigma_d} \quad (2.39)$$

$$a' = 318.2 + 0.377 \times q_u + 0.73 \times \%C + 2.26 \times PI - 0.92 \times \gamma_d - 2.19 \times S - 0.30 \times p\#200$$

$$b' = 2.10 + \frac{0.00039}{a} + 0.104 \times q_u + 0.09 \times LL - 0.10 \times p\#200$$

where  $M_R$  is in ksi,  $a$  = initial tangent modulus (psi),  $q_u$  = unconfined compressive strength (psi),  $PI$  = plastic index,  $\gamma_d$  = dry unit weight (pcf),  $S$  = degree of saturation (percent),  $p\#200$  = percent passing the #200 sieve,  $\%C$  = clay content (percent), and  $LL$  = liquid limit (percent).

Farrar and Turner (1991) reported a correlation between the resilient modulus and soil properties which include the deviatoric stress and confining pressure as variables within the correlation using Wyoming subgrade soils. The correlation, Equation 2.40, is valid only for fine-grained soils.

$$M_R = 30.280 - 0.359S - 0.325\sigma_d + 0.237\sigma_c + 0.086PI + 0.107(p\#200) \quad (2.40)$$

where  $M_R$  is in ksi,  $S$  = degree of saturation (percent),  $\sigma_d$  = deviatoric stress (ksi),  $\sigma_c$  = confining pressure (ksi),  $PI$  = plastic index, and  $p\#200$  = percent passing the #200 sieve.

Hudson et al. (1994) proposed a correlation between the resilient modulus and soil properties using Tennessee subgrade soils as shown in Equation 2.41. The correlation is valid only for fine-grained soils.

$$\begin{aligned} \log M_R = & 46.93 + 0.018 \times \sigma_d + 0.033 \times \Delta\gamma_d - 0.2222 \times \log \sigma_d \\ & + 0.468 \times S + 0.0085 \times CLASS^2 - 0.0033\Delta w^2 \\ & - 0.0012 \times \sigma_c^2 + 0.0001 \times PL^2 - 0.0278 \times LI^2 \\ & - 0.0017 \times S^2 - 38.44 \times \log S - 0.114 \times LI \end{aligned} \quad (2.41)$$

where  $M_R$  is in ksi,  $\sigma_d$  = deviatoric stress (ksi),  $\Delta\gamma_d$  = deviation from the standard Proctor maximum dry density,  $LI$  = liquidity index (percent),  $S$  = degree of saturation (percent),  $CLASS$  is the AASHTO classification,  $\Delta w$  = deviation from the optimum water content (percent),  $\sigma_c$  = confining pressure (ksi), and  $PL$  = plastic limit.

Rahim and George (2004) provided two correlations between the resilient modulus and basic soil properties using Mississippi subgrade soils. The first correlation, Equation 2.42, was developed for fine-grained soils and the second correlation, Equation 2.43, was developed for coarse-grained soils.

$$M_R = 2.429 \left[ \left( \frac{LL}{w} \times \frac{\gamma_d}{\gamma_{d-s}} \right)^{2.06} + \left( \frac{p\#200}{100} \right)^{-0.59} \right] \quad (2.42)$$

$$M_R = 44.58 \times \left( \frac{\gamma_d}{w} \right)^{0.86} \times \left( \frac{p\#200}{\log C_u} \right)^{-0.46} \quad (2.43)$$

where  $M_R$  is in ksi,  $LL$  = liquid limit,  $w$  = water content (percent),  $\gamma_d$  = in-situ dry density,  $\gamma_{d-s}$  = maximum standard Proctor dry density,  $p\#200$  = percent passing the #200 sieve, and  $C_u$  = uniformity coefficient.

### 2.3.3 Resilient Modulus Prediction Models

In practice, the resilient modulus at various stress states cannot be entirely determined from the laboratory resilient modulus tests. This reason brings mathematical models into the picture. These models correlate the resilient modulus with stresses and/or fundamental soil properties. This section will provide a few models that are widely used.

#### 2.3.3.1 Bulk stress model

Bulk stress defines as the sum of the principal stresses which are  $\sigma_1$ ,  $\sigma_2$ , and  $\sigma_3$ . This model is considered to be more suitable to predict the resilient modulus of granular materials (Titi et al., 2006). The equation of this model is provided as Equation 2.44.

$$M_R = k_1 \theta^{k_2} \quad (2.44)$$

where  $\theta$  is the bulk stress, and  $k_1$  and  $k_2$  are material specific regression coefficients.

According to May and Witczak (1981), this model was improved by adding a factor that account for shear stress/strain and volumetric strain as presented below.

$$M_R = K_1 k_1 \theta^{k_2} \quad (2.55)$$

where  $K_1$  is a function that correlates with pavement structure, applied load, and developed shear strain.

#### 2.3.3.2 Uzan model

According to Uzan (1985), deviatoric stress was included in the model to account for the actual field stress state. The model is presented as Equation 2.56.

$$M_R = k_1 \theta^{k_2} \sigma_d^{k_3} \quad (2.56)$$

where  $k_1$ ,  $k_2$  and  $k_3$  are material specific regression coefficients,  $\theta$  is the bulk stress, and  $\sigma_d$  is the deviatoric stress.

The equation above can be normalized and rewritten as Equation 2.57.

$$M_R = k_1 P_a \left[ \frac{\theta}{P_a} \right]^{k_2} \left[ \frac{\sigma_d}{P_a} \right]^{k_3} \quad (2.57)$$

where  $P_a$  is the atmospheric pressure (101.325 kPa)

As suggested by Uzan, Equation 2.56 and 2.57 can be used for all types of soils. Also, this model can be converted back to the bulk model by assuming  $k_3$  equals to 0.

#### 2.3.3.3 Octahedral shear stress model

Witzak and Uzan (1988) modified the Uzan model by replacing the deviatoric stress with octahedral shear stress. The model is presented as Equation 2.58.

$$M_R = k_1 P_a \left[ \frac{\theta}{P_a} \right]^{k_2} \left[ \frac{\tau_{oct}}{P_a} \right]^{k_3} \quad (2.58)$$

where  $k_1$ ,  $k_2$  and  $k_3$  are material specific regression coefficients,  $P_a$  is the atmospheric pressure (101.325 kPa),  $\theta$  is the bulk stress, and  $\tau_{oct}$  is the octahedral

shear stress  $\left\{ \frac{[(\sigma_1 - \sigma_2)^2 + (\sigma_2 - \sigma_3)^2 + (\sigma_3 - \sigma_1)^2]^{\frac{1}{2}}}{3} \right\}$ .

#### 2.3.3.4 Universal model

The universal model was named by Dai and Zollar (2002) since this model is applicable for all unbound materials and incorporates the effects of both deviatoric

stress and volumetric stress on the resilient modulus. This model was developed through NCHRP project 1-28A and was recommended by the AASHTO Guide for the Design of New and Rehabilitated Pavement Structures. The universal model is presented in Equation 2.59.

$$M_R = k_1 \times P_a \times \left(\frac{\sigma_b}{P_a}\right)^{k_2} \times \left(\frac{\tau_{oct}}{P_a} + 1\right)^{k_3} \quad (2.59)$$

where  $k_1$ ,  $k_2$ , and  $k_3$  are material specific coefficients;  $P_a$  is the atmospheric pressure (101.325 kPa);  $\sigma_b$  is the bulk stress; and  $\tau_{oct}$  is the octahedral shear stress.

#### 2.4 Summary

This chapter is intended to provide background information regarding this research. The chapter begins with the pavement failure caused by poor soils which can be categorized into three types, compressible soils, collapsible soils, and expansive soils. Subsequently, soil stabilization methods are addressed including the main method used in this research, the mechanical stabilization method. As an evaluation parameter of soil improvement, the resilient modulus is later presented. Furthermore, parameters that influence the resilient modulus are stated including types of soil, loading condition, compaction method, moisture content, density, soil index properties, thixotropy, and freeze-thaw. Several methods of resilient modulus measurement are also presented. The repeated load triaxial (RLT) test is selected as a method employed in this research. The last section provides information about resilient modulus models. The universal model is chosen to predict the resilient modulus results in this research.

## Chapter 3

### Experimental Program

#### 3.1 Introduction

The experimental program for the current research involves basic soil characterization and assessment of strength improvement. This chapter contains the procedural details and fundamental test results that are implicated in the clay-sand mixtures. The UCS and resilient modulus test procedures are presented in accordance with the ASTM D 2166 standard and AASHTO T 307-99 standard, respectively. In addition, apparatus details employed in the resilient modulus test are also stated.

#### 3.2 Laboratory Testing Program

##### *3.2.1 Physical Soil Properties*

The reference clay was collected from Dallas, Texas; the coarse sand used as an admixture in this research is industrial silica sand with grain size ranging between 0.92–0.95 mm. The coarse sand has a coefficient of uniformity ( $C_u$ ) of 1.016 and coefficient of curvature ( $C_c$ ) of 1.005. To determine the basic soil properties of Dallas clay, the following tests were performed.

##### 3.2.1.1 Particle size analysis

Particle size analysis consists of sieve and hydrometer analysis in accordance with the ASTM D 422 standard. First, wet sieve analysis was performed in order to know the percent of soil retained on No.200 sieve which was then used to perform a dry sieve analysis test. Second, hydrometer analysis was performed using the soil that

passed through No. 200 sieve to determine the percent finer of soil corresponding to the particle size. Both tests are presented as a particle size distribution curve in Figure 3.2.

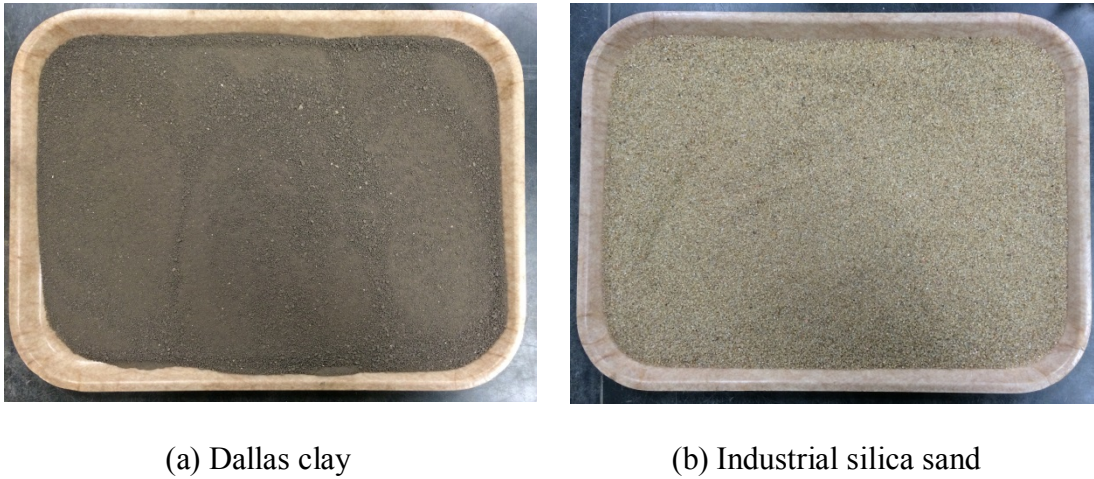


Figure 3.1 Pictures of soils using in this research

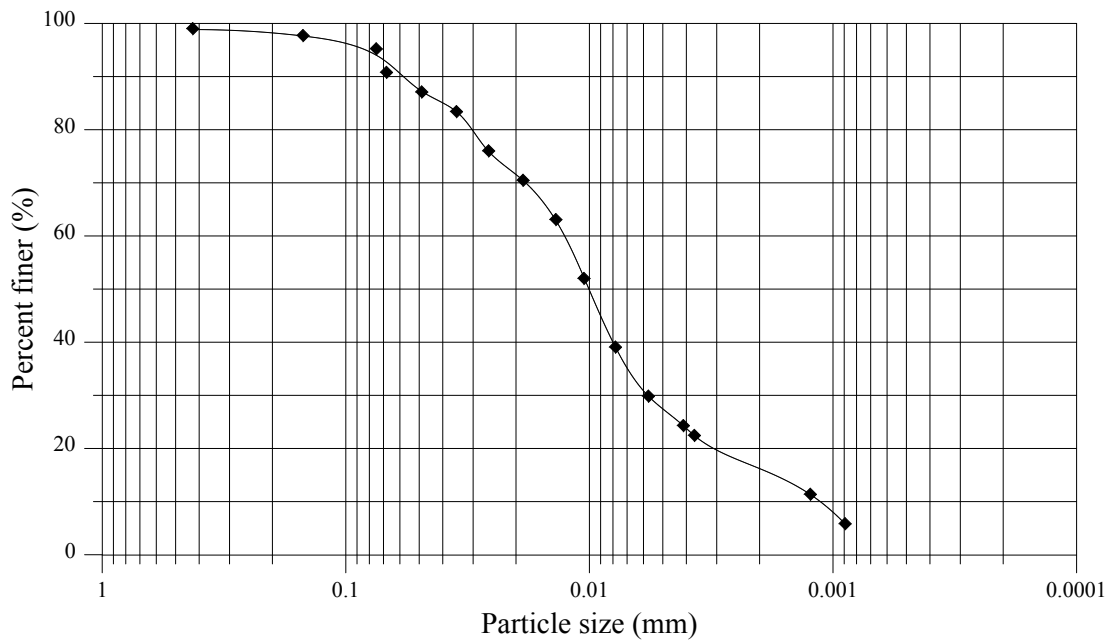


Figure 3.2 Particle size distribution of Dallas clay

### 3.2.1.2 Atterberg limits

Atterberg limits are based on the moisture content of soils in order to classify the soil type. In this research, liquid limit and plastic limit were determined with respect to the ASTM D 4318 standard. Liquid limit is defined as the moisture content (in percent) at which the soil changes from a liquid state to a plastic state. Plastic limit is defined as the moisture content (in percent) at which the soil changes from a plastic state to a semi-solid state. Both liquid limit and plastic limit of Dallas clay are presented in Table 3.1.

### 3.2.1.3 Specific gravity

Specific gravity is expressed as the ratio of the considered soil density to the density of distilled water which has an equal volume to the considered soil. The test was performed in accordance with the ASTM D 854 standard. The specific gravity result of Dallas clay is presented in Table 3.1.

Table 3.1 Physical properties of Dallas clay

<b>Physical Soil Property</b>	<b>Dallas Clay</b>
Percent Passing No. 200 Sieve	96
USCS Classification	CH
Liquid Limit, LL	58
Plastic Limit, PL	24
Plasticity Index, PI	34
Specific Gravity, $G_s$	2.79



### 3.2.2 Clay-Sand Mixtures

According to the mechanical stabilization method, the native soil is mixed with a coarse material in order to improve the overall soil properties as detailed in the previous chapter. Therefore, this research performed six types of clay-sand mixtures by inclusion of Dallas clay and industrial silica sand of 0, 5, 10, 20, 30, and 50 percent by weight of the total mixture as illustrated in Figure 3.3.

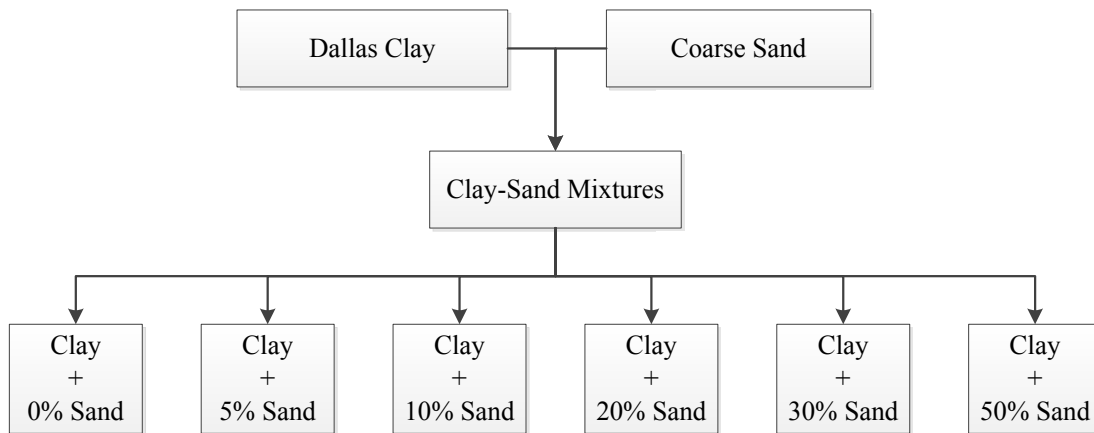


Figure 3.3 Flowchart of the clay-sand mixtures

### 3.2.3 Standard Proctor Compaction Test

In general, a subgrade soil is compacted to approximately reach its maximum dry density and optimum moisture content in order to improve soil strength. To determine the maximum dry density and optimum moisture content value of each clay-sand mixture, standard Proctor compaction tests were conducted in accordance with the ASTM D 698 standard. Table 3.2 shows a summary of the test specifications; Figure 3.4 shows the test procedures. Test results of the clay-sand mixtures are presented thereafter.

Table 3.2 Standard Proctor compaction specifications (ASTM D 698 Standard)

Volume of mold	1/30 ft <sup>3</sup> (943 cm <sup>3</sup> )
Height of mold	4.584 in. (116.43 mm)
Diameter of mold	4 in. (101.6 mm)
Weight of hammer	5.5 lb (24.4 N)
Height of hammer drop	12 in. (304.8 mm)
Number of layers	3
Number of blows per layer	25



(a) Preparation of soil and equipment



(b) Compaction process



(c) Mold after compaction



(d) Sample and mold after extrusion

Figure 3.4 Standard Proctor compaction procedure

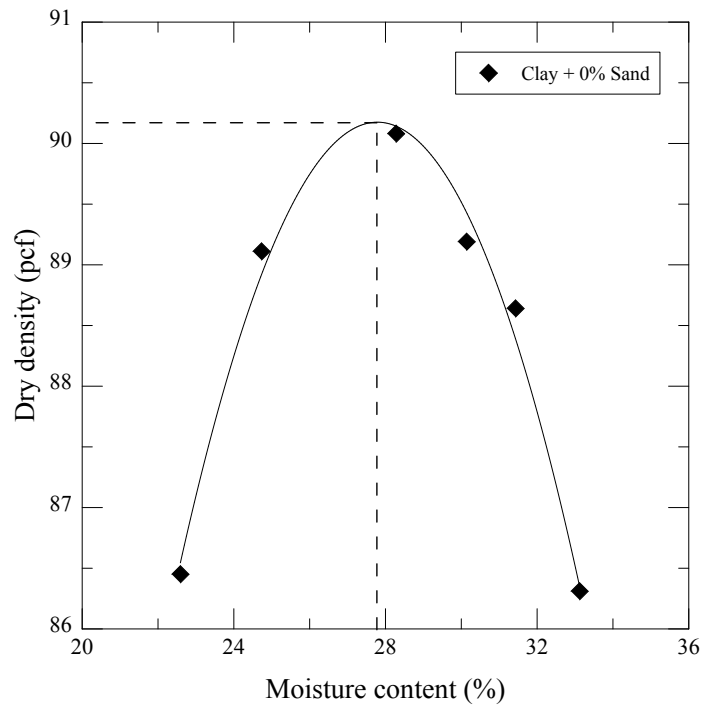


Figure 3.5 Compaction curve of Dallas clay with no sand admixture

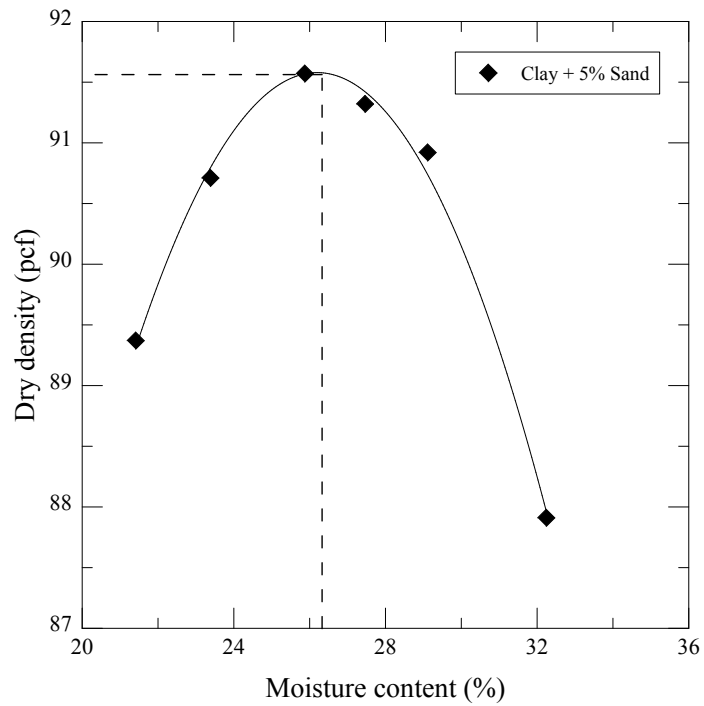


Figure 3.6 Compaction curve of Dallas clay with 5% sand admixture

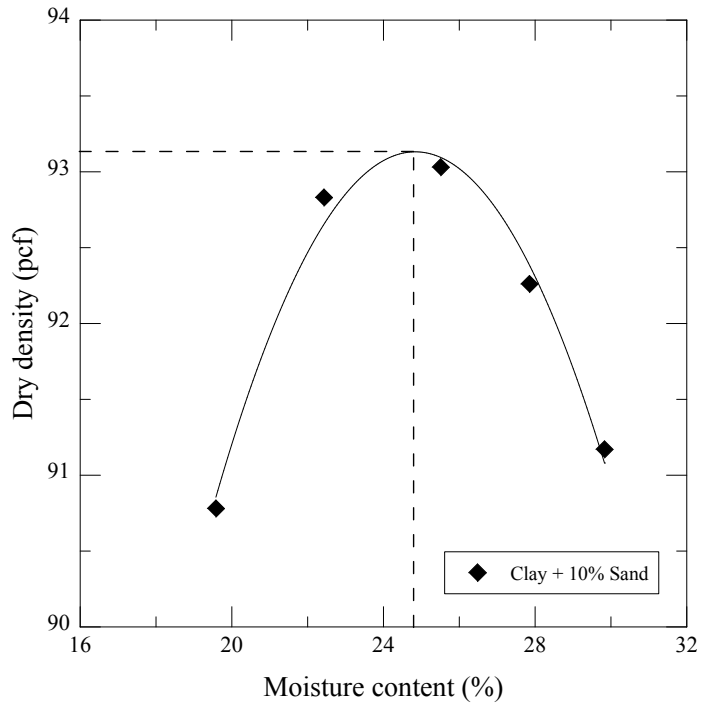


Figure 3.7 Compaction curve of Dallas clay with 10% sand admixture

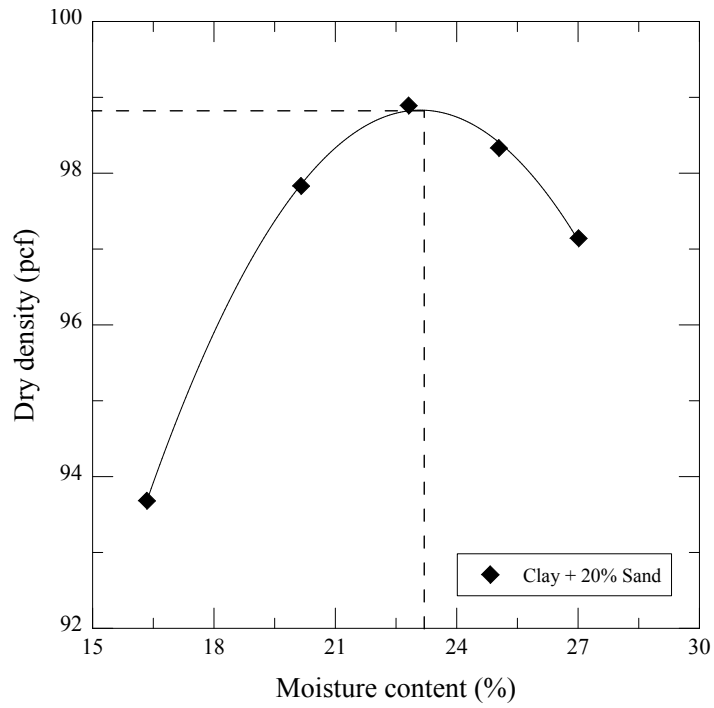


Figure 3.8 Compaction curve of Dallas clay with 20% sand admixture

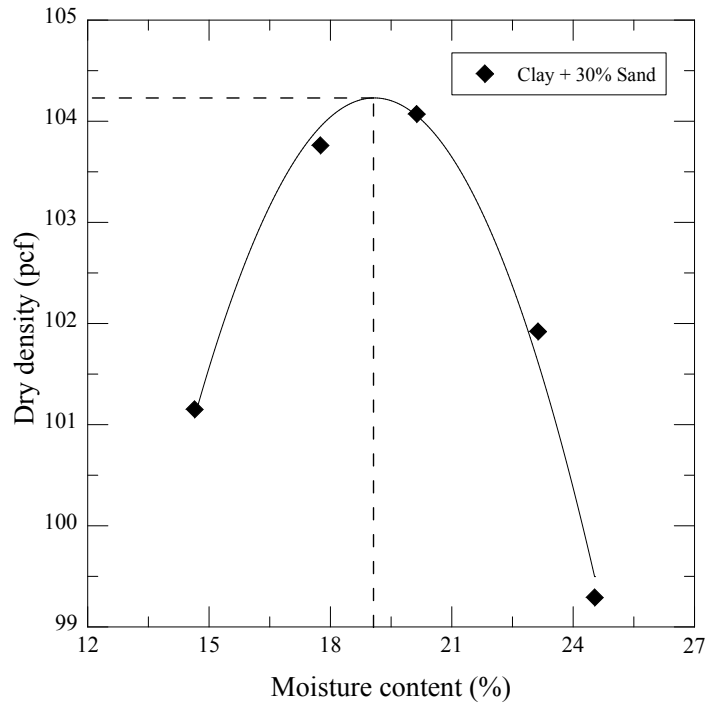


Figure 3.9 Compaction curve of Dallas clay with 30% sand admixture

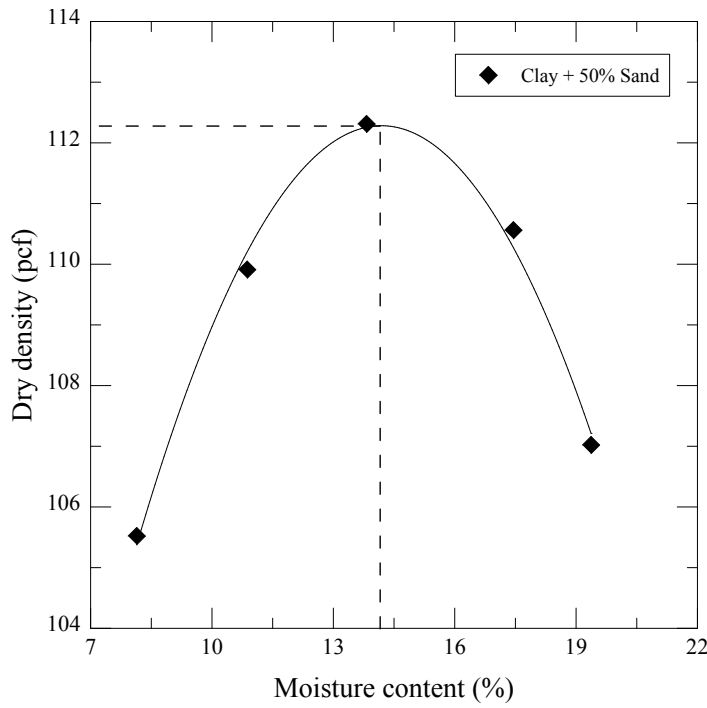


Figure 3.10 Compaction curve of Dallas clay with 50% sand admixture

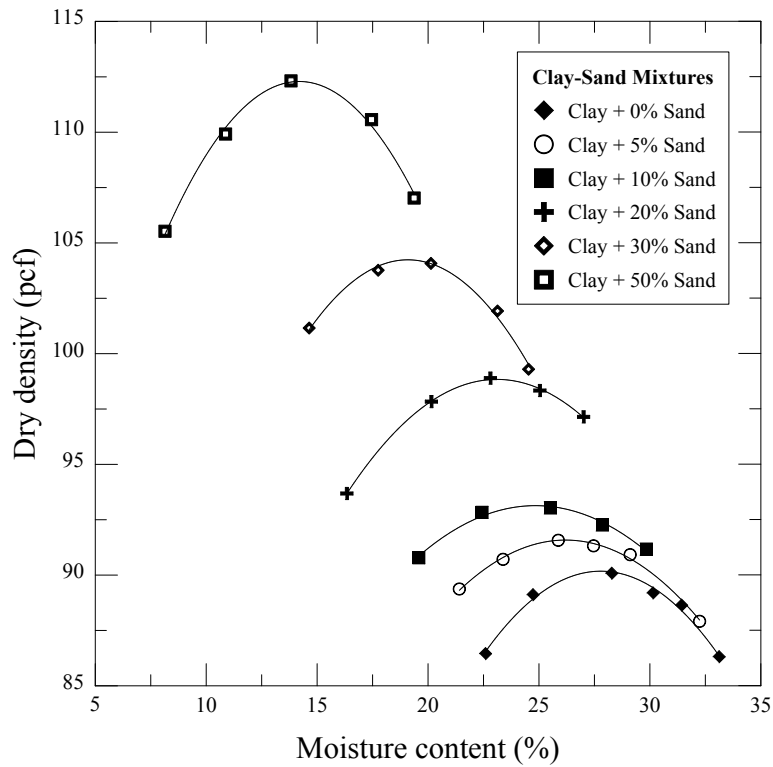


Figure 3.11 Total compaction curves of the clay-sand mixtures

Table 3.3 Summary of standard Proctor compaction results

Soil Mixture Type	Maximum Dry Density (pcf)	Optimum Moisture Content (%)
Clay	90.2	27.8
Clay + 5% Sand	91.6	26.2
Clay + 10% Sand	93.2	24.9
Clay + 20% Sand	98.8	23.1
Clay + 30% Sand	104.2	19.1
Clay + 50% Sand	112.3	14.2

### 3.2.4 Unconfined Compressive Strength Test

As an alternative method of soil strength measurement together with the resilient modulus test, the unconfined compressive strength (UCS) test was also

performed in this research. According to the ASTM D 2166 standard, the primary purpose of UCS test is to quickly obtain a compressive strength for soils that possess sufficient cohesion to allow testing in the unconfined state. The test procedure begins with placing a soil specimen on the loading platform before raising it until the top cap touches the top plate. After setup the triaxial test equipment, the test is done by lifting the specimen at a constant rate while the external LVDT (Linear Variable Displacement Transducer) and load cell measure the applied loads and displacement, respectively. The obtained maximum axial stress is an unconfined compressive strength of the soil specimen. Figure 3.12 shows the unconfined compressive strength equipment employed in this research.

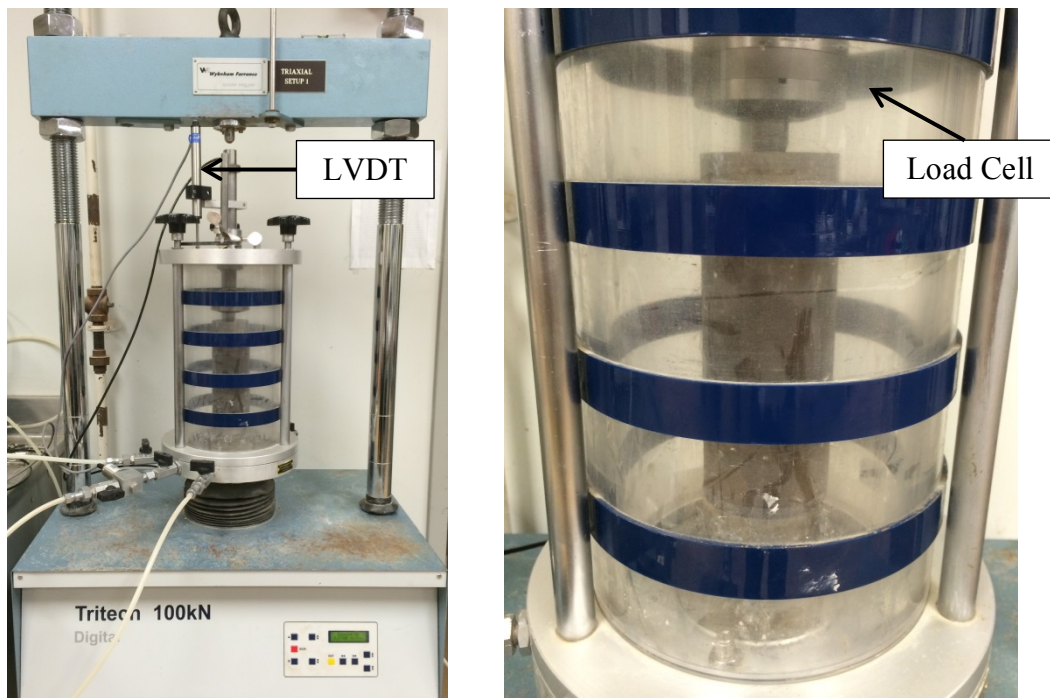


Figure 3.12 Unconfined compressive strength equipment

### *3.2.5 Repeated Load Triaxial Test*

To evaluate the soil strength increase by adding the coarse particles, the resilient modulus parameter was selected. In this research, the repeated load triaxial test was chosen as a method of resilient modulus measurement. This section will present information related to the repeated load triaxial test including sample preparation, apparatus details, and test procedures.

#### 3.2.5.1 Resilient modulus sample preparation

According to the AASHTO T 307-99 standard, Dallas clay is a Type 2 material which can be compacted using a static compaction method. In addition, the AASHTO standard also provided resilient modulus sampling procedures as presented below.

1. Prepare a soil mixture following its maximum dry density and optimum moisture content. Since the specimen has a diameter of 2.8" and height of 5.6", the total specimen volume can be calculated. From the maximum dry density and volume, the required soil mass can be measured.
2. Divide the prepared soil mass into five equal portions and fill the first soil portion into the mold which has a bottom plug placed inside.
3. Place a top plug into the mold and compact the soil by using a static loading machine until the compacted soil height reaches 1.12".
4. Take a top plug out and fill the second soil portion into the mold, and then place a top plug into the mold again.
5. Compact the soil until the compacted soil height reaches 2.24".



6. Take a top plug out and turn the mold upside down.
7. Fill the third soil portion into the mold, and then place a top plug into the mold again.
8. Compact the soil until the compacted soil height reaches 3.36".
9. Redo the process 6, 7, and 8 until the height of soil becomes 4.48", and 5.6" respectively.

The resilient modulus sampling procedures are illustrated in Figure 3.13 and Figure 3.14.

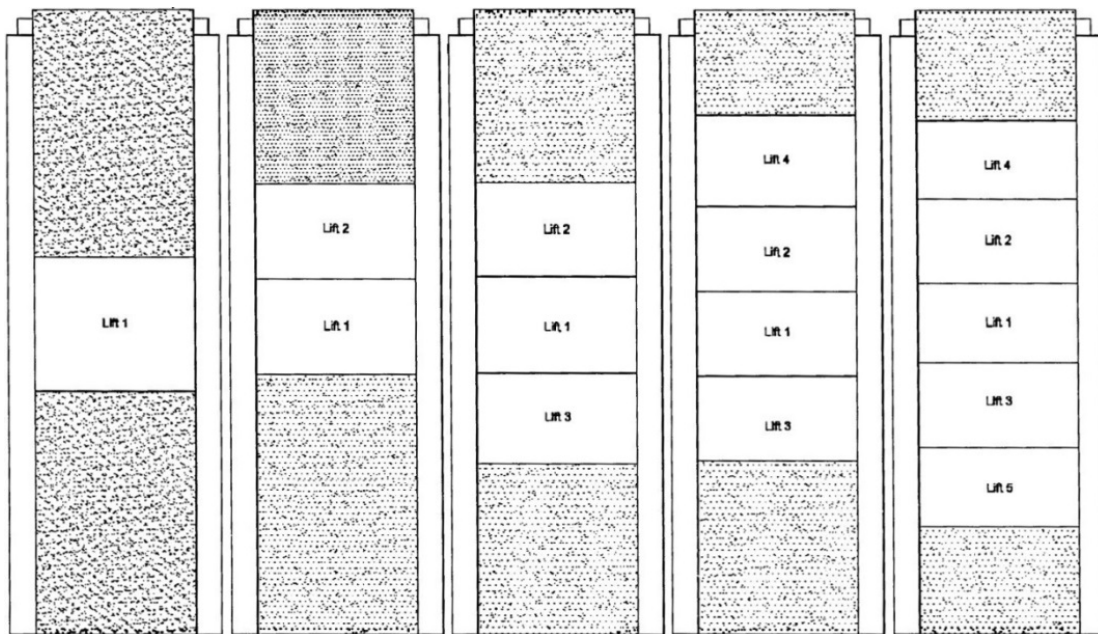


Figure 3.13 Soil specimen compaction steps from Lift 1 to Lift 5

(AASHTO T 307-99 Standard)



(a) Preparation of the soil mixture



(b) Compaction process (five layers)



(c) Mold set up at the sample extruder



(d) Soil specimen extrusion

Figure 3.14 Soil specimen preparation for the repeated load triaxial test

### 3.2.5.2 Cyclic triaxial system components

The resilient modulus apparatus employed in this research is the Universal Cyclic Triaxial System as shown in Figure 3.15. The apparatus consists of seven major components; triaxial load frame, pneumatic actuator, Integrated Multi-Axis Control System (IMACS), auxiliary air reservoir, water distribution panel, triaxial cell and submersible load cell, and Linear Variable Displacement Transducers (IPC Global, 2011).

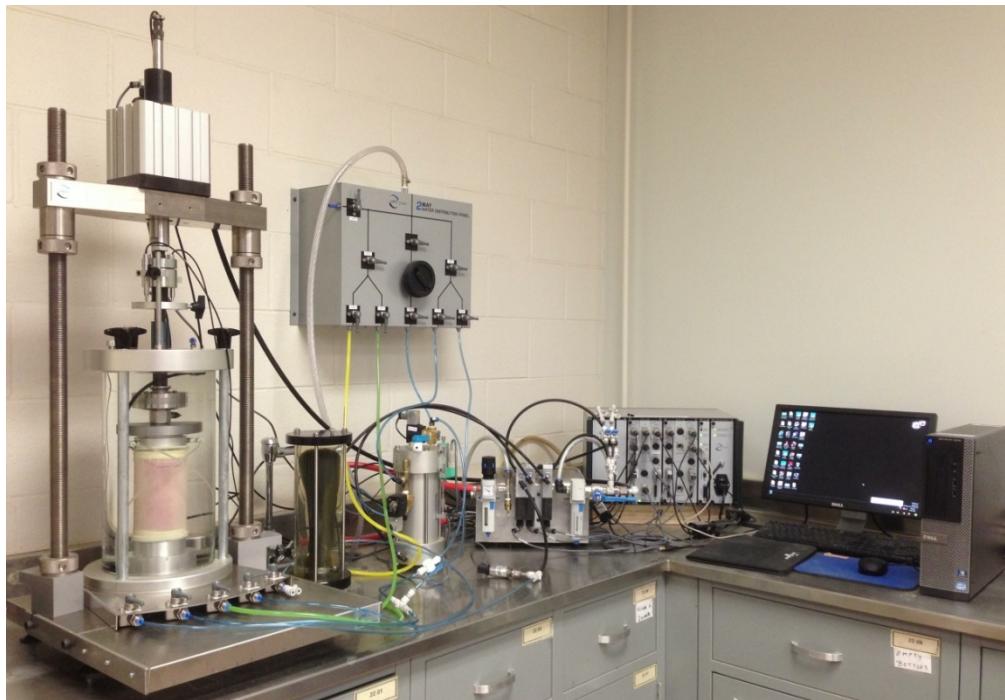


Figure 3.15 Cyclic triaxial system components

#### 3.2.5.2.1 Triaxial load frame

As shown in Figure 3.16, the load frame is supplied with the pneumatic actuator at its crosshead and has a heavy flat base plate supported on four leveling screws. The actual piston passes through the crosshead and has a special alignment

adapter to connect with the load cell which is located at the triaxial cell. The load frame is made of heavy materials in order to limit deflection and vibration which may affect the accuracy of measurements.

#### 3.2.5.2.2 *Pneumatic actuator*

The pneumatic actuator is located at the crosshead of the triaxial load frame and consists of a displacement transducer which is attached to the actuator shaft in order to connect with the triaxial cell as shown in Figure 3.16. The electrically controlled pneumatic servo valve is located close to the actuator so that the feedback from displacement and load transducers are reported back to the control system.

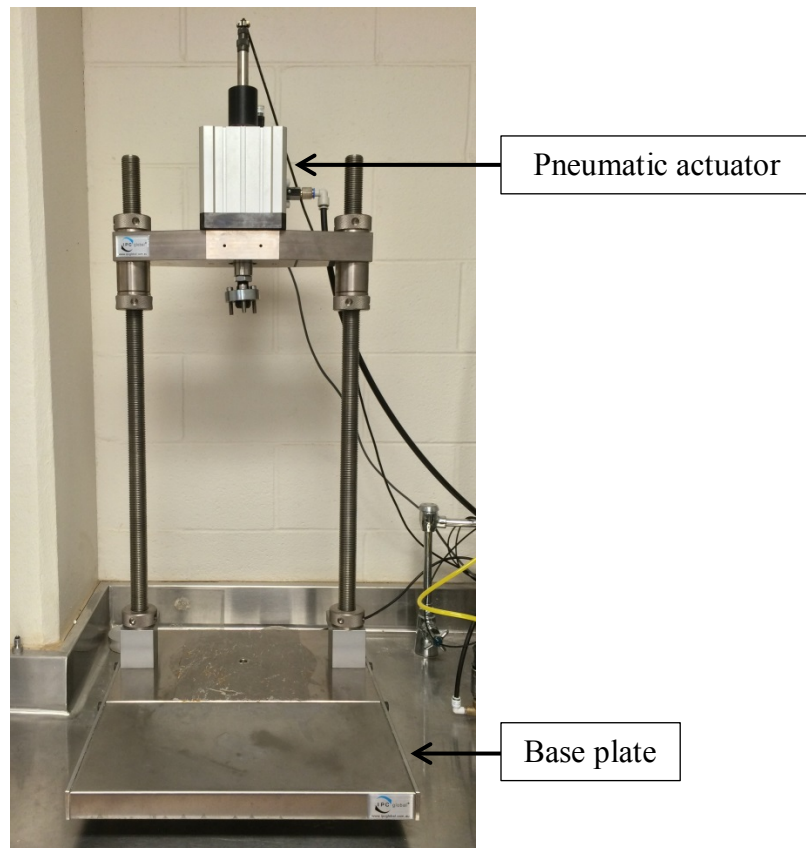


Figure 3.16 Triaxial load frame with pneumatic actuator



### 3.2.5.2.3 Integrated Multi-Axis Control System (IMACS)

The Integrated Multi-Axis Control System (IMACS) is a unit that controls the system including the communication between the system and computer, applied loads, displacement, confining pressure, and back pressure. All of the transducer cables are connected at the front panel of the IMACS as shown in Figure 3.17. The IMACS also captures data from the transducers and transfers to a computer for processing, presenting, and storing.



Figure 3.17 Integrated Multi-Axis Control System (IMACS)

### 3.2.5.2.4 Auxiliary air reservoir

The auxiliary air reservoir functions as a reservoir that maintains a ready supply of pressurized air. The reservoir also houses the water trap, mist separator, and servo valves which control the confining pressure and back pressure. The system requires this reservoir in order to smooth out any variations in the air supply pressure and prevent moisture from entering the servo valves.

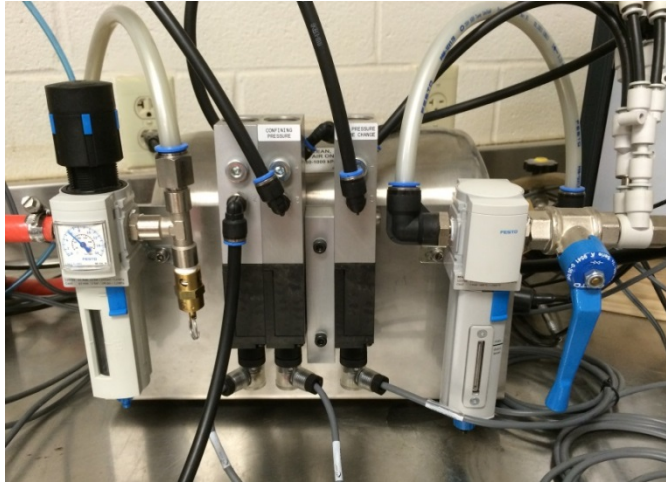


Figure 3.18 Auxiliary air reservoir

#### 3.2.5.2.5 Water distribution panel

The water distribution panel receives de-aired water to be directed to the confining cell and air/water interface that controls the water pressure applied to the confining cell. The panel has diagrammatic distribution channel marks to follow as shown in Figure 3.19.

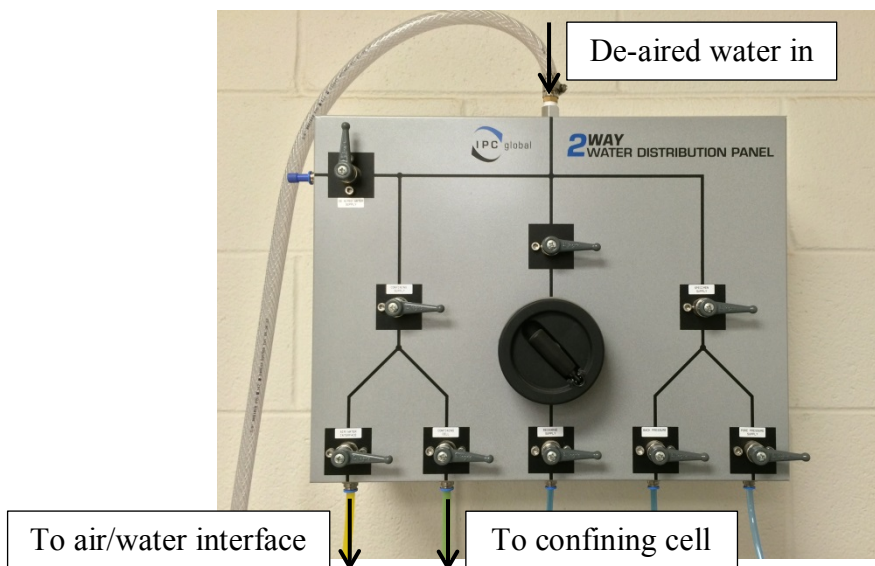


Figure 3.19 Water distribution panel

#### 3.2.5.2.6 Triaxial cell and submersible load cell

The triaxial cell is a clear acrylic chamber with a working pressure of 150 psi (1,000 kPa). The cell has a solid top and base, which provides a stable platform for easier aligning of the cell to the load frame, and three knobs that lock the cell with the base plate during the test process. At the top of the triaxial cell, a submersible load cell is attached within the cell in order to measure the load applied to the soil specimen as shown in Figure 3.20.

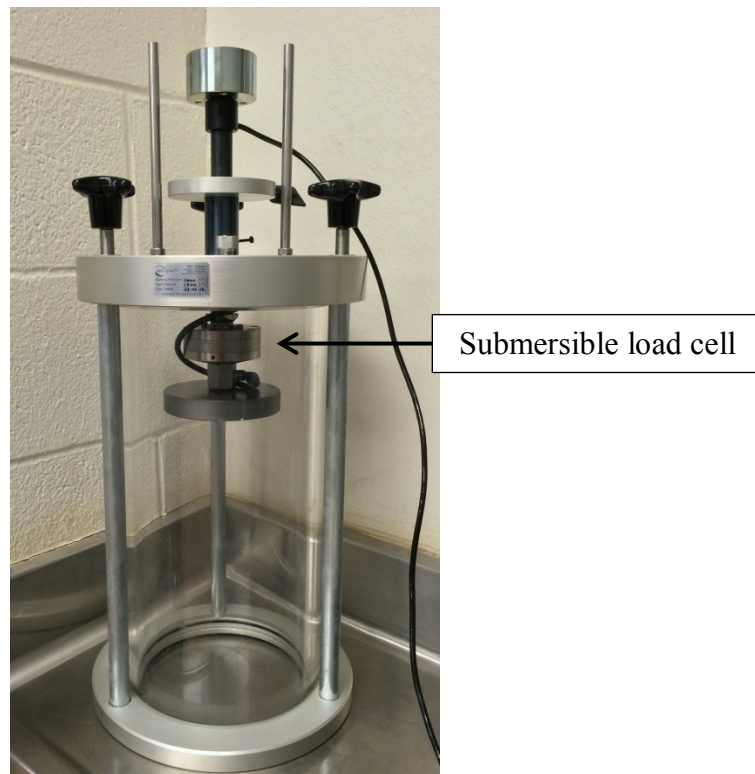


Figure 3.20 Triaxial cell

#### 3.2.5.2.7 Linear Variable Displacement Transducers (LVDTs)

According to the AASHTO T 307-99 standard, LVDTs are required to measure the displacements caused by the applied cyclic loads. LVDTs are installed at

the load shafts located at the top of the triaxial cell as shown in Figure 3.21. The output from each LVDT is measured and recorded individually of which the average result is used to determine the resilient modulus.

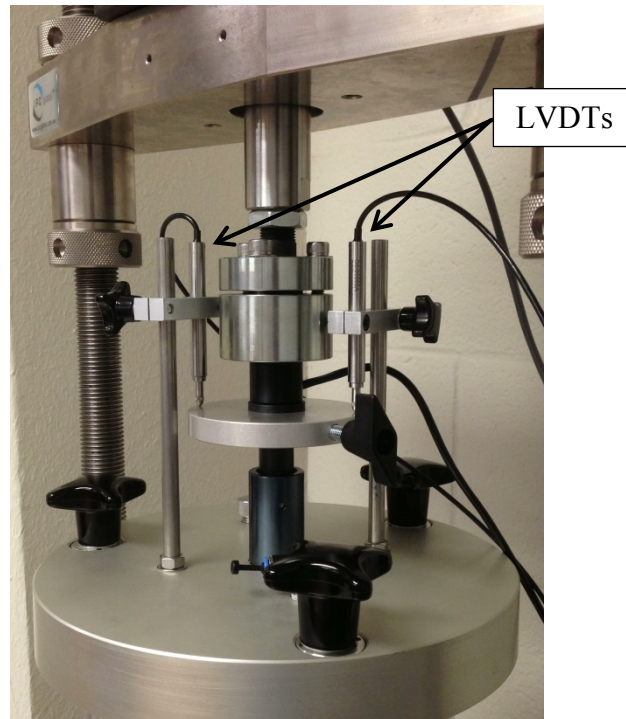


Figure 3.21 Linear Variable Displacement Transducers (LVDTs)

### 3.2.5.3 Resilient modulus test procedures

The prepared soil specimens were tested using the Universal Cyclic Triaxial System with respect to the AASHTO T 307-99 standard. The stress levels applied to the specimen are categorized into deviatoric stress and confining pressure. To simulate various stress situations caused from the real traffic to the soil, five different deviatoric stresses with three different confining pressures are performed within fifteen testing sequences as shown in Table 3.4. According to the standard, Sequence



No. 0 is performed in order to reduce the plastic strain to approximately zero. Therefore, beginning with the Sequence No. 1, strains caused by the applied loads are assumed to be elastic strains which are used to determine the resilient modulus from each sequence.

Table 3.4 Testing sequence for subgrade soil (AASHTO T 307-99 Standard)

No.	Confining Pressure		Max. Axial Stress		Cyclic Stress		Contact Stress		No. of Load Cycles
	kPa	psi	kPa	psi	kPa	psi	kPa	psi	
0	41.4	6	27.6	4	24.8	3.6	2.8	0.4	500–1000
1	41.4	6	13.8	2	12.4	1.8	1.4	0.2	100
2	41.4	6	27.6	4	24.8	3.6	2.8	0.4	100
3	41.4	6	41.4	6	37.3	5.4	4.1	0.6	100
4	41.4	6	55.2	8	49.7	7.2	5.5	0.8	100
5	41.4	6	68.9	10	62.0	9.0	6.9	1.0	100
6	27.6	4	13.8	2	12.4	1.8	1.4	0.2	100
7	27.6	4	27.6	4	24.8	3.6	2.8	0.4	100
8	27.6	4	41.4	6	37.3	5.4	4.1	0.6	100
9	27.6	4	55.2	8	49.7	7.2	5.5	0.8	100
10	27.6	4	68.9	10	62.0	9.0	6.9	1.0	100
11	13.8	2	13.8	2	12.4	1.8	1.4	0.2	100
12	13.8	2	27.6	4	24.8	3.6	2.8	0.4	100
13	13.8	2	41.4	6	37.3	5.4	4.1	0.6	100
14	13.8	2	55.2	8	49.7	7.2	5.5	0.8	100
15	13.8	2	68.9	10	62.0	9.0	6.9	1.0	100

Each deviatoric stress consists of cyclic stress and contact stress. The cyclic stress is an actual stress applied to the specimen, but the contact stress is a constant stress applied to the specimen in order to hold it during each test sequence. The contact stress is approximately equal to 10% of the deviatoric stress. In addition, the AASHTO T 307-99 standard requires the applied load to be a haversine-shaped waveform as shown in Figure 3.22. At each load cycle duration is composed of 0.1 second load duration and 0.9 second rest period.

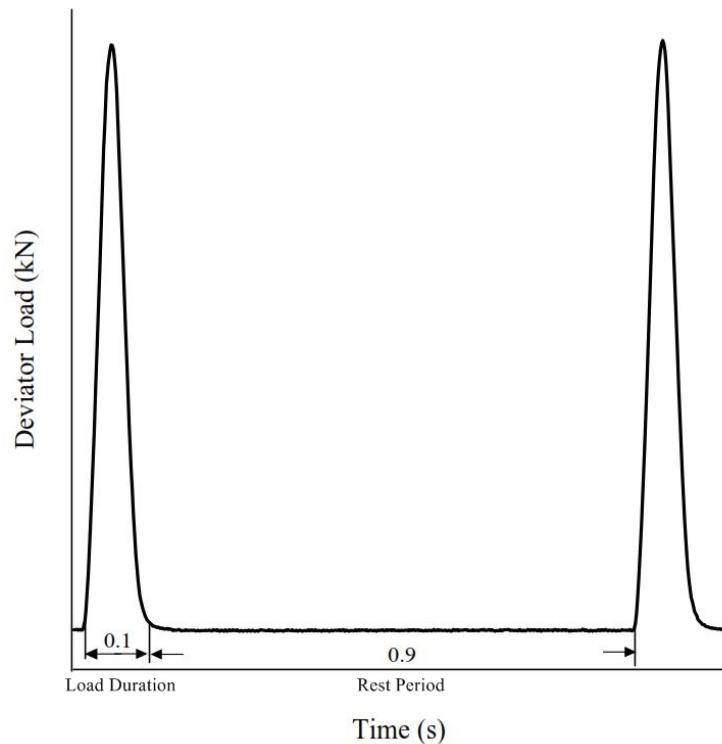


Figure 3.22 Load cycle duration of each deviatoric stress (Titi et al., 2006)

### 3.3 Summary

This chapter presents fundamental laboratory tests and results conducted as primary requirements to achieve the further testing programs. Compaction curves obtained from six types of the clay-sand mixtures are included in order to determine the maximum dry density and optimum moisture content for each clay-sand mixture. The resilient modulus sample preparation and test procedure are then discussed step by step with respect to the AASHTO T 307-99 standard. The resilient modulus apparatuses employed in this research are detailed including seven main components; triaxial load frame, pneumatic actuator, IMACS, auxiliary air reservoir, water distribution panel, triaxial cell and submersible load cell, and Linear Variable Displacement Transducers (LVDTs).

## Chapter 4

### Test Results and Analysis

#### 4.1 Introduction

After the specimen preparation process as detailed in the previous chapter, the unconfined compression tests and the resilient modulus tests were conducted on the specimens. Both test results are presented in this chapter. In the beginning, the unconfined compressive strength results are presented and analyzed. Thereafter, the resilient modulus results obtained from six types of the clay-sand mixtures are presented including one comprehensive example of the full resilient modulus results. The resilient modulus results are then analyzed by using the universal model; these results are presented in this chapter. The analysis of the resilient modulus improvement with various percentages of the sand admixture is subsequently addressed.

#### 4.2 Unconfined Compression Test

Two statically compacted specimens, named as Sample A and Sample B, for one type of the clay-sand mixtures were prepared in compliance with their optimum moisture content and maximum dry density. Each specimen had a diameter and height of 2.8 and 5.6 inch, respectively. The prepared specimens were kept in the humidity room for at least 24 hours before testing. The unconfined compression tests were conducted with respect to the ASTM D 2166 standard as detailed in the previous chapter. Table 4.1 summarizes the UCS test results obtained from both Sample A and Sample B per one type of the clay-sand mixtures.

Table 4.1 Summary of unconfined compression test results

Soil Mixture Type	Unconfined Compressive Strength					
	Sample A		Sample B		Average	
	kPa	psi	kPa	psi	kPa	psi
Clay	177.9	25.8	171.0	24.8	174.5	25.3
Clay + 5% Sand	179.9	26.1	186.9	27.1	183.4	26.6
Clay + 10% Sand	184.1	26.7	195.1	28.3	189.6	27.5
Clay + 20% Sand	203.4	29.5	214.5	31.1	208.9	30.3
Clay + 30% Sand	221.3	32.1	230.9	33.5	226.1	32.8
Clay + 50% Sand	268.2	38.9	275.9	40.0	272.1	39.5

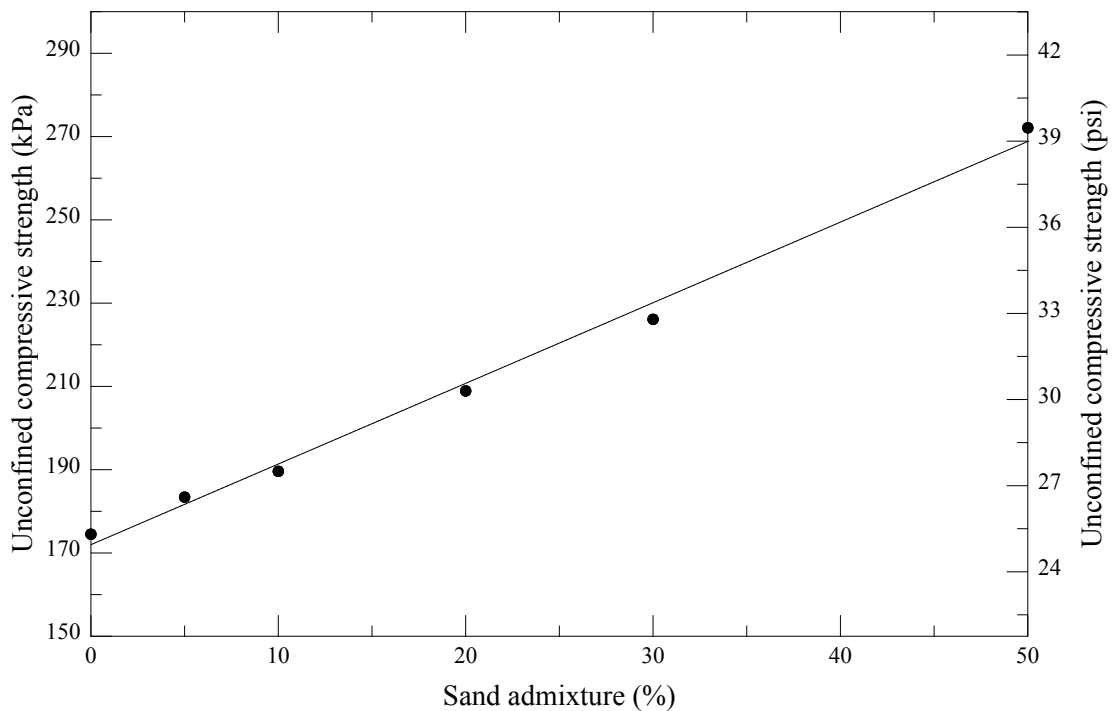


Figure 4.1 Average of the UCS results with various percentages of the sand admixture

The UCS results linearly increased when the content of the sand admixture was increased. The average strength obtained from the UCS results of Dallas clay

with no sand admixture was 174.5 kPa, whereas the average strength obtained from Dallas clay with 50% sand admixture increased to 272.1 kPa. The maximum strength improvement was 55.9%, which achieved from the clay-sand mixture with 50% sand admixture. This improving trend is expected since the sand admixture forms the skeleton and the pores around the skeleton are filled with fine grains causing higher soil strength as detailed in Chapter 2.

#### 4.3 Resilient Modulus Test

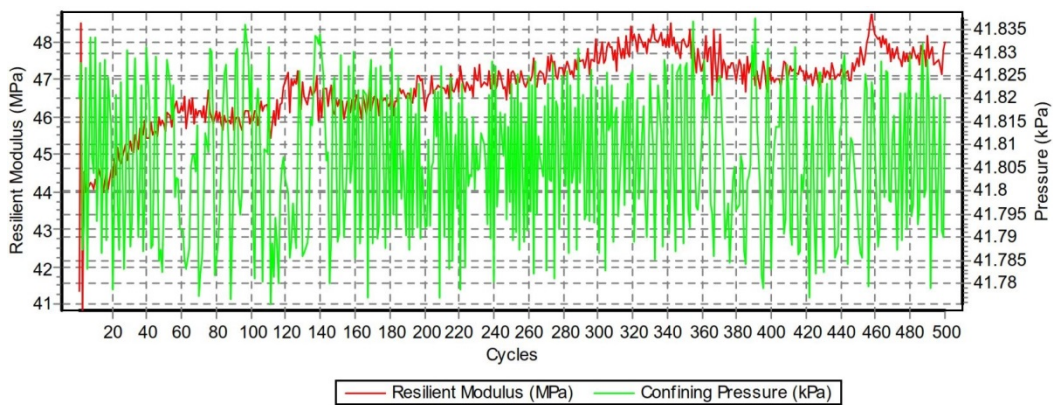
Two resilient modulus specimens, named as Sample A and Sample B, for one type of the clay-sand mixtures were prepared in compliance with their optimum moisture content and maximum dry density. The sampling procedures were adhered to the AASHTO T 307-99 standard as detailed in Chapter 3. The resilient modulus tests were conducted with respect to the AASHTO T 307-99 standard using the Universal Cyclic Triaxial System as stated in the previous chapter. As a subgrade soil, five different deviatoric stresses (13.8, 27.6, 41.4, 55.2, and 68.9 kPa) with three different confining pressures (13.8, 27.6, and 41.4 kPa) were applied to the specimen creating fifteen test sequences.

During the test procedure, each vertical deformation of the specimen caused by the applied load is used to determine the resilient modulus. Therefore, one test sequence will have a hundred values of the resilient modulus. However, the AASHTO T 307-99 standard requires only an average of the last five resilient modulus values obtained from each sequence to be a representative of the whole sequence. In the following subsection, an example of the complete resilient modulus

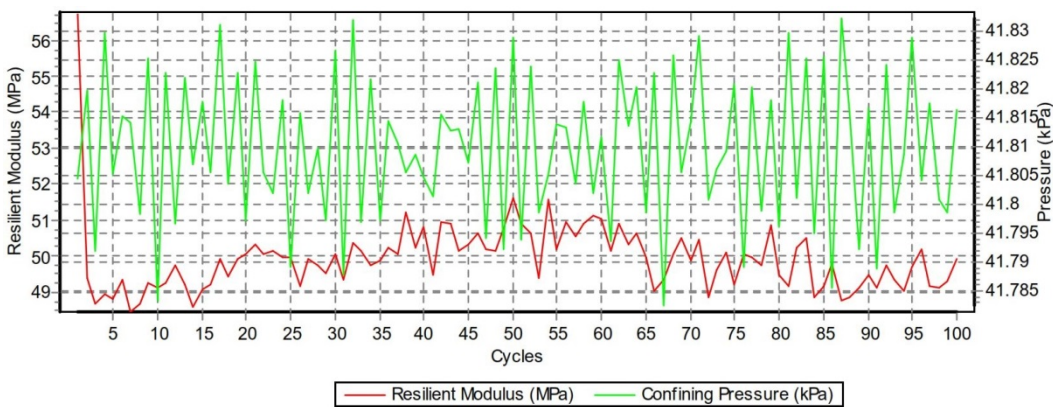
test results from Sequence No.1 to Sequence No. 15 is presented. The resilient modulus results of the clay-sand mixtures as required by the AASHTO T 307-99 standard are provided subsequently.

#### 4.3.1 Example of Complete Resilient Modulus Test Results

The complete resilient modulus test results of Dallas clay with no sand admixture (Sample A) are presented as follows.

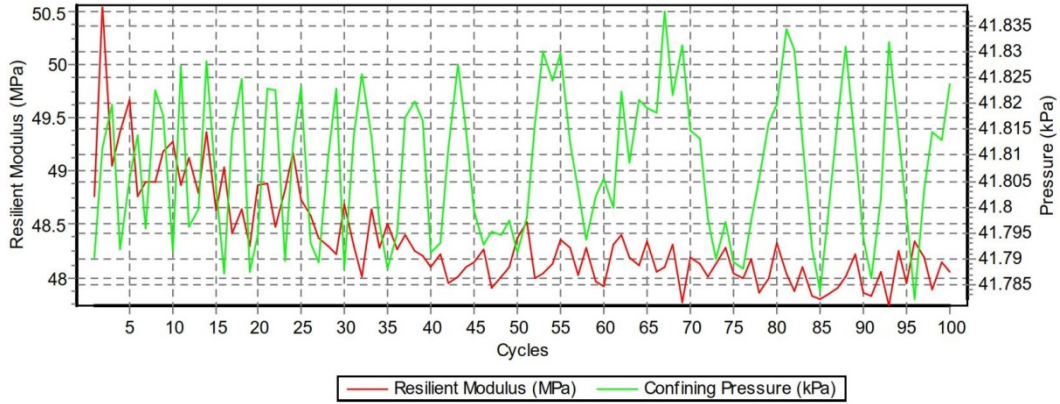


(a) Sequence No. 0

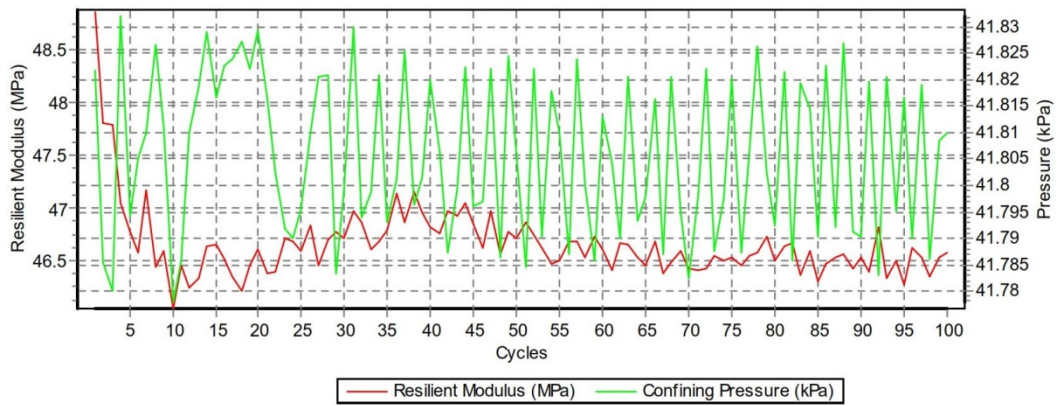


(b) Sequence No. 1

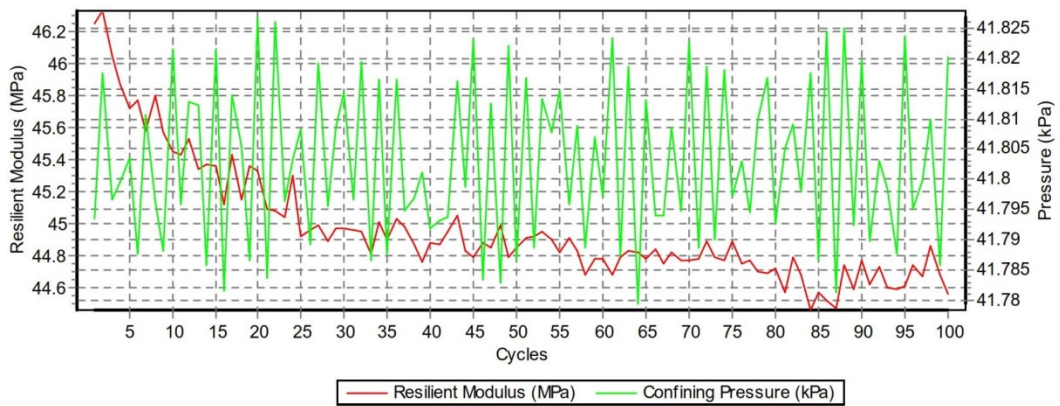
Figure 4.2 Example of the complete  $M_R$  test results, Sequence No. 0 and 1



(a) Sequence No. 2



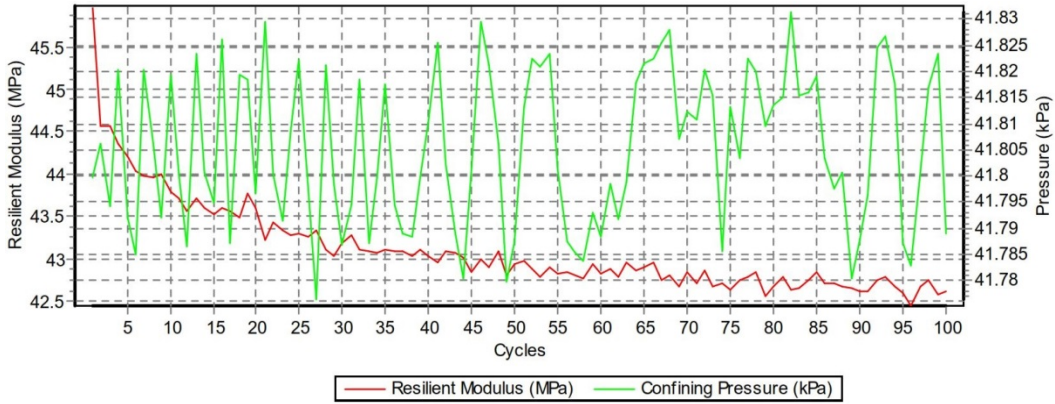
(b) Sequence No. 3



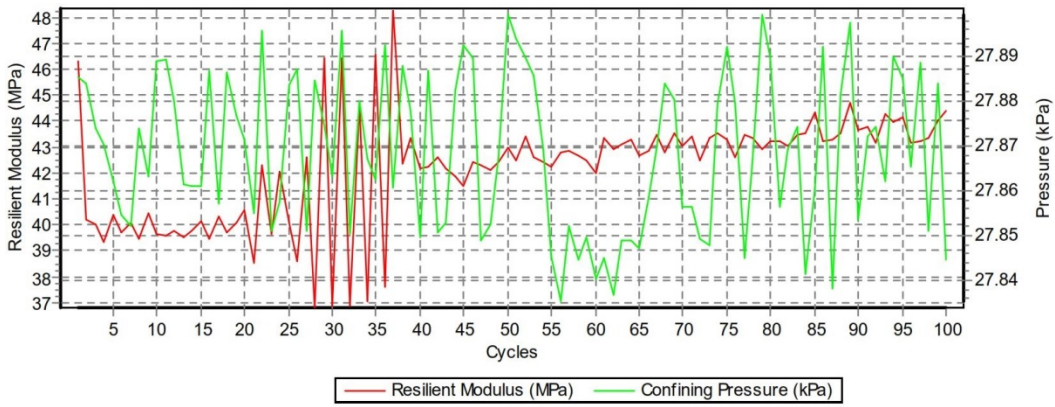
(c) Sequence No. 4

Figure 4.3 Example of the complete  $M_R$  test results, Sequence No. 2, 3, and 4

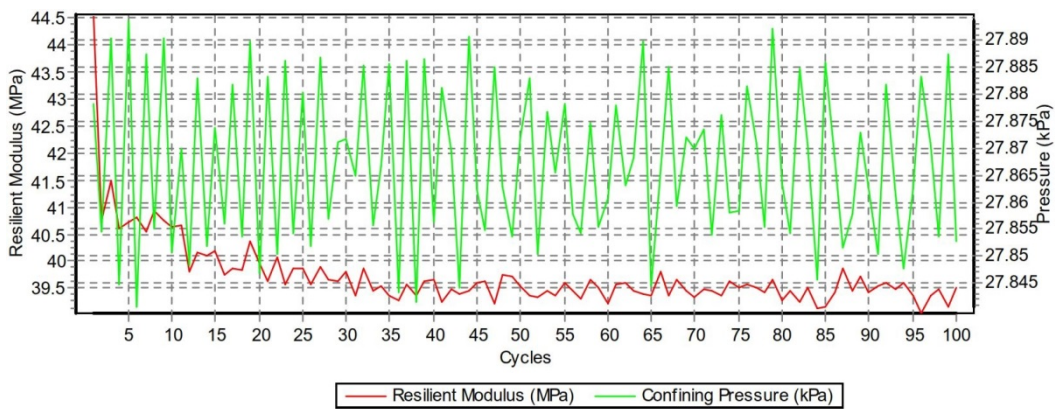




(a) Sequence No. 5

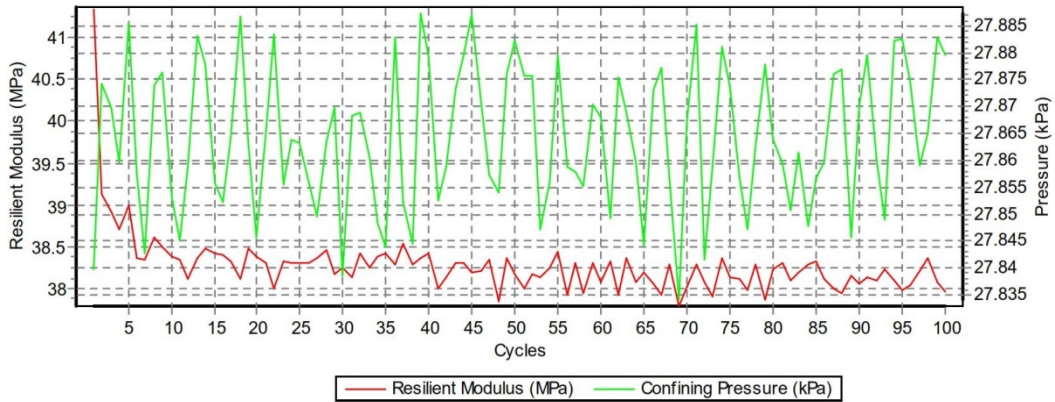


(b) Sequence No. 6

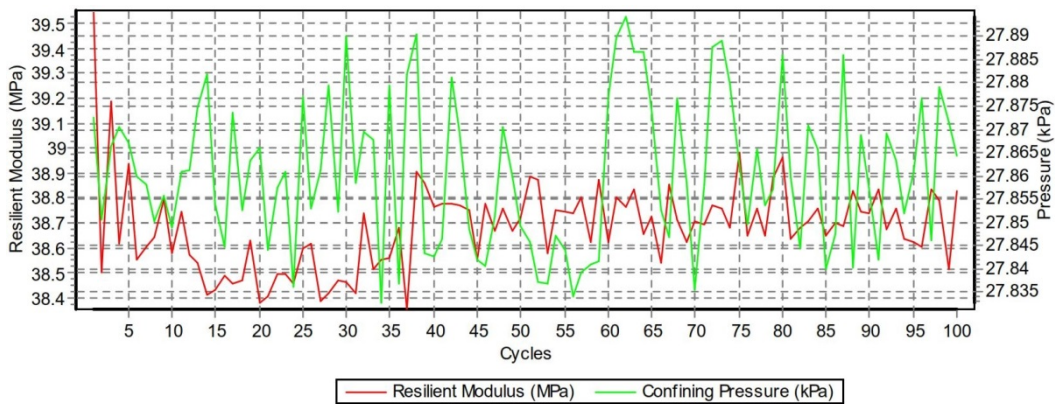


(c) Sequence No. 7

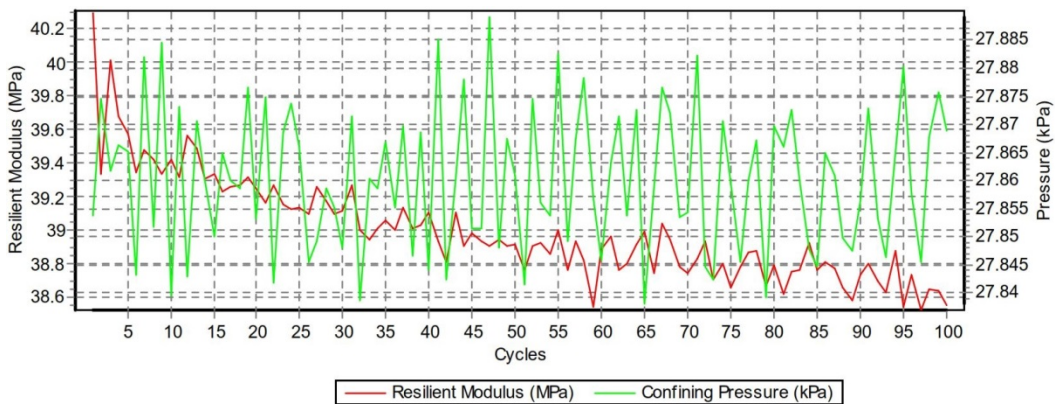
Figure 4.4 Example of the complete  $M_R$  test results, Sequence No. 5, 6, and 7



(a) Sequence No. 8



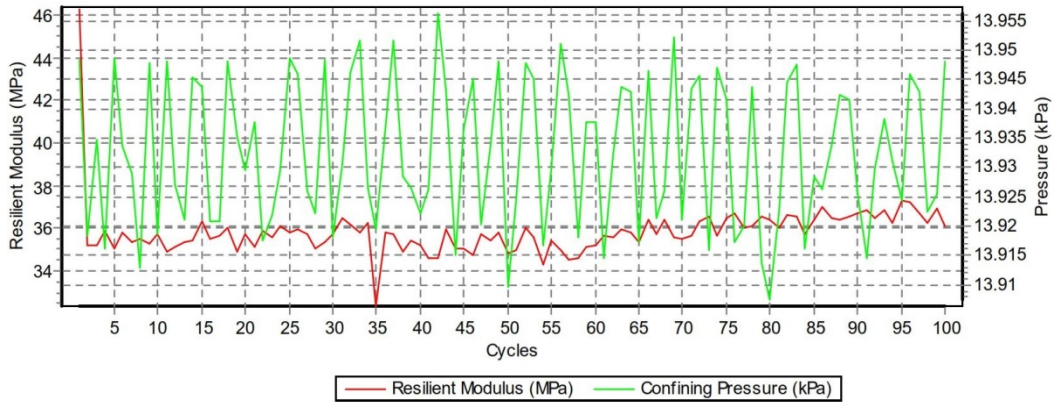
(b) Sequence No. 9



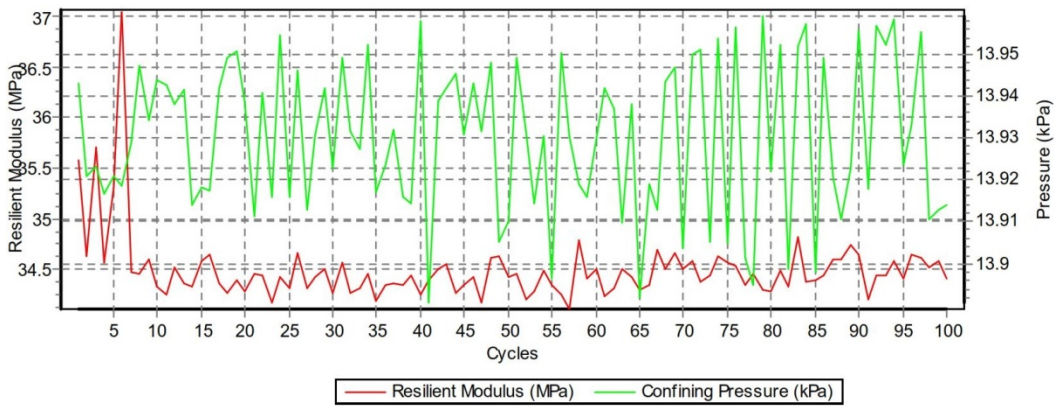
(c) Sequence No. 10

Figure 4.5 Example of the complete  $M_R$  test results, Sequence No. 8, 9, and 10

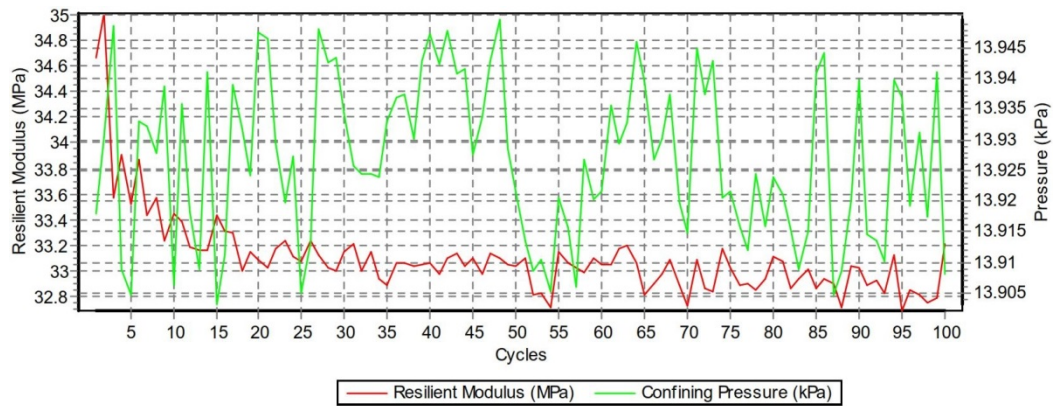




(a) Sequence No. 11

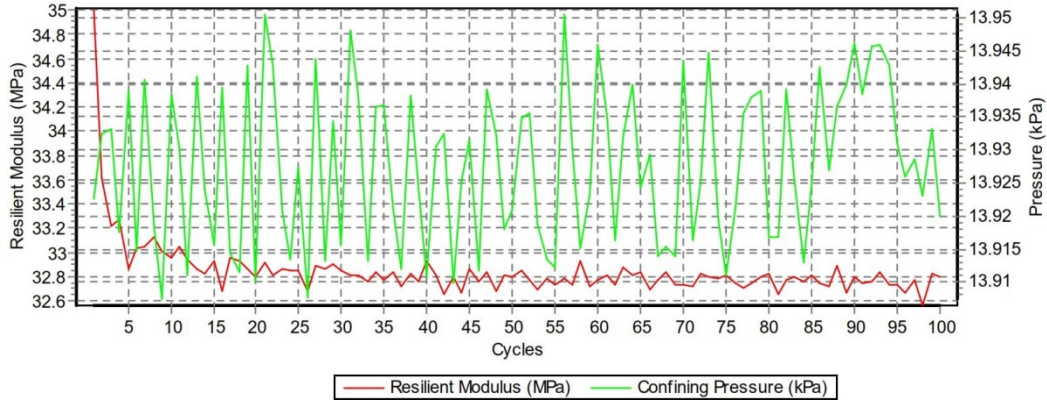


(b) Sequence No. 12

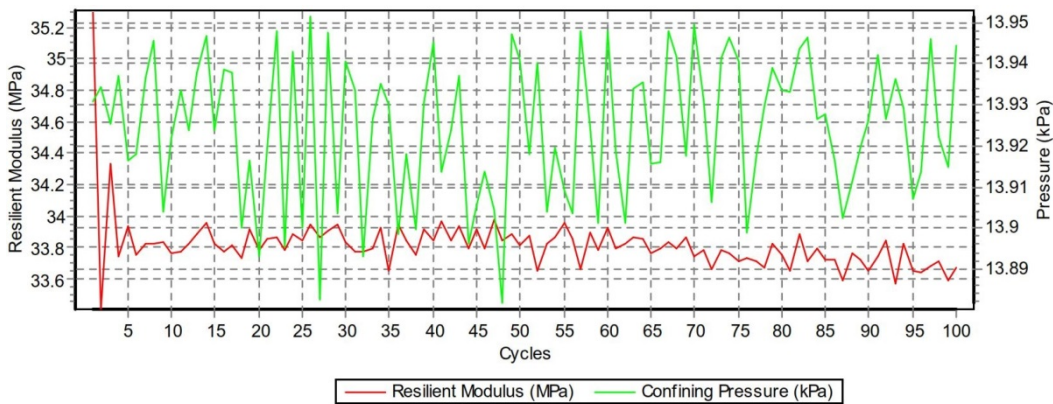


(c) Sequence No. 13

Figure 4.6 Example of the complete  $M_R$  test results, Sequence No. 11, 12, and 13



(a) Sequence No. 14



(b) Sequence No. 15

Figure 4.7 Example of the complete  $M_R$  test results, Sequence No. 14 and 15

#### 4.3.2 Measured Resilient Modulus Results

The resilient modulus test results of each clay-sand mixture are presented both Sample A and Sample B. Therefore, in one figure, fifteen points representing the resilient modulus values from Sequence No. 1–15 are addressed. Since the deviatoric stress is the main concerned parameter used to simulate the real traffic load, the horizontal axis is displayed as the deviatoric stress instead of the confining pressure. The resilient modulus test results are presented from Figure 4.8 to Figure 4.19.

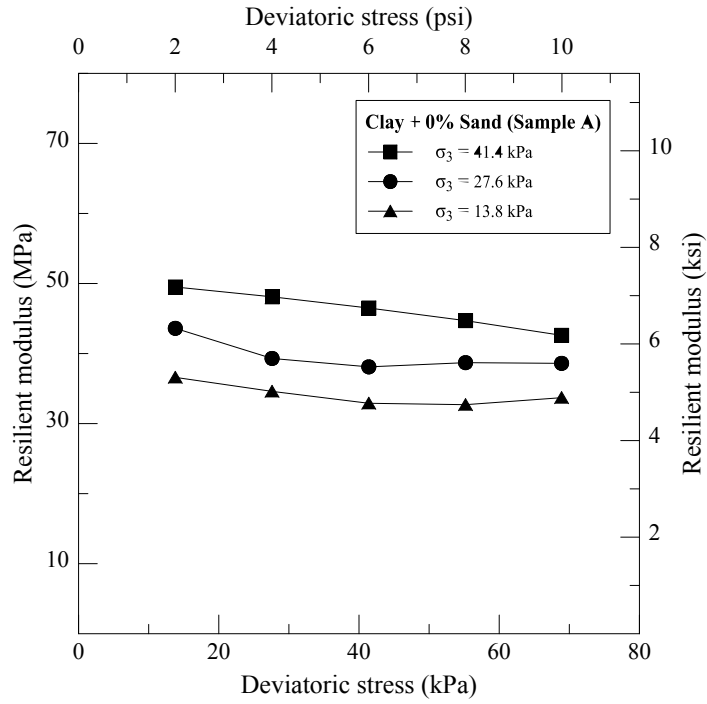


Figure 4.8  $M_R$  results of Dallas clay with no sand admixture, Sample A

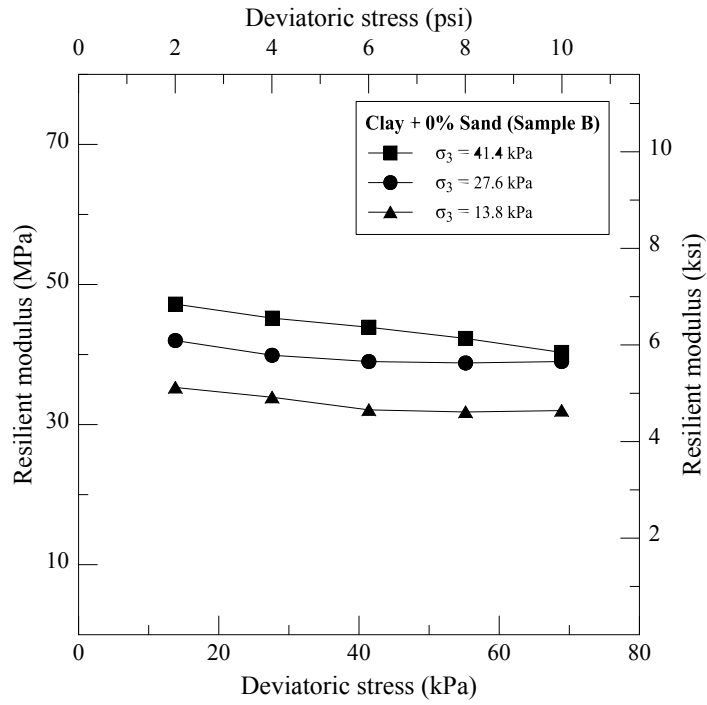


Figure 4.9  $M_R$  results of Dallas clay with no sand admixture, Sample B

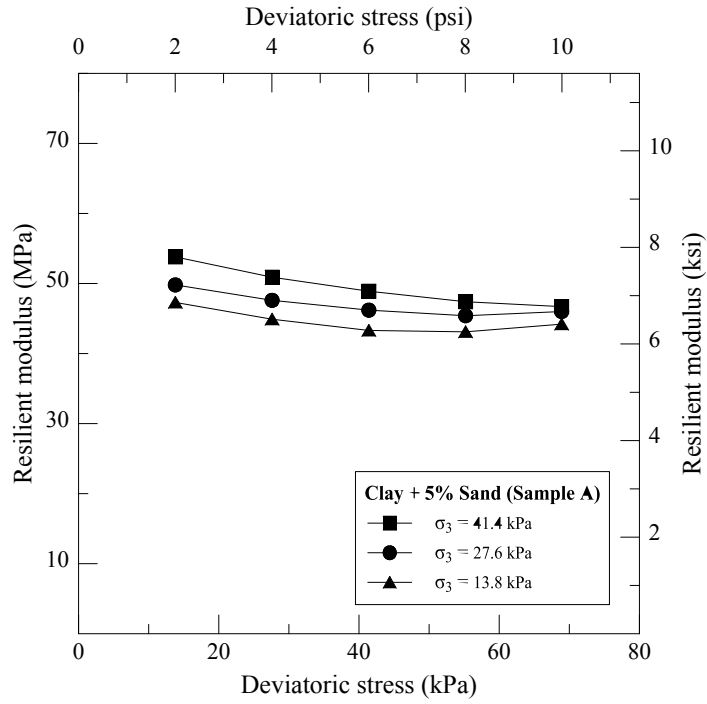


Figure 4.10  $M_R$  results of Dallas clay with 5% sand admixture, Sample A

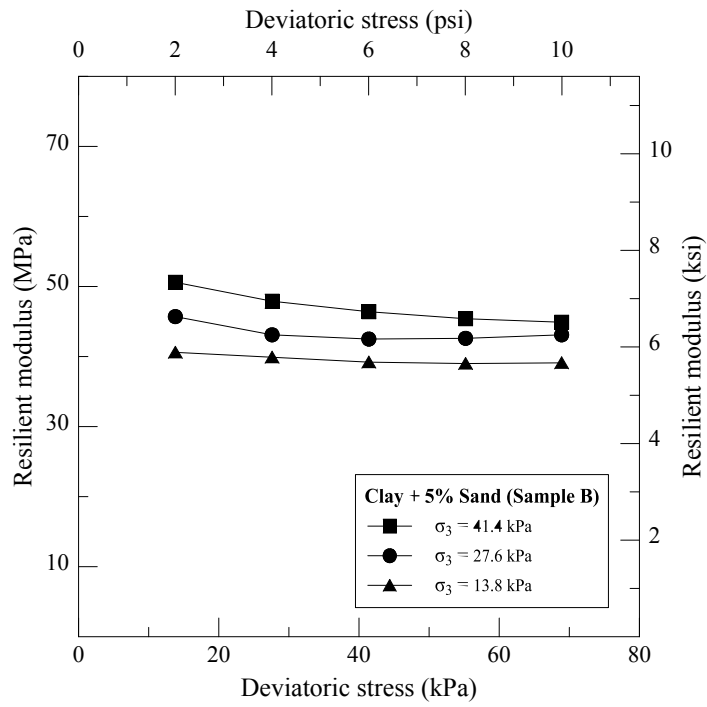


Figure 4.11  $M_R$  results of Dallas clay with 5% sand admixture, Sample B

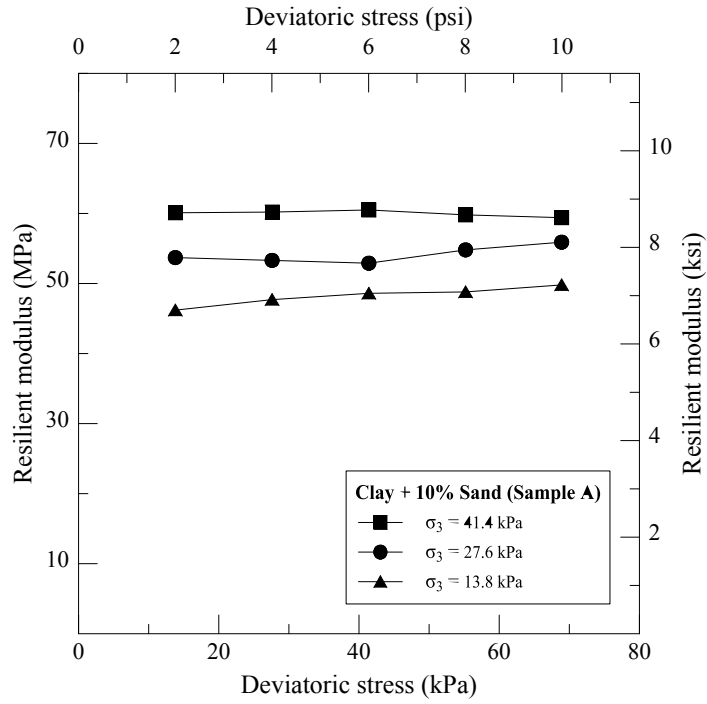


Figure 4.12  $M_R$  results of Dallas clay with 10% sand admixture, Sample A

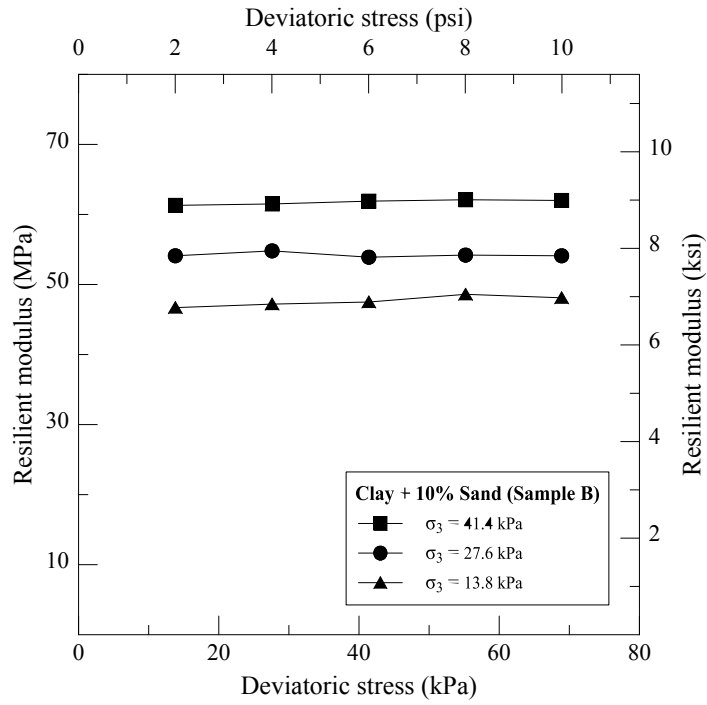


Figure 4.13  $M_R$  results of Dallas clay with 10% sand admixture, Sample B

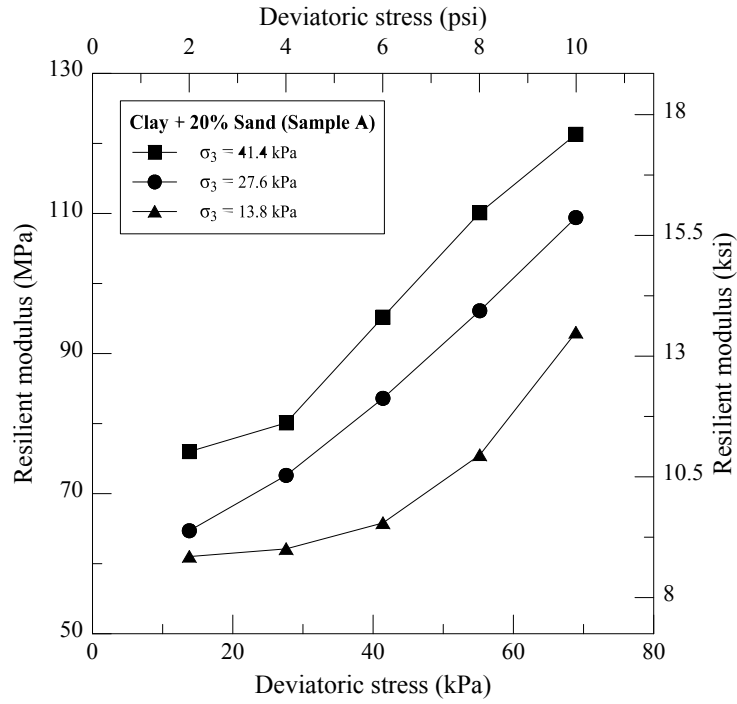


Figure 4.14  $M_R$  results of Dallas clay with 20% sand admixture, Sample A

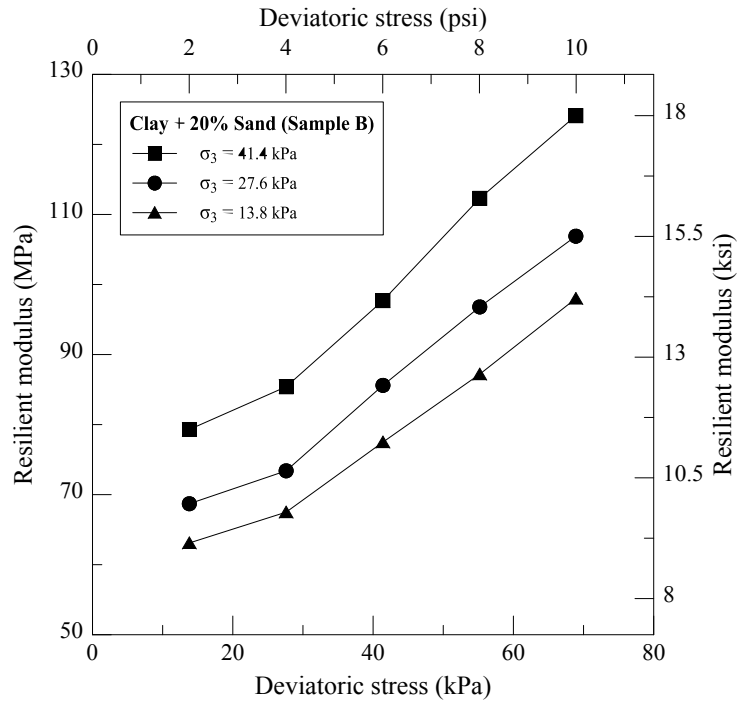


Figure 4.15  $M_R$  results of Dallas clay with 20% sand admixture, Sample B



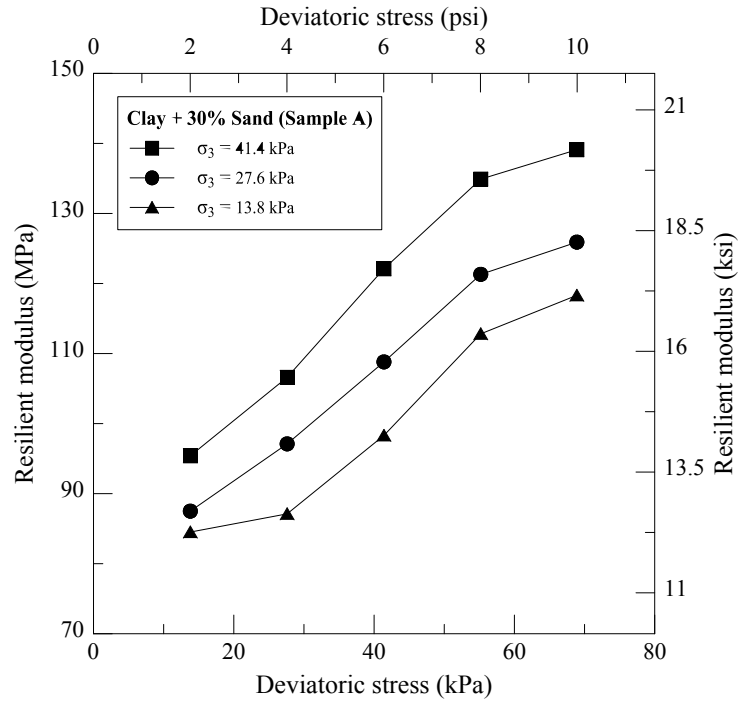


Figure 4.16  $M_R$  results of Dallas clay with 30% sand admixture, Sample A

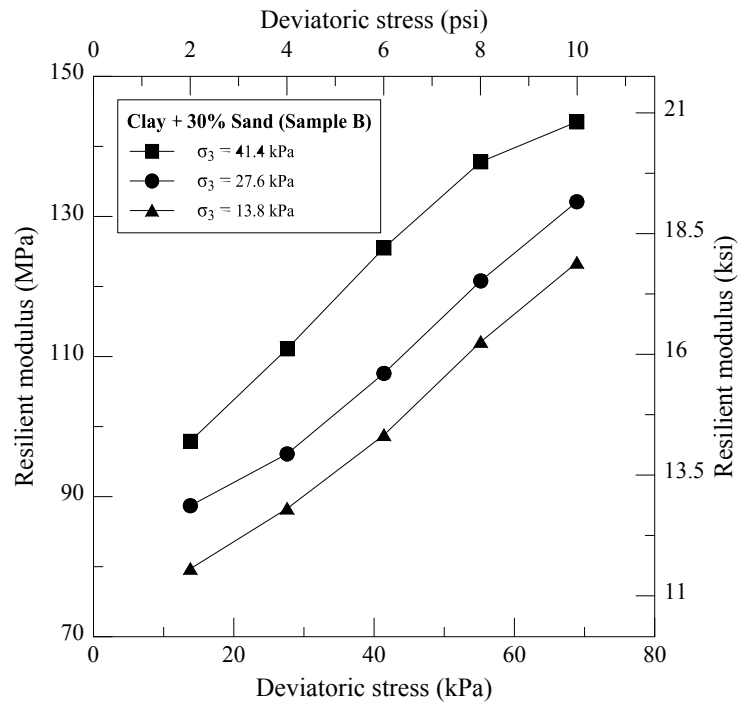


Figure 4.17  $M_R$  results of Dallas clay with 30% sand admixture, Sample B

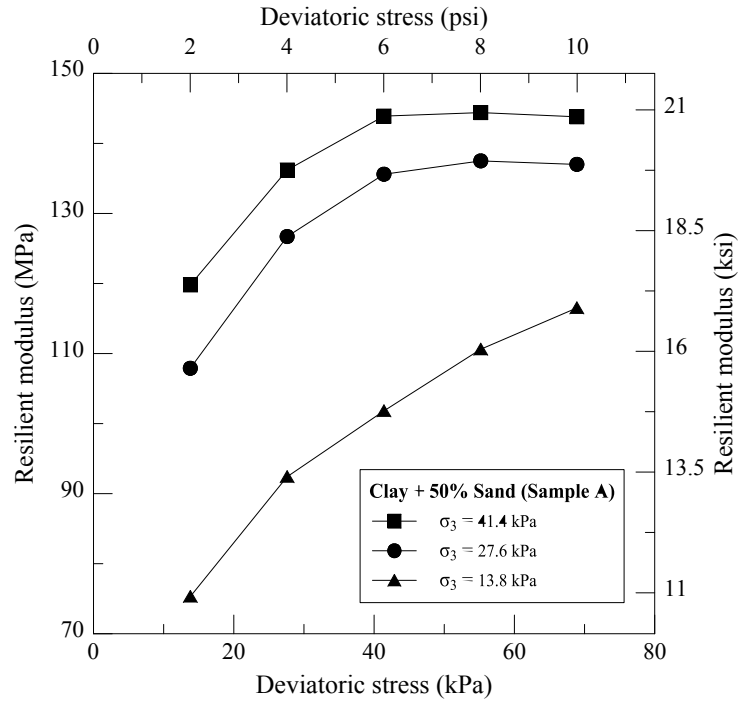


Figure 4.18  $M_R$  results of Dallas clay with 50% sand admixture, Sample A

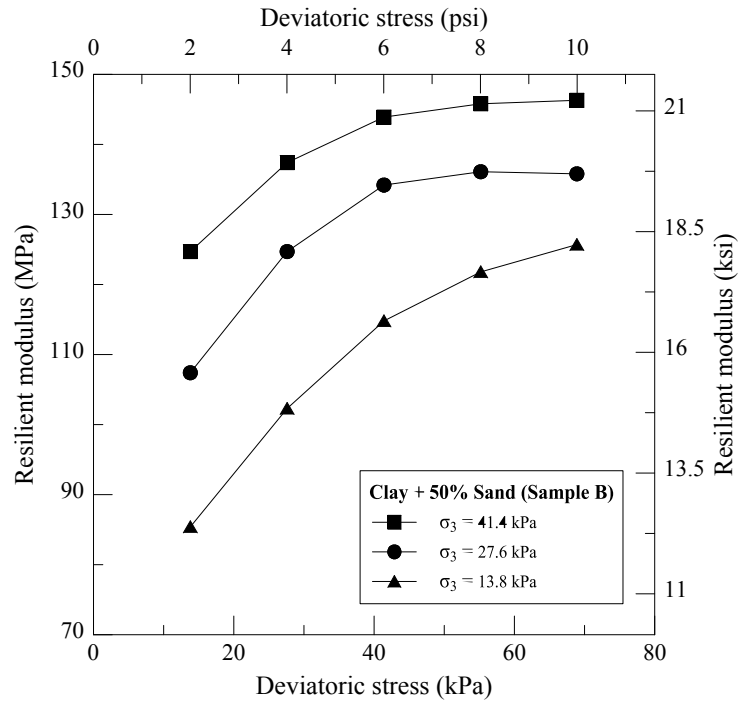


Figure 4.19  $M_R$  results of Dallas clay with 50% sand admixture, Sample B

According to the resilient modulus results, it can be observed that the resilient modulus increased when the percentage of the sand admixture was increased. This behavior is expected as the sand admixture formed the intra skeleton inside the clay-sand mixture resulting in a stronger material. This improving behavior is detailed in the next section.

Another remarkable observation is that both deviatoric stress and confining pressure have a significant influence on the resilient modulus results. As expected, the resilient modulus increased when the confining pressure was increased since the greater confining pressure helped the specimen to develop more strength. An increase in the deviatoric stress resulted in decreasing of the resilient modulus at the low percentage of the sand admixture. At 10% sand admixture, an increase in the deviatoric stress resulted in approximately the same value of the resilient modulus. As for the percentage of the sand admixture more than 10, an increase in the deviatoric stress resulted in increasing of the resilient modulus. These various effects of deviatoric stress on the resilient modulus can be explained as an interaction of soil particles between Dallas clay and the sand admixture. For the percentage of the sand admixture lower than 10, the clay-sand mixture behaved like a stress-softening material. On the other hand, for the percentage of the sand admixture more than 10, the clay-sand mixture behaved like a stress-hardening material.

### 4.3.3 Analysis of Resilient Modulus Test Results

The resilient modulus test results obtained from the repeated load triaxial test were used to develop correlations for predicting the resilient modulus model parameters by using the universal model as shown in Equation 4.1.

$$M_R = k_1 \times P_a \times \left(\frac{\sigma_b}{P_a}\right)^{k_2} \times \left(\frac{\tau_{oct}}{P_a} + 1\right)^{k_3} \quad (4.1)$$

where  $k_1$ ,  $k_2$ , and  $k_3$  are material specific regression coefficients;  $P_a$  is the atmospheric pressure;  $\sigma_b$  is the bulk stress; and  $\tau_{oct}$  is the octahedral shear stress.

In this research, the statistical software was used to analyze and determine the material specific regression coefficients for each type of the clay-sand mixtures. The resilient modulus test results of Sample A and Sample B were averaged and then inputted to the software. After the model parameters ( $k_1$ ,  $k_2$ , and  $k_3$ ) are calculated, these parameters will be used to determine the predicted resilient modulus results. Table 4.2 shows material specific regression coefficients of the clay-sand mixtures. The predicted resilient modulus results are presented in Figure 4.20–4.25.

Table 4.2 Material specific regression coefficients of the clay-sand mixtures

<b>Soil Mixture Type</b>	<b>k<sub>1</sub></b>	<b>k<sub>2</sub></b>	<b>k<sub>3</sub></b>	<b>R<sup>2</sup></b>
Clay	466.2	0.398	-1.429	0.95
Clay + 5% Sand	499.0	0.189	-0.828	0.93
Clay + 10% Sand	566.8	0.325	-0.629	0.97
Clay + 20% Sand	623.2	0.348	1.390	0.95
Clay + 30% Sand	828.1	0.254	1.273	0.97
Clay + 50% Sand	1083.6	0.422	0.261	0.93

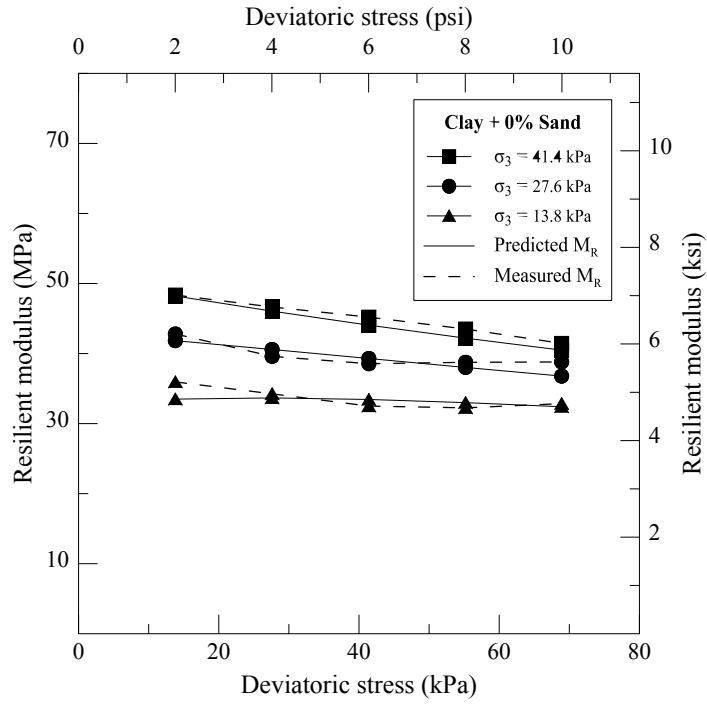


Figure 4.20 Predicted  $M_R$  results of Dallas clay with no sand admixture

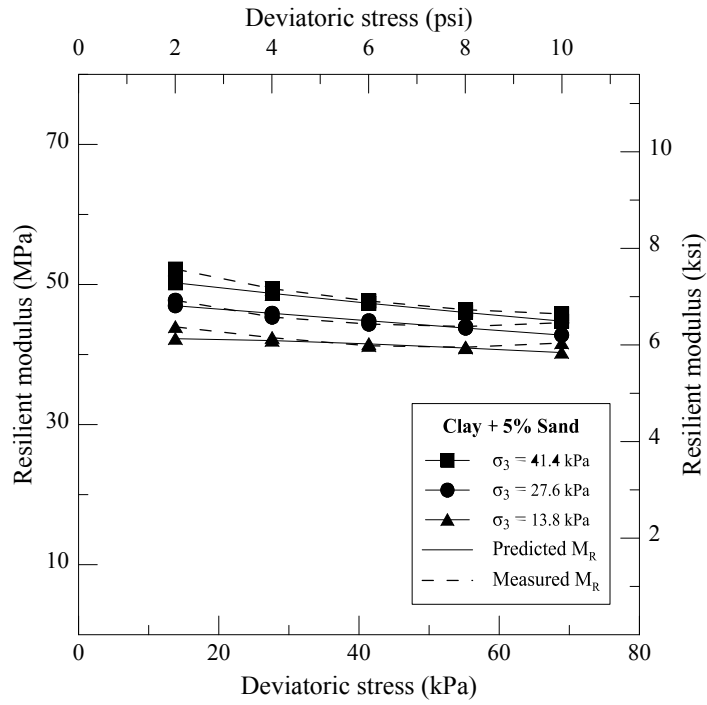


Figure 4.21 Predicted  $M_R$  results of Dallas clay with 5% sand admixture

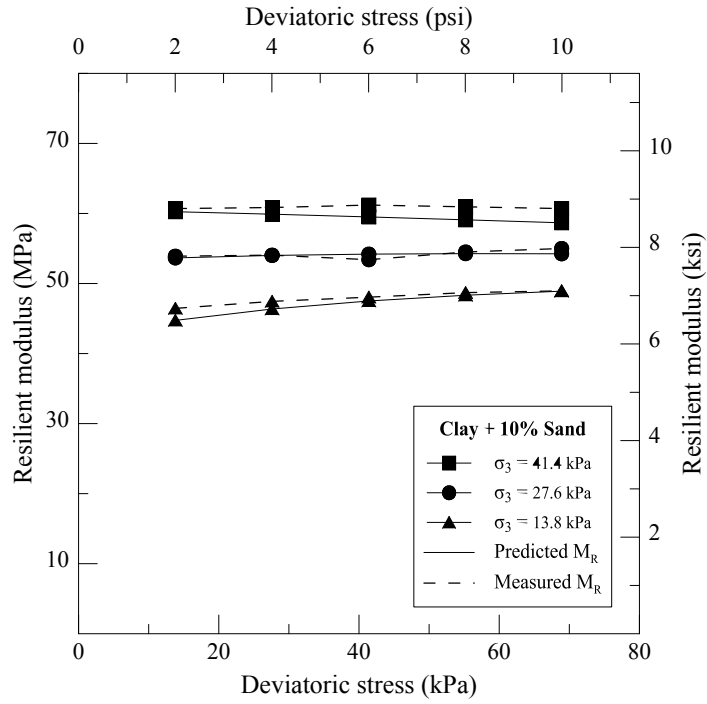


Figure 4.22 Predicted  $M_R$  results of Dallas clay with 10% sand admixture

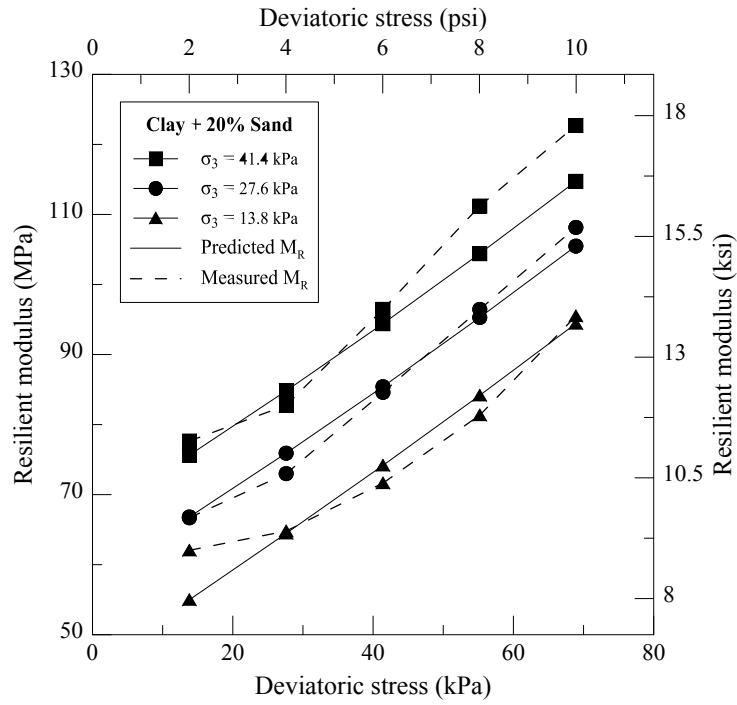


Figure 4.23 Predicted  $M_R$  results of Dallas clay with 20% sand admixture

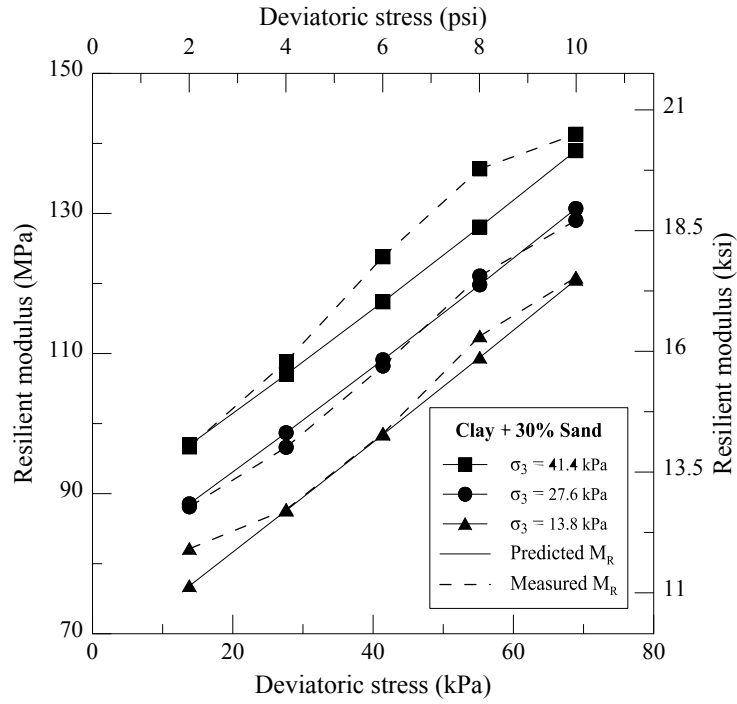


Figure 4.24 Predicted  $M_R$  results of Dallas clay with 30% sand admixture

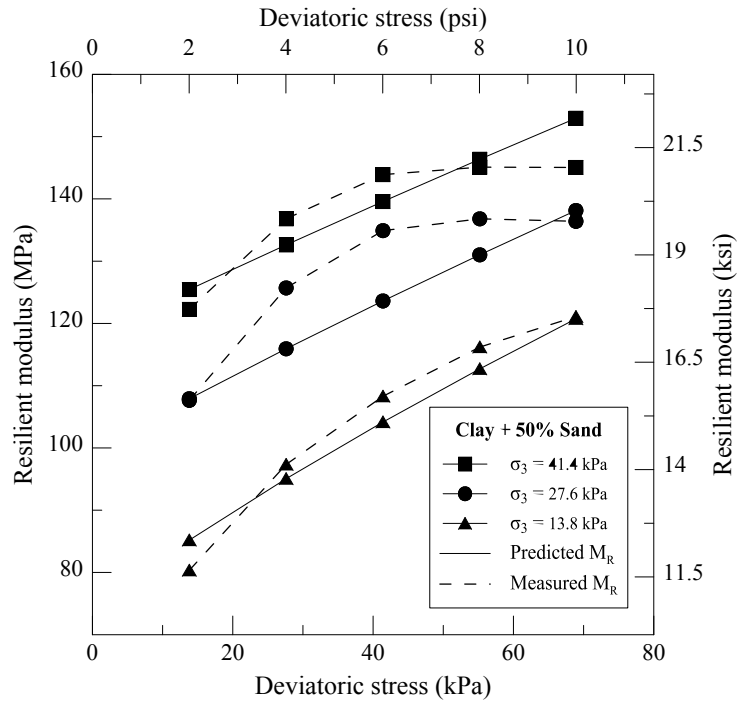


Figure 4.25 Predicted  $M_R$  results of Dallas clay with 50% sand admixture

The behavior of the predicted resilient modulus results was similar to the measured resilient modulus results. The resilient modulus increased when the content of the sand admixture was increased. Also, when the percentage of the sand admixture was increased to 10%, the mixture changed its behavior from a stress-softening material to stress-hardening material. The detailed explanation for these behaviors was provided in the previous section. Figure 4.26 depicts a comparison between the measured versus predicted resilient modulus values. From the figure, it can be observed that the predicted resilient modulus values are well matched with the measured resilient modulus values since the original constants are derived from the same experimental test results.

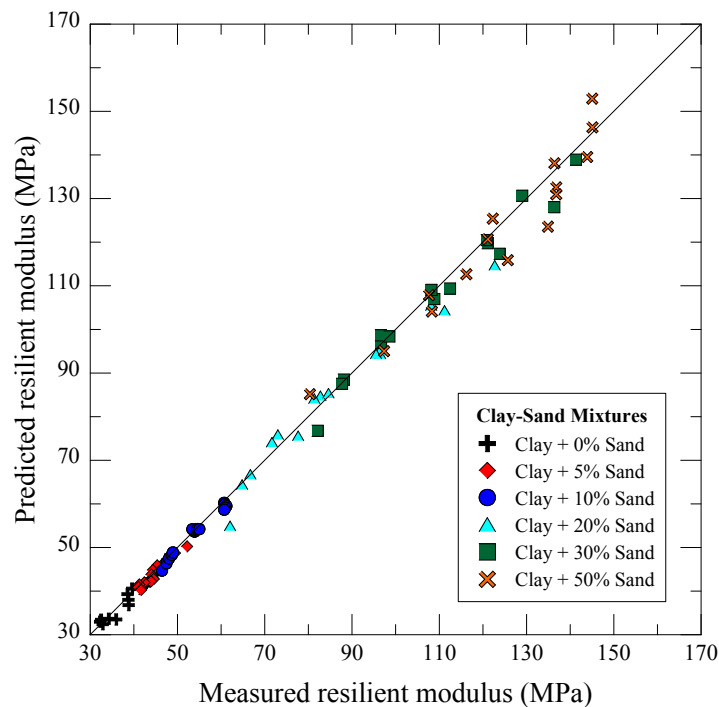


Figure 4.26 Comparison between the predicted and measured  $M_R$  results of the clay-sand mixtures



#### *4.3.4 Analysis of Resilient Modulus Improvement by Sand Admixture*

The measured resilient modulus results from the previous section are rearranged in order to analyze for the resilient modulus behavior with various percentages of the sand admixture. Since the deviatoric stress is the main concerned parameter used to simulate the real traffic load, this section will analyze the resilient modulus results by allocating the deviatoric stress to a constant parameter.

According to the AASHTO T 307-99 standard, five different deviatoric stresses (13.8, 27.6, 41.4, 55.2, and 68.9 kPa) are applied to the specimen. Therefore, five different plots are illustrated in Figure 4.27–4.31. The vertical axis of each plot presents an increase in the measured resilient modulus results, which are the comparisons between the resilient modulus results of every clay-sand mixture and Dallas clay (with no sand admixture). Therefore, each plot starts at the origin. It should be noticed that the measured resilient modulus results in each plot were averaged from Sample A and Sample B.

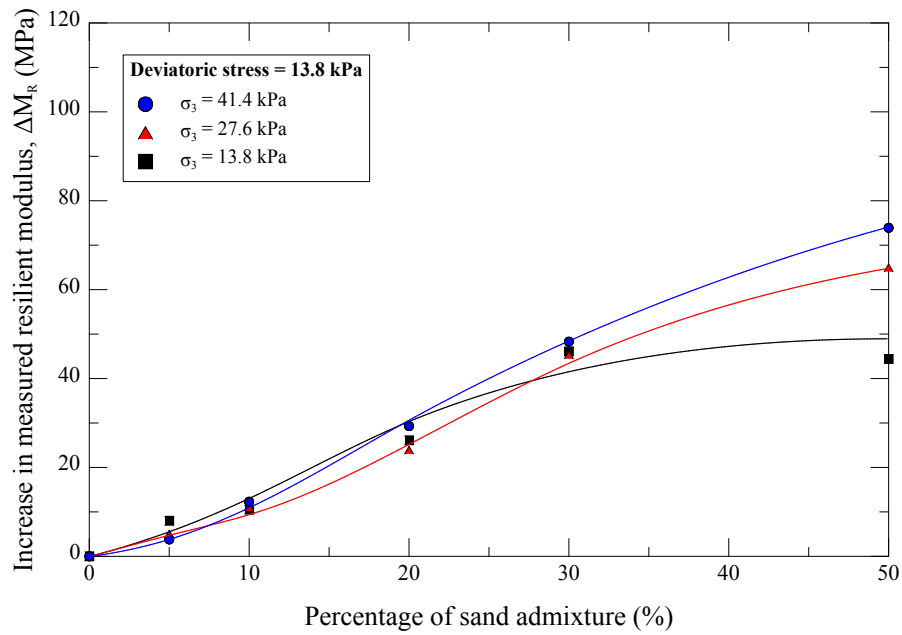


Figure 4.27 Relationship between an increase in the measured resilient modulus and percentage of the sand admixture (at deviatoric stress of 13.8 kPa)

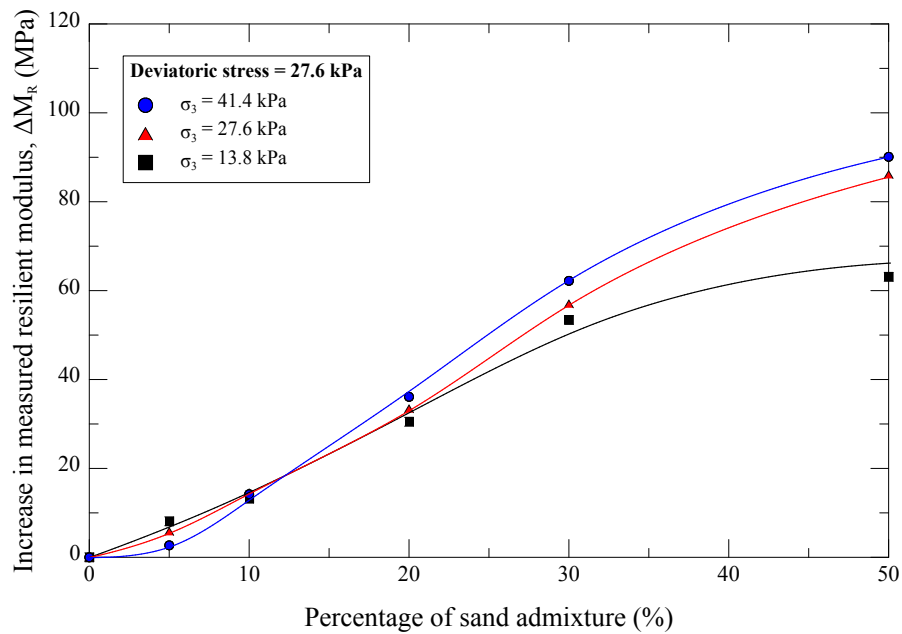


Figure 4.28 Relationship between an increase in the measured resilient modulus and percentage of the sand admixture (at deviatoric stress of 27.6 kPa)

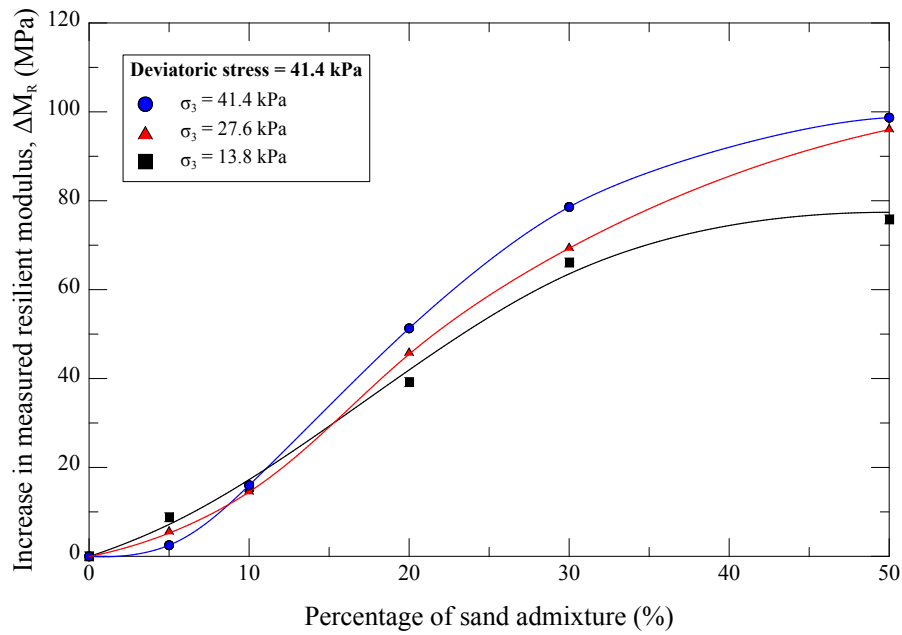


Figure 4.29 Relationship between an increase in the measured resilient modulus and percentage of the sand admixture (at deviatoric stress of 41.4 kPa)

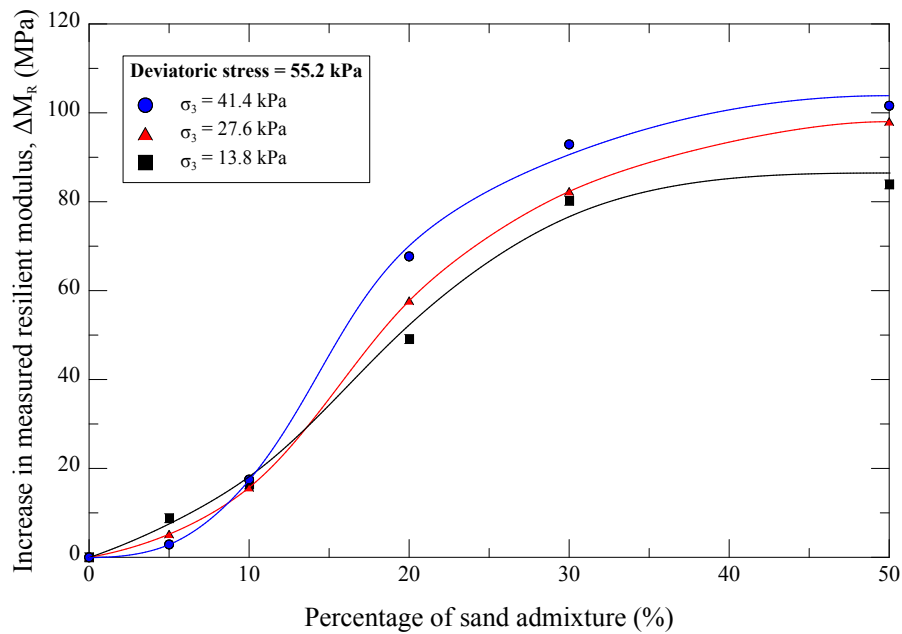


Figure 4.30 Relationship between an increase in the measured resilient modulus and percentage of the sand admixture (at deviatoric stress of 55.2 kPa)

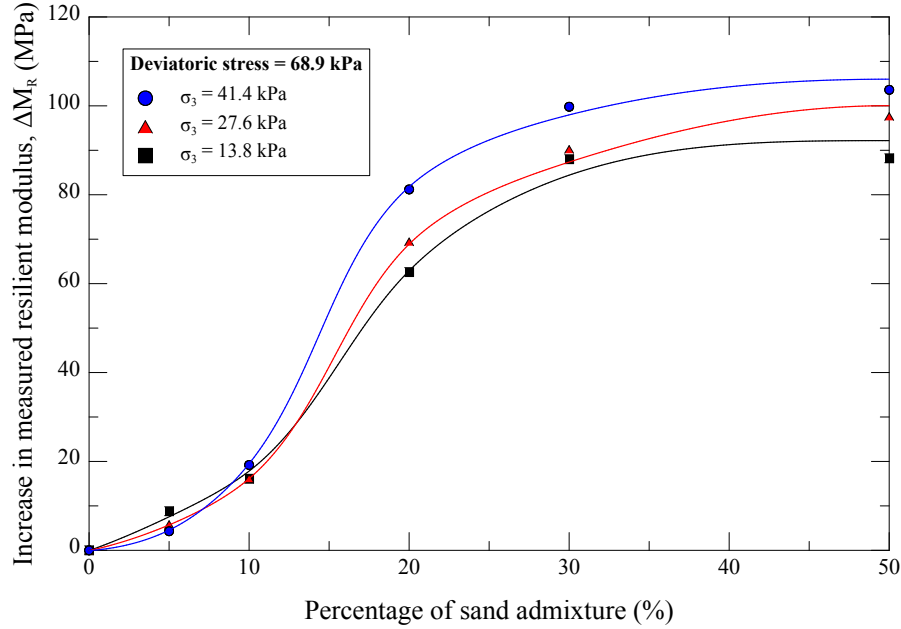


Figure 4.31 Relationship between an increase in the measured resilient modulus and percentage of the sand admixture (at deviatoric stress of 68.9 kPa)

From Figure 4.27–4.31, it can be observed that the resilient modulus increased when the content of the sand admixture was increased. Except for the resilient modulus improvement results obtained from 30–50% sand admixture at the deviatoric stress of 68.9 kPa, the improvement was almost constant. In addition, at the percentage of the sand admixture between 0–10, the resilient modulus results did not exhibit any significant improvement when compared to the results at the higher percentage of the sand admixture. This behavior is explicitly observed at the deviatoric stress of 41.4, 55.2, and 68.9 kPa. Therefore, it can be concluded that adding ten percent of the sand admixture to Dallas clay can be the threshold percent value for the effective resilient modulus improvement.

#### 4.4 Summary

This chapter aims to present and analyze the soil strength improvement with various percentages of the sand admixture by using resilient modulus ( $M_R$ ) as the main parameter and unconfined compressive strength (UCS) as the second parameter. From the unconfined compression test results, it is clearly observed that the UCS linearly increased when the content of the sand admixture was increased.

For the  $M_R$ , an example of one complete  $M_R$  results including full fifteen sequences is initially provided. Subsequently, the  $M_R$  results as required by the AASHTO T 307-99 standard are presented from Dallas clay with no sand admixture to Dallas clay with 50% sand admixture inclusive. The measured  $M_R$  results were then analyzed by a statistical model and presented as predicted  $M_R$  results. From both measured and predicted  $M_R$  results, deviatoric stresses and confining pressures have a significant influence on the results. The last section presents the  $M_R$  improvement by the sand admixture. From the analysis, adding ten percent of the sand admixture to Dallas clay was found to be a threshold percent for the effective resilient modulus improvement.

## Chapter 5

### Conclusions and Recommendations

#### 5.1 Conclusions

The research described in this thesis presented subgrade soil strength improvement by a sand admixture using both unconfined compression strength and resilient modulus as the evaluation parameters. Dallas clay was selected as a reference clayey subgrade soil, and industrial silica sand was selected as a sand admixture material. To determine the subgrade strength improvement behavior, six types of clay-sand mixtures were prepared from Dallas clay with 0%, 5%, 10%, 20%, 30%, and 50% sand admixture, respectively.

In practice, subgrade soil is compacted to approximately reach its maximum dry density (MDD) and optimum moisture content (OMC) obtained from Proctor tests. Therefore, the preparation of clay-sand mixtures in this research was adhered to their MDD and OMC as well. Method of resilient modulus measurement used in this research is the repeated load triaxial test. As provided by the AASHTO T 307-99 standard, the resilient modulus sampling was conducted by preparing two specimens per one type of the clay-sand mixtures. The resilient modulus tests were then performed on the prepared specimens.

All the resilient modulus test results were summarized and presented in accordance with the referred standard. The measured resilient modulus results were then analyzed with the universal model to obtain the predicted resilient modulus results. As for the resilient modulus improvement analysis, the measured resilient

modulus results were adjusted to compare with various percentages of the sand admixture. Based on the experimental results and analyses provided in this research, the following conclusions are set forth:

1. From the compaction curves of the clay-sand mixtures, the maximum dry density increased with an increase in the percentage of the sand admixture. Similar to the maximum dry density, the optimum moisture content decreased with an increase in the percentage of the sand admixture. These behaviors confirm that adding the sand admixture results in higher density that leads to lower moisture content.
2. As an alternative soil strength evaluation parameter, the unconfined compression test results showed that the unconfined compressive strength linearly increased with an increase in the percentage of the sand admixture. This behavior supports that adding the sand admixture can efficiently improve the soil strength.
3. The measured resilient modulus results obtained from six types of the clay-sand mixtures are well matched with the predicted resilient modulus results based on the universal modeling analysis indicating that this model captures both stress-hardening and stress-softening responses. The third parameter of the model,  $k_3$ , presents this response as negative parameter that shows softening behavior with repeated loading.
4. From both measured and predicted resilient modulus results, it can be concluded that both deviatoric stress and confining pressure have a significant

effect on the resilient modulus property. The resilient modulus increased when the confining pressure was increased. As for the effect of the deviatoric stress, an increase in the deviatoric stress resulted in decreasing of the resilient modulus at the percentage of the sand admixture lower than 10. At 10% sand admixture, an increase in the deviatoric stress at the same confining pressure resulted in the similar value of the resilient modulus. When the percentage of the sand admixture was more than 10, an increase in the deviatoric stress resulted in increasing of the resilient modulus.

5. From the resilient modulus improvement analysis, it can be summarized that the resilient modulus significantly increased when the content of the sand admixture was increased. However, the resilient modulus improvements obtained from the sand admixture less than 10% were small. Therefore, the 10% value was termed as a threshold percent of the effective resilient modulus improvement.

This study demonstrates that the mixing of sandy soil to the clay soil can enhance the resilient behavior of the cohesive subgrades. This application can be implemented in low to medium volume pavement conditions. This method is sustainable as no chemical additives will be expended and hence no pollutions are anticipated.

## 5.2 Recommendations

Based on the experiments and analyses conducted in this research, the following recommendations are made for future research activities:



1. Various types of the reference clayey soil and sand admixture should be tested so that the behavior of the test results will reflect better accuracy to be referred at a broader range of soil types.
2. Suction controlled resilient modulus test with different matric suction values should be performed in order to simulate the unsaturated soil condition of the subgrade.

## References

- AASHTO, 1986. "Guide for Design of Pavement Structures," American Association of State Highway and Transportation Officials (AASHTO), Washington, D.C.
- AASHTO, 1993. "Guide for Design of Pavement Structures," American Association of State Highway and Transportation Officials (AASHTO), Washington, D.C.
- AASHTO, 1991. "Interim Method of Test for Resilient Modulus of Subgrade Soils and Untreated Base/Subbase Materials," AASHTO Designation: T 292-91I, American Association of State Highway and Transportation Officials (AASHTO), Washington, D.C.
- AASHTO, 2007. "Standard Method of Test for Determining the Resilient Modulus of Soils and Aggregate Materials," AASHTO Designation: T 307-99, American Association of State Highway and Transportation Officials (AASHTO), Washington, D.C.
- AASHTO, 1992. "Standard Method of Test for Resilient Modulus of Unbound Granular Base/Subbase Materials and Subgrade Soil-SHRP Protocol P46," AASHTO Designation: T 294-92, American Association of State Highway and Transportation Officials (AASHTO), Washington, D.C.
- AASHTO, 1982. "The Standard Method of Testing for Resilient Modulus of Subgrade Soils," AASHTO Designation: T 274-82, American Association of State Highway and Transportation Officials (AASHTO), Washington, D.C.

- Al-Rawas, A. A. and Goosen, M. F. A., 2006. "Expansive Soils: Recent Advances in Characterization and Treatment," Taylor & Francis/Balkema, AK Leiden, The Netherlands, 544 pp.
- Asphalt Institute, 1981. "Thickness Design: Asphalt Pavements for Highways and Streets, 9th edition," Manual Series MS-1, Asphalt Institute, College Park, Maryland, 110 pp.
- Asphalt Institute, 1982. "Research and Development of the Asphalt Institute's Thickness Design Manual (MS-1), 9th Edition," Research Report No. 82-2, Asphalt Institute, College Park, Maryland, 204 pp.
- ASTM Standard D 1883, 2007. "Standard Test Method for CBR (California Bearing Ratio) of Laboratory-Compacted Soils," American Society for Testing and Materials, West Conshohocken, Pennsylvania.
- ASTM Standard D 2166, 2006. "Standard Test Method for Unconfined Compressive Strength of Cohesive Soil," American Society for Testing and Materials, West Conshohocken, Pennsylvania.
- ASTM Standard D 2844, 2007. "Standard Test Method for Resistance R-Value and Expansion Pressure of Compacted Soils," American Society for Testing and Materials, West Conshohocken, Pennsylvania.
- ASTM Standard D 4429, 2007. "Standard Test Method for CBR (California Bearing Ratio) of Soils in Place," American Society for Testing and Materials, West Conshohocken, Pennsylvania.

- ASTM Standard D 6951-03, 2005. "Standard Test Method for Use of the Dynamic Cone Penetrometer in Shallow Pavement Applications," American Society for Testing and Materials, West Conshohocken, Pennsylvania.
- Barker, W. R., 1982. "Prediction of Pavement Roughness," Report No. Miscell. Paper GL-82-11, U.S. Army Engineer Waterways Experiment Station, Vicksburg, Mississippi, 91 pp.
- Barksdale, R. D., Alba, J., Khosla, P. N., Kim, R., Lambe, P. C., and Rahman, M. S., 1997. "Laboratory Determination of Resilient Modulus for Flexible Pavement Design," NCHRP Web Document 14, Federal Highway Administration, Washington, D.C., 486 pp.
- Bergan A. T. and Fredlund D. G., 1973. "Characterization of Freeze-Thaw Effects on Subgrade Soils," Symp. On Frost Action of Roads, Organization for Economic Cooperation and Development, Oslo, Norway, pp. 119–143.
- Buu, T., 1980. "Correlation of Resistance R-value and Resilient Modulus of Idaho Subgrade Soil," Idaho Department of Transportation, Division of Highways, Special Report No. ML-08-80-G, 21 pp.
- Carmichael, R. F. and Stuart, E., 1985. "Predicting Resilient Modulus: A Study to Determine the Mechanical Properties of Subgrade Soils," TRB 1043, Transportation Research Board, National Council, Washington, D.C., pp. 145–148.
- Chamberlain E. J., 1973. "A Model for Predicting the Influence of Closed System Freeze-Thaw on the Strength of Thawed Soils," Symp. On Frost Action on

- Roads, Organization for Economic Cooperation and Development, Oslo, Norway, pp. 94–97.
- Chen, D. H., Wang J. N., and Bilyen, J., 2001. “Application of the DCP in Evaluation of Base and Subgrade Layers,” Transportation Research Board, National Research Council, Washington, D.C., pp. 1–10.
- Chen, D. H., Lin, D. F., Liao P. H., and Bilyen, J., 2007. “A Correlation Between Dynamic Cone Penetrometer Data and Pavement Layer Moduli,” Geotechnical Testing Journal, Vol. 28, No. 1, pp. 42–49.
- Choubane, B. and McNamara R. L., 2000. “Flexible Pavement Embankment Moduli Using Falling Weight Deflectometer (FWD) Data,” Research Report FL/DOT/SMO/00-442, State Materials Office, Florida Department of Transportation, Tallahassee.
- Christopher, B. R., Schwartz, C., and Boudreau, R., 2006. “Geotechnical Aspects of Pavements,” Reference Manual of the United States Federal Highway Administration, U.S. Department of Transportation Publication No. FHWA NHI-05-037, 888 pp.
- Coduto, D. P., 2000. “Foundation Design: Principles and Practices, 2nd Edition,” Prentice-Hall, Upper Saddle River, New Jersey, 883 pp.
- Cosentino, P. and Chen, Y., 1991. “Correlating Resilient Moduli from Pressuremeter Tests to Laboratory California Bearing Ratio Tests,” TRB 1309, Transportation Research Board, National Research Council, Washington, D.C., pp. 56–65.

- Dawson, A. R., Thom, N. H., and Paute, J. L., 1996. "Mechanical Characteristics of Unbound Granular Materials as a Function of Condition," Flexible Pavements, Proc., Eur., Symp. Euroflex 1993, A. G. Correia, ed., Balkema Rotterdam, the Netherlands, pp. 35–44.
- Department of the Army, 1992. "Military Soils Engineering," FM 5-410, Washington D.C.
- Joint Departments of the Army and Air Force, USA, 1994. "Soil Stabilization for Pavements," TM 5-822-14/AFMAN 32-8010, Departments of the Army, and the Air Force, Washington, D.C.
- Jones, D., Rahim, A., Saadeh, S., and Harvey, J., 2010. "Guidelines for the Stabilization of Subgrade Soils in California," Research Report UCD-ITS-RR-10-38, Institute of Transportation Studies, University of California, Davis, Davis, California.
- Dai, S. and Zollars, J., 2002. "Resilient Modulus of Minnesota Road Research Project Subgrade Soil," TRB 1786, Transportation Research Board, National Research Council, Washington, D.C., pp. 20–28.
- Drumm, E. C., Boateng-Poku, Y., and Pierce, T. J., 1990. "Estimation of Subgrade Resilient Modulus from Standards Tests," Journal of Geotechnical Engineering, Vol. 116, No. 5, pp. 774–789.
- Elliot, R. P. and Thornton, S. I., 1988. "Resilient Modulus and AASHTO Pavement Design," Transportation Research Record 1196, pp. 116–124.

- Elliott, R. P., Thornton, S. I., Foo, K. W., Siew, K. W., and Woodbridge, R., 1988. "Resilient Properties of Arkansas Subgrades," Final Report TRC-94, Arkansas State Highway and Transportation Department, Report No. FHWA/AR-89/004, 105 pp.
- Farrar, M. J. and Turner, J. P., 1991. "Resilient Modulus of Wyoming Subgrade Soils," MPC Final Report No. 91-1, Mountain Plains Consortium, 100 pp.
- George, K. P. and Uddin, W., 2000. "Subgrade Characterization for Highway Design," Final Report, University of Mississippi, in cooperation with the Mississippi Department of Transportation, U.S. Department of Transportation, and Federal Highway Administration, Oxford, Mississippi.
- Green, J. L. and Hall, J. W., 1975. "Nondestructive Vibratory Testing of Airport Pavements Volume I: Experimental Test Results and Development of Evaluation Methodology and Procedure," Federal Aviation Administration Report No. FAA-RD-73-205-1, 214 pp.
- Hassan, A., 1996. "The Effect of Material Parameters on Dynamic Cone Penetrometer Results for Fine-grained Soils and Granular Materials, Ph.D. Dissertation, Oklahoma State University, Stillwater, Oklahoma.
- Heukelom, W. and Klomp J. G., 1962. "Dynamic Testing as a Means of Controlling Pavements During and After Construction," Proceedings International Conference on the Structural Design of Asphalt Pavements, Ann Arbor, Michigan, pp. 667-679.

- Hick, R. G., 1970. "Factors Influencing the Resilient Properties of Granular Materials," Ph.D. Dissertation, University of California, Berkeley, Berkeley, California.
- Hicks, R. G. and Monismith, C. L., 1971. "Factors Influencing the Resilient Modulus Properties of Granular Materials," Highway Research Record 345, pp. 15–31.
- Hicks, R. G., 2002. "Alaska Soil Stabilization Design Guide," Alaska Department of Transportation and Public Facilities, FHWA-AK-RD-01-6B.
- Hopkins, T. C., 1991. "Bearing Capacity Analysis of Pavements," Research Report KTC-91-8, University of Kentucky Transportation Center, College of Engineering, Lexington, Kentucky.
- Hopkins, T. C., Beckham, T. L., and Hunsucker, D. Q., 1995. "Modification of Highway Soil Subgrades," Research Report KTC-94-11, University of Kentucky Transportation Center, College of Engineering, Lexington, Kentucky.
- Huang, J., 2001. "Degradation of Resilient Modulus of Saturated Clay Due to Pore Water Pressure Buildup under Cyclic Loading," Master's Thesis, Department of Civil Engineering and Environmental Engineering, Ohio State University, Columbus, Ohio.
- Huang, Y. H., 2004. "Pavement Analysis and Design, 2nd Edition," Pearson Prentice Hall, Upper Saddle River, New Jersey, 775 pp.
- Hudson, J. M., Drumm, E. C., and Madgett, M., 1994. "Design Handbook for the Estimation of Resilient Response of Fine-Grained Subgrades, Proceedings of



- the 4th International Conference on the Bearing Capacity of Roads and Airfields, University of Minnesota, Minneapolis, Vol. 2, pp. 917–931.
- IPC Global, 2011. “Universal Cyclic Tri-axial System,” 0002-2620 Technical Reference Version: 1d1, IPC Global, Victoria, Australia.
- Janoo, V. C. and Bayer II J. J., 2001. “The Effect of Aggregate Angularity on Base Course Performance,” U.S. Army Corps of Engineers, ERDC/CRREL TR-01-14.
- Jones, R., 1958. “In-Situ Measurement of the Dynamic Properties of Soil by Vibration Methods,” *Geotechnique*, Vol. 8, pp. 1–21.
- Jones, M. P. and Witczak, M. W., 1972. “Subgrade Modulus on the San Diego Test Road,” TRB 641, Transportation Research Board, National Research Council, Washington, D.C., pp. 1–6.
- Jorenby, B. N. and Hicks, R. G., 1986. “Base Course Contamination Limits,” TRB 1095, Transportation Research Board, Washington, D.C., pp. 86–101.
- Kim, J. R., Kang, H. B., Kim, D., Park, D. S., and Kim, W. J., 2006. “Evaluation of In-Situ Modulus of Compacted Subgrades Using Portable Falling Weight Deflectometer as an Alternative to Plate Bearing Load Test,” Transportation Research Board 2006 Annual Meeting: Soil and Rock Properties Committee (AFP30), Transportation Research Board, National Research Council, Washington, D.C.

- Kolisoja, P., 1997. "Resilient Deformation Characteristics of Granular Materials," Ph.D. Dissertation, Tampere University of Technology, Publication No. 223, Tampere, Finland.
- Lawton, E. C., Fragaszy, R. J., and Hetherington, M. D., 1992. "Review of Wetting-Induced Collapse in Compacted Soil," *Journal of Geotechnical Engineering*, ASCE, 118-9 (1992) 1376-94.
- Lee, W. J., 1993. "Evaluation of In-Service Subgrade Resilient Modulus with Consideration of Seasonal Effects," Ph.D. Dissertation, Purdue University, West Lafayette, Indiana.
- Lee, W. J., Bohra, N. C., Altschaeffl. A. G., and White, T. D., 1997. "Resilient Modulus of Cohesive Soils," *Journal of Geotechnical and Geoenvironmental Engineering*, ASCE, Vol. 123, No. 2, pp. 131–136.
- Lekarp, F., Isacsson, U., and Dawson, A., 2000. "State of the Art. II: Permanent Strain of Unbound Aggregates," *Journal of Transportation Engineering*, Vol. 126, No. 1, pp. 76–83.
- Lenke, L. R., McKeen, R. G., and Grush M. P., 2001. "Evaluation of a Mechanical Stiffness Gauge for Compaction Control of Granular Media," Report NM99MSC-07.2, New Mexico State Highway and Transportation Department, Albuquerque, New Mexico.
- Liu, C. and Evett, J. B., 2008. "Soils and Foundations, 7th Edition," Pearson Prentice Hall, Upper saddle River, New Jersey, 528 pp.

- Lofti, H. A., 1984. "Development of a Rational Compaction Specification for Cohesive Soils," Ph.D. Dissertation, University of Maryland, College Park, Maryland.
- Lofti, H. A., Schwartz, W., and Witzak, M. W., 1988. "Compaction Specification for the Control of Pavement Subgrade Rutting," TRB 1196, Transportation Research Board, National Research Council, Washington, D.C., pp. 108–115.
- Maher, A., Bennert T., Gucunski, N., and Papp, W. J., 2000. "Resilient Modulus of New Jersey Subgrade Soils," FHWA Report No. 2000-01, Washington, D.C.
- May, R. W. and Witzak, M. W., 1981. "Effective Granular Modulus to Model Pavement Responses," Transportation Research Record No. 810, Transportation Research Board, pp. 1–9.
- Mohammad, L. N., Puppala, A. J., and Alavilli, P., 1994. "Influence of Testing Procedure and LVDTs Location on Resilient Modulus of Soils," Journal of the Transportation Research Board, National Academy of Science, Transportation Research Board, No. 1462, Washington D.C., pp. 91–101.
- Mohammad, L. N., Puppala, A. J., and Alavilli, P., 1994. "Resilient Properties of Laboratory Compacted Subgrade Soils," Journal of the Transportation Research Board, National Academy of Science, Transportation Research Board, No. 1504, Washington, D.C., pp. 87–102.
- Mohammad, L. N., Puppala, A. J., and Alavilli, P., 1995. "Resilient Properties of Laboratory Compacted Subgrade Soils," TRB 1196, Transportation Research Board, National Research Council, Washington, D.C., pp. 87–102.

- Mohammad, L. N., Titi, H. H., and Herath, A., 2000. "Investigation of the Applicability of Intrusion Technology to Estimate the Resilient Modulus of Subgrade Soil," FHWA/LA-00/332, Louisiana Transportation Research Center, Baton Rouge, Louisiana.
- Mohammad, L. N., Titi, H. H., and Herath, A., 2002. "Effect of Moisture Content and Dry Unit Weight on the Resilient Modulus of Subgrades Soils Predicted by Cone Penetration Test," FHWA/LA-00/355, Louisiana Transportation Research Center, Baton Rouge, Louisiana.
- Mohammad, L. N., Gaspard, K., Herath, A., Nazzal, M., 2007. "Comparative Evaluation of Subgrade Resilient Modulus from Non-Destructive , In-Situ and Laboratory Methods, FHWA/LA-06/417, Louisiana Transportation Research Center, Baton Rouge, Louisiana.
- Muench, S. T., Mahoney, J. P., and Pierce, L. M., 2009. "WSDOT Pavement Guide," Washington State Department of Transportation, Olympia, Washington.
- Nazarian, S. and Feliberti, M., 1993. "Methodology for Resilient Modulus Testing of Cohesionless Subgrades," Transportation Research Record No. 1406, Transportation Research Board, pp. 108–115.
- Nazarian, S., Baker, M., and Crain, K., 1995. "Use of Seismic Pavement Analyzer in Pavement Evaluation," TRB 1505, Transportation Research Board, National Research Council, Washington, D.C., pp. 1–8.
- Nazarian, S., Yuan, D., Tandon, V., and Arrellano, M., 2003. "Quality Management of Flexible Pavement Layers with Seismic Methods," Research Report 1735-

3F, Center for Highway Materials Research, The University of Texas at El Paso, El Paso, Texas.

Nazarian, S., Yuan, D., and Tandon, V., 2005. "Quality Management of Flexible Pavement Layers with Seismic Methods," Research Report 0-1735-S, Center for Highway Materials Research, The University of Texas at El Paso, EL Paso, Texas.

Nelson, D. and Miller, D. J., 1992. "Expansive Soils Problems and Practice in Foundation and Pavement Engineering," John Wiley & Sons, New York, 259 pp.

Nelson, C. R., Petersen, R. L., Rudd, J. C., and Sellman, E., 2004. "Design and Compaction Control for Foundation Soil Improvements," T.H. 61 Reconstruction, New Port, Minnesota (CD-ROM), Presented at the 83rd Annual Meeting of the Transportation Research Board, Washington, D.C.

O'Flaherty, C., A. 2002. "Highways: The Location, Design, Construction and Maintenance of Road Pavements, 4th Edition," Butterworth-Heinemann, Burlington, Massachusetts, 576 pp.

Ohio DOT, 2008. "Pavement Design Manual," Ohio Department of Transportation, Office of Pavement Engineering, Columbus, Ohio.

Pezo, R., Claros, G., Hudson, W.R., and Stoke, K.H., 1992. "Development of a Reliable Resilient Modulus Test for Subgrade and Non-Granular Subbase Materials for Use in a Routine Pavement Design," Research Report 1177-4F., University of Texas at Austin, Austin, Texas.

- Pezo, R. and Hudson, W.R., 1994. "Prediction Models of Resilient Modulus for Nongranular Materials," *Geotechnical Testing Journal*, GTJODJ, Vol. 17, No. 3, pp. 349–355.
- Pfalzer, W., Tollner, N., and Hopkins, T. C., 1995. "The Kentucky Geotechnical Data Bank," University of Kentucky Transportation Center, Lexington, Kentucky.
- Ping, W. V., Xiong, W., and Yang, Z., 2003. "Implementing Resilient Modulus Test for Design of Pavement Structures in Florida," Research Report No. FL/DOT/RMC/BC-352-6 (F)/ 6120-567-39, Department of Civil Engineering, FAMU-FSU College of Engineering, Tallahassee, Florida.
- Ruttanaporamakul, P., 2012. "Resilient Properties of Compacted Unsaturated Subgrade Soils," Master's Thesis, The University of Texas at Arlington, Arlington, Texas, 118 pp.
- Powell, W. D., Potter, J. F., Mayhew, H. C., and Nunn, M. E., 1984. "The Structural Design of Bituminous Roads," Transportation and Road Research Laboratory, TRRL Laboratory Report 1132, Department of Transport, Berkshire, United Kingdom.
- Puppala, A. J., Mohammad, L. N., and Allen, A., 1996. "Non-Linear Model for Resilient Modulus Characterization of Granular Soils," Proceedings, 1996 ASCE Engineering Mechanics Conference, Fort Lauderdale, Florida.
- Puppala, A. J., Cumbaa, S. L., and Temple, W. H., 1996. "Comparisons Between Laboratory Measured and FWD Backcalculated Resilient Moduli,"

- Proceedings, 1996 ASCE Engineering Mechanics Conference, Fort Lauderdale, Florida.
- Puppala, A. J. and Mohammad, L. N., 1997. "A Regression Model for Better Characterization of Resilient Properties of Subgrade Soils," Proceedings, 8th International Conference on Asphalt Pavements, Conference Proceedings, Seattle, Washington.
- Puppala, A. J. and Suppakit, C., 1999. "Geotextile Reinforcement Effects on Resilient and Strength Properties of a Clayey Soil," Sixth International Conference on Composites Engineering, ICCE/6, Orlando, Florida.
- Puppala, A. J. and Hanchanloet, S., 1999. "Evaluation of a Chemical Treatment Method (Sulphuric Acid and Lignin Mixture) on Strength and Resilient Properties of Cohesive Soils," Proceedings, Transportation Research Board, CD ROM Preprints, National Research Council, National Academy of Science, Washington, D.C.
- Puppala, A. J. and Ramakrishna, A., 2002. "Resilient Modulus Properties of Control and Chemically Treated Soils," Proceedings, Annual Indian Geotechnical Conference, Allahabad, India.
- Puppala, A. J., Ramakrishna, A., and Hoyos, L. R., 2003. "Resilient Moduli of Treated Clays from Repeated Load Triaxial Test," Journal of the Transportation Research Board, National Academy of Science, Transportation Research Board, No. 1821, Washington, D.C., pp. 68–74.

- Puppala, A. J., 2008. "Estimating Stiffness of Subgrade and Unbound Materials for Pavement Design," NCHRP Synthesis 382, Transportation Research Board, National Research Council, Washington, D.C., 139 pp.
- Puppala, A. J., Hoyos, L. R., and Potturi, A., 2011. "Resilient Moduli Response of Moderately Cement Treated Reclaimed Asphalt Pavement Aggregates," Journal of Material, ASCE, 23, No. 7, pp. 990–998.
- Rada, G. and Witczak, M. W., 1981. "Comprehensive Evaluation of Laboratory Resilient Moduli Results for Granular Material," Transportation Research Record No. 810, Transportation Research Board, National Research Council, Washington, D.C., pp. 23–33.
- Rahim, A. M. and George, K. P., 2004. "Subgrade Soil Index Properties to Estimate Resilient Modulus," Proceedings 83th Annual Meeting of the Transportation Research Board, CD-ROM, 24 pp.
- Richart, F. E., 1975. "Some Effects of Dynamics Soil Properties on Soil-Structure Interaction," Journal of Geotechnical Engineering Division, Vol. 101, No. 12, pp. 1193–1240.
- Robinson, R. G., 1974. "Measurement of the Elastic Properties of granular Materials Using a Resonance Method," TRRL Supplementary Report No. 111UC, TRRL.
- Saparamado, A. A. D. O. P., 1962. "Soil Stabilization as Applied to Highway and Airfield Construction with Special Reference to Ceylon," Institution of Engineers, Ceylon, Sri Lanka.



- Schaefer, V., Stevens, L., White, D., and Ceylan, H., 2008. "Design Guide for Improved Quality of Roadway Subgrades and Subbases," Report No. IHRB Project TR-525, Center for Transportation Research and Education, Iowa State University, Ames, Iowa.
- Seed, H. B. and Chan, C. K., 1957. "Thixotropic Characteristics of Compacted Clays," Journal of Soil Mechanics and Foundation Engineering Division, ASCE, Vol. 83, No. 6, pp. 31–47.
- Seed, H. B. and Chan, C. K., 1958. "Effect of Stress History and Frequency of Stress Application on Deformation of Clay Subgrades under Repeated Loading," Proc., Highway Research Record, Vol. 37, Highway Research Board, Washington, D.C., pp. 555–575.
- Seed, H. B. and Chan, C. K., 1959. "Structure and Strength Characteristics of Compacted Clays," Journal of Soil Mechanics and Foundation Engineering Division, ASCE, Vol. 85, No. 5, pp. 87–128.
- Seed, H., Chan, C., and Lee, C., 1962. "Resilient Characteristics of Subgrade Soils and Their Relation to Fatigue Failures in Asphalt Pavements," Proceedings, International Conference on Structural Design of Asphalt Pavements, University of Michigan, Ann Arbor, Michigan, pp. 611–636.
- Seed H. B., Mitry F. G., Monismith C. L., and Chan C. K., 1967. "Prediction of Flexible Pavement Deflections from Laboratory Repeated-Loads Tests," NCHRP Report 35, Highway Research Board, Washington, D.C.

- Seim D. K., 1989. "A Comprehensive Study on the Resilient Modulus of Subgrade Soils," Workshop on Resilient Modulus Testing, Oregon State University, Corvallis, Oregon.
- Selig, E. T. and Lutenecker, A. J., 1991. "Assessing Railroad Track Subgrade Performance Using In-Situ Tests," Geotechnical Report No. AAR91-369F, University of Massachusetts, Amherst, Amherst, Massachusetts.
- Selig, E. T. and Waters, J., 1994. "Track Geotechnology and Substructure Management," Thomas Telford Publications.
- Smith, W. S. and Nair, K., 1973. "Development of Procedures for Characterization of Untreated Granular Base Course and Asphalt-Treated Base Course Materials," Report No. FHWA-RD-74-61, Federal Highway Administration, Washington, D.C.
- Sukumaran, B., Kyatham, V., Shah, A., and Sheth, D., 2002. "Suitability of Using California Bearing Ratio Test to Predict Resilient Modulus," Proceedings: Federal Aviation Administration Airport Technology Transfer Conference, 9 pp.
- Tanomota, K. and Nishi, M., 1970. "On Resilience Characteristics of Some Soils under Repeated Loading, Solid and Foundations, JSSMFE, Vol. 10 pp. 75–92.
- Thom, N. H. and Brown, S. F., 1988. "The Effect of Grading and Density on the Mechanical Properties of a Crushed Dolomitic Limestone," Proc., 14th ARRB Conf., Vol. 14, Part 7, pp. 94–100.

- Thom, N. H. and Dawson, A. R., 1989. "The Permanent Deformation of a Granular Material Modelled Using Hollow Cylinder Testing," Transportation research Board, Paper Presented at the 68th Annual Meeting, Washington, D.C.
- Thompson, M. R. and LaGrow, T. G., 1988. "A Proposed Conventional Flexible Pavement Thickness Design Procedure," FHWA-IL-UI-223, University of Illinois at Urbana-Champaign, Urbana and Champaign, Illinois, 47 pp.
- Thompson, M. R. and Robnett, Q. L., 1976. "Resilient Properties of Subgrade Soils," Final Report, Illinois Cooperative Highway and Transportation Serial No. 160, University of Illinois Urbana-Champaign, Urbana and Champaign, Illinois.
- Thompson, M. R. and Robnett, Q. L., 1979. "Resilient Properties of Subgrade Soils," Journal of Transportation Engineering, ASCE, Vol. 105, No. 1, pp. 71–89.
- Titi, H. H., Elias, M. B., and Helwany S., 2006. "Determination of Typical Resilient Modulus Values for Selected Soils in Wisconsin," Wisconsin Highway Research Program ID 0092-03-11, Final Report, Department of Civil Engineering and Mechanics, University of Wisconsin – Milwaukee, Milwaukee, Wisconsin.
- Uzan, J., 1985. "Characterization of Granular Material," Transportation Research Record No. 1022, pp. 52–59.
- Vanicek, I. and Vanicek, M., 2008. "Earth Structures: In Transport, Water and Environmental Engineering, 1st Edition," Springer Science+Business Media, New York, New York, 637 pp.

- Vuong, B., 1992. "Influence of Density and Moisture Content on Dynamic Stress-Strain Behaviour of a Low Plasticity Crushed Rock." *Road and Transport Research*, 1(2), pp. 88–100.
- Wilson, B. E., Sargand, S. M., Hazen, G. A., and Green, R., 1990. "Multiaxial Testing of Subgrade", TRB 1278, Transportation Research Board, National Research Council, Washington, D.C., pp. 91–95.
- Witczak, M. W. and Uzan, J., 1988. "The Universal Airport Pavement Design System, Report I of IV: Granular Material Characterization," University of Maryland, College Park, Maryland.
- Witczak, M. W., Qi, X., and Mirza, M. W., 1995. "Use of Nonlinear Subgrade Modulus in AASHTO Design Procedure," *Journal of Transportation Engineering*, Vol. 121, No. 3, pp. 273–282.
- Witczak, M. W. and Uzan, J., 1988. "The Universal Airport Pavement Design System," Report I of V: Granular Material Characterization, University of Maryland, College Park, Maryland.
- Yeh, S-T. and Su, C-K., 1989. "Resilient Properties of Colorado Soils," Colorado Department of Highways, Final Report No. CDOH-DH-SM-89-9, 75 pp.
- Yoder, E. J. and Witczak, M. W., 1975. "Principles of Pavement Design," John Wiley and Sons, New York, New York.

## Biographical Information

Chatuphat Savigamin was born in Greenville, Texas and stayed in Dallas, Texas for two years before moving to Thailand. He completed his high school diploma at Patumwan Demonstration School, Bangkok, Thailand and obtained his bachelor's degree in civil engineering from Chulalongkorn University, Bangkok, Thailand.

In 2012, Chatuphat Savigamin entered the University of Texas at Arlington to pursue a master's degree in civil engineering with a specialization in geotechnical engineering. He had an opportunity to be a graduate research assistant since January 2013 under the guidance of Dr. Anand J. Puppala. During his position, he worked on various research projects including Project TX 0-6740 "Improvement of Construction Quality Control by Using Intelligent Compaction Technology for Base and Soil" funded by TxDOT, Project 56022-01 "Pilot Implementation Using Geofoam for Repair of Bridge Approach Slabs and Adjoining Roadway" funded by TxDOT, and Project "Extended Monitoring and Modeling of Field Testing Sections" funded by U.S. Army Corps of Engineers.